

University of Massachusetts Medical School

eScholarship@UMMS

GSBS Dissertations and Theses

Graduate School of Biomedical Sciences

2012-03-29

Localization of Insulin Receptor Substrate-2 in Breast Cancer: A Dissertation

Jennifer L. Clark

University of Massachusetts Medical School

Let us know how access to this document benefits you.

Follow this and additional works at: https://escholarship.umassmed.edu/gsbs_diss



Part of the [Amino Acids, Peptides, and Proteins Commons](#), [Biological Factors Commons](#), [Cancer Biology Commons](#), [Hormones, Hormone Substitutes, and Hormone Antagonists Commons](#), [Neoplasms Commons](#), and the [Skin and Connective Tissue Diseases Commons](#)

Repository Citation

Clark JL. (2012). Localization of Insulin Receptor Substrate-2 in Breast Cancer: A Dissertation. GSBS Dissertations and Theses. <https://doi.org/10.13028/gn9c-v713>. Retrieved from https://escholarship.umassmed.edu/gsbs_diss/587

This material is brought to you by eScholarship@UMMS. It has been accepted for inclusion in GSBS Dissertations and Theses by an authorized administrator of eScholarship@UMMS. For more information, please contact Lisa.Palmer@umassmed.edu.

LOCALIZATION OF INSULIN RECEPTOR SUBSTRATE-2 IN BREAST CANCER

A Dissertation Presented

By

JENNIFER LYNN CLARK

Submitted to the Faculty of the
University of Massachusetts Graduate School of Biomedical Sciences, Worcester
in partial fulfillment of the requirements for the degree of

DOCTOR OF PHILOSOPHY

MARCH 29, 2012

CANCER BIOLOGY

LOCALIZATION OF INSULIN RECEPTOR SUBSTRATE-2 IN BREAST CANCER

A Dissertation Presented

By

JENNIFER LYNN CLARK

The signatures of the Dissertation Defense Committee signify completion and approval as to style and content of the Dissertation

Leslie M. Shaw, Ph.D., Thesis Advisor

Ashraf Khan, M.D., Member of Committee

Mary Munson, Ph.D., Member of Committee

Andrea L. Richardson, M.D., Ph.D., Member of Committee

Karl Simin, Ph.D., Member of Committee

The signature of the Chair of the Committee signifies that the written dissertation meets the requirements of the Dissertation Committee

Stephen Doxsey, Ph.D., Chair of Committee

The signature of the Dean of the Graduate School of Biomedical Sciences signifies That the student has met all graduation requirements of the school.

Anthony Carruthers, Ph.D., Dean of the Graduate School of Biomedical Sciences

MD/PhD Program

March 29, 2012

ACKNOWLEDGEMENTS

First, I would like to acknowledge the support of my thesis advisor, Dr. Leslie Shaw, who has been a wonderful teacher and mentor. In addition, I would like to thank colleagues in my own lab and others for frequent assistance, advice, equipment, and reagents throughout the course of my thesis work. These include Dr. Shannon Pankratz, Dr. Katerina Mardilovich, Dr. Xiaoqing Yang, Jenny Janusis, Justine Landis, Rasika Rohatgi Kapoor, Dr. Anuradha Seshadri, Jose Mercado-Matos, Bryan Pursell, Michael Roche, Dr. Kyle Draheim, Sambra Redick, and Heidi Malaby.

For assistance with the tumor project outlined in Chapter II, I would like to acknowledge Karen Dresser, Dr. Ashraf Khan, and Dr. Chung-Cheng Hsieh, as well as Dr. Celina Kleer and Dr. Michael Sabel from the University of Michigan for sharing their tumor microarray and Dr. Qin Liu for helpful advice on the statistical analysis. In addition, Dr. Stephen Lyle provided access to the institutional tissue bank, and Michael Roche provided tumor sections and patient data on many occasions.

For assistance with the project outlined in Chapter III, I would like to acknowledge Jean Underwood and Dr. Jeffrey Nickerson for access to the confocal microscope and help with imaging, Jenny Janusis and Jose Mercado-Matos for assistance with several experiments, and Dr. Stephen Doxsey for helpful advice and sharing reagents.

Finally, I would like to acknowledge many classmates, friends, and family who have supported me throughout the last six years of my education. In particular, I thank my husband and my parents for their unwavering support and constant aid.

ABSTRACT

The insulin-like growth factor-1 receptor (IGF-1R) and many of its downstream signaling components have long been implicated in tumor progression and resistance to therapy. The insulin receptor substrate-1 (IRS-1) and IRS-2 adaptor proteins are two of the major downstream signaling intermediates of the IGF-1R. Despite their considerable homology, previous work in our lab and others has shown that IRS-1 and IRS-2 play divergent roles in breast cancer cells. Signaling through IRS-1 promotes cell proliferation, whereas signaling through IRS-2 promotes cell motility and invasion, as well as glycolysis. Moreover, using a mouse model of mammary tumorigenesis, our lab demonstrated that IRS-2 acts as a positive regulator of metastasis, while IRS-1 cannot compensate for this function.

The focus of my thesis research is to understand how IRS-2, but not IRS-1, promotes breast carcinoma cell invasion and metabolism to support metastasis. In preliminary studies, I have found that IRS-1 and IRS-2 exhibit different expression patterns in both cell lines and human tumors with correlations to patient survival, which provides a potential mechanism for their distinct functions. The localization of IRS-1 and IRS-2 within separate intracellular compartments would determine their access to downstream effectors and substrates, and this would result in unique cellular outcomes. Specifically, I have observed that IRS-2, but not IRS-1, co-localizes with microtubules in breast carcinoma cell lines with implications for signaling through AKT and mTORC2.

The goal of this research is to determine how the localization of IRS-2 contributes to its regulation of breast cancer progression and response to therapy and how this information could be used to better predict patient outcomes.

TABLE OF CONTENTS

Signature Page	ii
Acknowledgements	iii
Abstract	v
Table of Contents	vii
List of Tables	ix
List of Figures	x
Preface	xii
Chapter I: Introduction	1
Breast Cancer Statistics and Significance.....	2
IGF-1 Signaling: An Overview.....	2
IGF-1 Signaling: Insulin Receptor Substrates.....	5
IRS Divergent Roles: Differential Expression and Localization.....	8
IGF-1 Signaling: AKT.....	9
Microtubules in Cancer and Therapy.....	12
Microtubule Associated Proteins.....	14
Rationale for Thesis Work.....	15
Chapter II: Membrane localization of Insulin Receptor Substrate-2 (IRS-2) is associated with decreased overall survival in breast cancer	16
Abstract.....	17
Introduction.....	18
Materials and Methods.....	21
Results.....	26
Discussion.....	47
Acknowledgements.....	52
Chapter III: Interaction of Insulin Receptor Substrate-2 (IRS-2) with microtubules and KIF2A: Impact on AKT signaling	53
Introduction.....	54
Materials and Methods.....	57
Results.....	63
Discussion.....	87
Acknowledgements.....	92
Chapter IV: Discussion	93
Summary of Findings.....	94
Explanation for Divergent Roles of IRS-1 and IRS-2.....	95
Clinical Relevance of IRS-2 Expression Patterns in Tumors.....	96
Further Study of the Punctate Cytoplasmic IRS-2 Expression Pattern.....	98
The Role of the Microtubules in AKT Activation.....	100
Potential Relevance of KIF2A in Breast Cancer.....	102
Potential Role of Microtubules in Differential Signaling to AKT Substrates.....	106
Novel Finding that Microtubules May Be Required for mTORC2 Activation.....	106

Overall Significance.....	107
Appendix: Interaction of Insulin Receptor Substrate-2 (IRS-2) with mTORC2..	110
Bibliography.....	114

LIST OF TABLES

Table 2.1. Clinical characteristics of tumor datasets

Table 2.2. Survival analysis of clinical parameters in the two datasets

Table 2.3. Survival analysis for IRS-2 staining patterns

Table 2.4. Survival analysis for diffuse and punctate IRS-2 staining patterns

Table 3.1. Nocodazole response summary

LIST OF FIGURES

Figure 1.1. Summary of Insulin Receptor Substrate signaling

Figure 2.1. Analysis of IRS-2 antibody specificity

Figure 2.2. IRS expression in normal human breast tissue and benign breast lesions

Figure 2.3. IRS expression in human breast tumors and cell lines

Figure 2.4. IRS-2 localization in human breast tumors

Figure 2.5. Analysis of IRS-2 staining patterns, progesterone receptor status, and overall survival

Figure 2.6. Analysis of IRS-2 diffuse staining pattern, progesterone receptor status, and overall survival

Figure 2.7. Analysis of IRS-2 punctate staining pattern, progesterone receptor status, and overall survival

Figure 3.1. Localization of the IRS proteins in breast carcinoma cells

Figure 3.2. Association of IRS-2 with the microtubule cytoskeleton

Figure 3.3. Impact of taxol and nocodazole treatment on IGF-1 stimulated AKT activation

Figure 3.4. Evaluation of the role of the microtubule cytoskeleton in IGF-1R signaling pathway activation

Figure 3.5. Evaluation of the role of the microtubule cytoskeleton in IGF-1 stimulation of mTORC1 and mTORC2 activation

Figure 3.6. Selective impact of nocodazole on IRS-2 mediated signaling

Figure 3.7. Differential sensitivity of breast carcinoma cells to nocodazole

Figure 3.8. Interaction of IRS-2 with microtubule associated proteins (MAPs)

Figure 3.9. Role of IRS-2 in the cellular response to microtubule disruption

Figure 4.1. Model of IRS-2-mediated AKT activation

Figure A.1. Association of IRS-2 with mTORC2

PREFACE

Though the majority of the work presented in this thesis is my own, some results represent the work of others.

In Chapter II, the tissue sections and immunochemistry presented in Figures 2.1c, 2.2, 2.3a, and 2.4a-c,j were prepared by Karen Dresser. The paraffin-embedded MDA-MB-231 cells in Figure 2.1a and the tumor microarray in Figure 2.4d-i were also stained by Karen Dresser. All slides were viewed and interpreted by me. The statistical analysis and accompanying Kaplan-Meier survival graphs in Tables 2.1, 2.2, 2.3, and 2.4 and Figures 2.5, 2.6, and 2.7 were prepared by Dr. Chung-Cheng Hsieh. All interpretation is my own work.

In Chapter III, the images pictured in Figure 3.1i were taken by Jean Underwood. The cell preparation and immunofluorescent staining was performed by me. The immunoprecipitation, SDS-PAGE, and immunoblots presented in Figure 3.8b,c,d were prepared by Jenny Janusis from lysates prepared by me. The cell cycle analysis presented in Figure 3.9 was performed by Jose Mercado-Matos.

CHAPTER I

Introduction

Breast Cancer Statistics and Significance

Breast cancer is the leading cancer diagnosis and second leading cause of cancer-related death among women in the United States. Approximately 12% of American women will be diagnosed with breast cancer in their lifetime, and 40,000 will die each year of the disease [1]. Public health efforts have improved screening for early detection, and scientific advances in treatment have prolonged survival for women with this disease; but breast cancer remains a serious and significant medical concern worldwide.

Death from breast cancer, as with most cancers, is generally caused by the metastasis, or spreading, of tumor cells to other sites in the body and subsequent compression and invasion of the parenchyma of vital organs. Common sites for metastasis of breast carcinoma include local lymph nodes, lung, bone, brain, and liver. Metastasis of a tumor cell to a distant site involves invasion of a blood or lymph vessel, travel in the circulation, invasion of a distant organ, and proliferation and survival in that organ. Such a cell must possess the properties of invasiveness, motility, and resistance to hypoxic and metabolic stress [2]. Metastatic disease is particularly difficult to treat, as the metastatic process has selected for an aggressive and resilient cellular phenotype more likely to resist standard treatment measures.

IGF-1 Signaling: An Overview

A variety of signaling pathways mediate the ability of a tumor cell to metastasize or resist pharmacologic treatment. Among others, insulin-like growth factor-1 receptor

(IGF-1R) signaling has been well studied in breast cancer. High serum IGF-1 levels are associated with an increased risk of developing breast cancer, and breast cancer patients have higher levels than healthy controls [3, 4]. The receptor tends to be overexpressed and hyperactivated in breast carcinoma cells [5, 6]; and inhibition of the receptor suppresses cell adhesion, invasion, and metastasis and increases sensitivity to taxol treatment [7]. Additionally, IGF-1R expression is increased by estrogen, a primary mediator of tumor cell growth in many breast cancers, and IGF-1 signaling can positively influence estrogen-inducible genes [8, 9].

The dimeric IGF-1R is made up of two monomers, each containing an alpha and beta subunit, joined by disulfide bonds [10]. The extracellular alpha subunit is responsible for ligand binding, while the transmembrane and intracellular beta subunit is responsible for signaling [10]. Hybrid receptors containing an alpha and beta subunit of the insulin receptor (IR) are also possible. Multiple ligands may activate the receptor. These include IGF-1 and IGF-2, as well as insulin to a lesser extent [11]. Although IGF levels are controlled in an endocrine manner, plasma ligand levels are also modulated in part by a group of IGF binding proteins (IGFBPs) which sequester IGF-1 in the plasma and prevent receptor binding and activation [11]. Specifically, IGFBP3 and IGFBP5 have been well studied in breast cancer. Both proteins have additional functions outside of the IGF-1 signaling pathway, and both have been correlated to breast cancer risk, prognosis, and sensitivity to therapy in several studies [12-19]. IGFBP3 mediates antiproliferative effects independent of IGF-1 through binding to cell surface proteins and

receptors [20, 21]. Additionally, IGFBP3 inhibits estrogen-stimulated growth when added to estrogen-treated MCF7 cultures, and antiestrogen treatment results in an accumulation of IGFBP3 with growth-inhibitory effects [22]. IGFBP5 has also been implicated in mediating growth inhibition by antiestrogens, as well as vitamin D-related compounds [23, 24]. IGFBP5 has also been found to enhance the antiproliferative effects of tumor necrosis factor- α (TNF α) [25].

Upon binding of IGF-1, an autophosphorylation event on the intracellular domain of the IGF-1R activates the receptor [26]. This key tyrosine phosphorylation serves to recruit effectors, including insulin receptor substrate (IRS) proteins, Grb10, and SHC which bind by virtue of their phosphotyrosine binding (PTB) or SH2 domains [27-29]. These effectors can then be phosphorylated by the receptor tyrosine kinase on specific tyrosine residues, facilitating the recruitment of other mediators of downstream signaling [30]. Most notably, PI3K is recruited to the receptor through the phosphorylated IRS proteins, where it converts phosphatidylinositol 4,5-bisphosphate (PIP₂) to phosphatidylinositol 3,4,5-trisphosphate (PIP₃) on the inner leaflet of the plasma membrane [31, 32]. Proteins that contain pleckstrin homology (PH) domains may then associate with PIP₃ at the membrane, facilitating signaling by bringing important molecules into close proximity. For example, 3-phosphoinositide dependent protein kinase-1 (PDK1) activates AKT in this manner.

IGF-1 Signaling: Insulin Receptor Substrates

In addition to the IGF-1R, the IRS proteins serve as adaptors for the IR and a number of cytokine receptors [33]. These proteins were originally identified and studied in the context of insulin signaling, and they serve to recruit downstream mediators of insulin action to the membrane receptor [34]. There are six known family members. IRS-1 and IRS-2 are expressed ubiquitously in humans [34]. The roles of IRS-1 and IRS-2 are not entirely redundant, though both mediate insulin signaling and regulate sensitivity [35-37]. Knockout studies in mice have revealed a role for Irs-1 in total body growth, whereas Irs-2 is involved in maintenance of pancreatic beta cell function and brain development [35-38]. Although loss of either Irs-1 or Irs-2 causes insulin resistance, only the loss of Irs-2 leads to diabetes [33]. Irs-3 is expressed in rodents only, and Irs-4 is limited in its tissue distribution with knockout resulting only in mild phenotypes [33, 39-41]. Two additional family members, IRS-5 and IRS-6, are truncated at the C-terminus but do associate with the IR and IGF-1R through intact PH and PTB domains [42]. Their function is relatively unknown.

IRS-1 and IRS-2 share considerable homology [43]. In particular, the PH domain closest to the N-terminus and the adjacent PTB domain are highly conserved between IRS-1 and IRS-2 [43] (Figure 1.1a). IRS-2 also contains a unique kinase regulatory loop binding (KRLB) domain involved in receptor interaction, which may have inhibitory effects that modulate IRS-2 activity downstream of the IR [44] (Figure 1.1a). The C-terminal region of the IRS proteins contains a number of confirmed and putative tyrosine

Figure 1.1. Summary of Insulin Receptor Substrate signaling

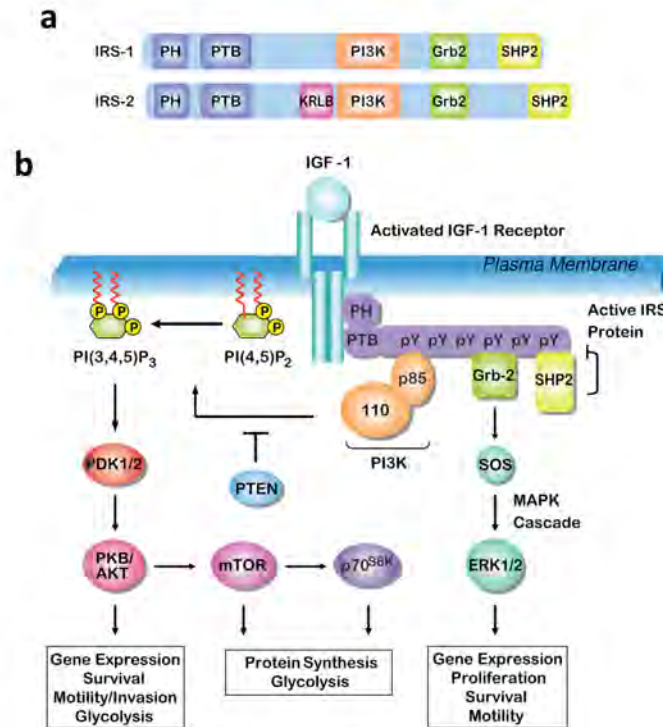


Figure 1.1. Summary of Insulin Receptor Substrate signaling. (a) Structural domains (purple and pink) and binding regions (orange, green, and yellow) of IRS-1 and IRS-2. (b) Overview of IRS signaling pathways.

and serine phosphorylation sites [43, 45] (Figure 1.1a). Though many of these sites are conserved between IRS-1 and IRS-2, many are unique and are likely partially responsible for differences in signaling downstream of these two proteins [43]. The tyrosine phosphorylation sites that have been best studied mediate binding of the p85 subunit of PI3K, Grb2, and Shp2 [43] (Figure 1.1a). IRS signaling is summarized in Figure 1.1b. Serine phosphorylation has been associated with suppressing activity of the IRS proteins [46, 47]. In the context of insulin signaling, specific serine residues on IRS-1 are phosphorylated by S6 Kinase (S6K) downstream of the active insulin receptor, leading to feedback inhibition of signaling [48]. The function of serine phosphorylation in IRS-2 has not been as well studied at this time.

IRS-1 and IRS-2 are of particular interest in breast cancer. In human breast cancer, IRS-1 expression is associated with increased recurrence rates and more lymph node metastasis [49, 50]; and a certain polymorphism of *IRS1* is associated with increased breast cancer risk in a subset of women [51]. IRS-2 has not been studied in this context. In a mouse model of mammary tumorigenesis, overexpression of either *Irs-1* or *Irs-2* enhances tumorigenesis, supporting a common role for the IRS proteins in transformation [52]. However, the roles of IRS-1 and IRS-2 in malignant breast tumor cells differ quite markedly [43]. *In vitro* studies have revealed that IRS-1 primarily regulates signals for proliferation and survival, whereas signaling through IRS-2 promotes motility, invasion, and glycolysis [53-61]. Restoration of IRS-1 in a model system lacking endogenous IRS protein expression enhances proliferation, but expression

of IRS-2 instead promotes motility [53]. In our own studies using the MMTV:PyV-MT mouse model of mammary tumorigenesis, metastasis is increased in the absence of Irs-1 expression, when Irs-2 expression is elevated, and diminished in the absence of Irs-2 expression [57, 58]. Tumor cells derived from Irs-2^{-/-} mice exhibit decreased invasiveness and lower rates of glycolysis, while Irs-1^{-/-} tumor cells, which signal through Irs-2 only, are highly invasive [58, 59]. Taken together, these results suggest that IRS-2 is uniquely associated with tumor aggressiveness and disease progression, while IRS-1 may actually have suppressive effects.

IRS Divergent Roles: Differential Expression and Localization

Despite considerable evidence for the divergent roles of IRS-1 and IRS-2 in breast cancer, a mechanistic explanation is lacking. Differential regulation of the expression of these proteins could partially explain differences in function. IRS-1 gene expression and activity is positively regulated by estrogen [62]; and in the nucleus, IRS-1 complexes with estrogen receptor α (ER α) at the estrogen response element (ERE) in other gene promoters to regulate gene expression [63, 64]. In contrast, IRS-2 is a primary progesterone response gene [65]. Progesterone induces IRS-2 mRNA, increases total protein levels, and enhances activation in response to IGF-1 [55, 65, 66]. However, IRS-2 can also be regulated by other means, including hypoxia and epidermal growth factor (EGF) signaling [67, 68]. Some differences in IRS expression patterns have been reported and might also explain divergent roles in breast cancer [69]. In the mouse mammary gland, Irs-1 is expressed in only a subset of ductal epithelial cells while Irs-2 is

expressed homogenously throughout the duct and in the terminal end buds [70]. The study of normal ducts and malignant lesions in humans is still needed to elucidate IRS-1 and IRS-2 expression patterns in the human mammary gland.

IGF-1 Signaling: AKT

The IRS proteins are important mediators of the PI3K/AKT/mTOR axis downstream of the activated IGF-1R. Signaling through the PI3K/AKT axis has been shown to play an important role in breast carcinoma cell survival, as well as to impact patient outcome, response to therapy, and drug resistance [71-76]. Human breast tumors tend to overexpress the serine and threonine kinase AKT compared to normal breast epithelium, and overexpression in MCF7 cells increases IGF-1-independent survival and proliferation, enhances responsiveness to IGF-1 stimulation, and suppresses induction of apoptosis by TNF and ultraviolet radiation [71-73]. Activation of AKT is associated with recurrence and distant metastasis, as well as resistance of MCF7 cells to chemotherapeutic drugs, including doxorubicin and the antiestrogens tamoxifen and fulvestrant [74-76].

Activation of AKT is achieved through phosphorylation of two essential sites. The threonine 308 (T308) site in the activation loop is a PDK1 phosphorylation site [77-79], whereas phosphorylation of serine 473 (S473) in the hydrophobic motif (HM) C-terminal domain is dependent on the mTORC2 complex [80]. An additional phosphorylation site at threonine 450 (T450) in the turn motif is also mTORC2-

dependent and stabilizes AKT by protecting the HM from dephosphorylation [81-83]. Phosphorylation on T308 by PDK1 is thought to result from association of the N-terminal PH domain with PIP₃ on the inner leaflet of the plasma membrane [84]. However, the mechanism of AKT activation by mTORC2 has not yet been fully elucidated. The mTORC2 complex is defined by the association of mTOR with rictor and also contains SIN1, mLST8, PRR5, and DEPTOR [85]. Other substrates of mTORC2 include the AGC kinases Protein Kinase C- α (PKC- α), a kinase involved in the regulation of the actin cytoskeleton, and Serum- and Glucocorticoid-induced Kinase 1 (SGK1), which regulates a number of processes including ion transport [83, 86]. In contrast to mTORC1, the mTORC2 complex is generally rapamycin-insensitive [87]. mTORC2 is activated downstream of PI3K, but the specific mechanism is unknown [88]. Limited evidence suggests that mTORC2 can be directly activated by association with ribosomes or through interaction with PIP₃ [89, 90]. Although rictor has been shown to be directly phosphorylated on a threonine residue by S6K1, causing an upregulation in phosphorylation of the S473 site on AKT, this event is not associated with increased complex formation or kinase activity [91].

There are three AKT isoforms with both overlapping and distinct functions [92]. AKT1 mainly functions in cell growth, AKT2 in glucose metabolism, and AKT3 in neuronal development, though there is considerable overlap [92]. All three isoforms have been shown to cause cellular transformation upon overexpression, and all three have been implicated in breast cancer [71, 73, 93-95]. AKT1 expression is increased in breast

tumors compared to normal mammary epithelium [71]. AKT2 is both frequently mutated and overexpressed in breast cancer, particularly in the HER2/Neu positive subset [73, 93]; and this isoform has been implicated in resistance to chemotherapy in several studies [96-98]. AKT3 mRNA is upregulated and protein activity enhanced in ER negative (ER-) breast tumors [94].

AKT has a wide number of downstream targets which function in proliferation, metabolism, and survival [99]. AKT regulates proliferation through modulation of the cell cycle. For example, phosphorylation of Glycogen Synthase Kinase 3 (GSK3) by AKT is inhibitory, relieving the inhibition of GSK3 on cyclin D1 and allowing the cell cycle to move forward [100]. Other targets include WEE1, MYT1, KIP1, and CIP1, inhibitors of the cell cycle which are themselves inhibited upon phosphorylation by AKT [101-104]. AKT also regulates metabolism through a number of pathways which regulate protein synthesis, glycogen synthesis, and glucose transport. AKT can regulate protein synthesis by activating the nutrient sensing complex mTORC1 either directly or through inactivation of the inhibitory Tuberous Sclerosis Complex (TSC) proteins [105]. mTORC1 may then activate 4E-BP1 to release eIF-4E for mRNA translation, as well as S6, another effector of protein synthesis, downstream of p70 S6K [105, 106]. AKT inhibits glycogen synthesis through inhibition of GSK3, which itself activates glycogen synthase [107]. Glucose transport is upregulated by activation of AS160, a Rab GTPase activating protein (RabGAP) involved in GLUT4 trafficking [108, 109]. Finally, AKT

promotes cell survival predominantly through the inhibitory phosphorylation of pro-apoptotic proteins, including FOXO1, BIM, BAX, and BAD [110-113].

Microtubules in Cancer and Therapy

Due to the importance of microtubules in many cellular functions, most notably mitosis, they have been an attractive target for cancer chemotherapy. The vinca alkaloids, which include the drugs vinblastine, vincristine, and vinorelbine, cause disaggregation of the microtubules through binding to tubulin dimer, resulting in disruption of replication and mitosis [114]. In contrast, the taxane drugs paclitaxel and docetaxel bind to microtubules causing a stabilization that prevents the dynamic changes necessary for cell cycle progression [114]. Both drug classes are associated with clinically significant myelosuppression and neuropathy, as well as drug resistance [114]. Studies of the mechanisms by which these drugs exert killing effects on cells, as well the study of modes of resistance to these drugs, will be important in developing and modifying cancer treatments for better clinical outcomes.

The microtubule cytoskeleton is a dynamic structure made up of polymerized tubulin which functions in the maintenance of cell architecture, protein and vesicle trafficking, cell division, and movement [115]. Tubulin polymerization and depolymerization is in constant flux, with many tubules growing and others shrinking at any moment in time [116]. The steady state length and stability of microtubules is highly regulated, likely due to the drastic reorganization which must take place during mitosis,

and this varies by cell type and context [117]. Tubulin polymerization is dependent on binding of guanosine triphosphate (GTP) to the beta subunit, and hydrolysis to guanosine diphosphate (GDP) occurs simultaneously with polymerization [115, 118]. Binding of GDP has a destabilizing effect, contributing to depolymerization and the dynamic nature of microtubules [115].

Though cancer treatment has focused on the role of the microtubules in mitosis, the microtubule cytoskeleton serves other important roles in cancer progression. In particular, the dynamic nature of the microtubules is required to effect changes in cell morphology for the purposes of motility and invasion. In a study of breast tumors, the microtubule associated protein (MAP) intracellular hyaluronic acid binding protein (IHABP) was strongly expressed in the tumor stroma, as well as in the carcinoma cells at the tumor edges, and this was associated with worse overall survival, suggesting that changes in microtubule stability may mediate tumor aggressiveness [119]. In MDA-MB-231 cells, hypoxia induces a stabilization of the microtubules which is required for invasiveness mediated by $\alpha 6\beta 4$ integrin [120]. The epithelial-to-mesenchymal transition (EMT) is associated with accumulation of deetyrosinated tubulin at the invasive tumor front and the formation of microtentacles which aid in invasion of the vascular endothelium [121].

The microtubules may also impact the outcome of signaling. Of relevance to IGF-1 and insulin signaling, many glycolytic enzymes are bound to the microtubules, and

changes in microtubule length and stability can modulate their activity [122]. Regarding glucose transport, the microtubules are targets of insulin signaling, as well as downstream effectors of GLUT4 trafficking [123]. It has been suggested that the microtubules are required to organize an insulin signaling complex and provide the surface necessary for the mobility of GLUT4 [124]. Similar mechanisms likely exist for IGF-1 signaling.

Microtubule Associated Proteins

A variety of microtubule associated proteins bind to polymerized tubulin and modulate stability and dynamicity. For example, the MAP2/tau family of proteins are known to stabilize microtubules, though they have diverse functions in signaling and transport [125]. Family members include MAP2 and tau which are mainly expressed in neurons and MAP4 which has a wider tissue distribution [125]. Other families of MAPs bind only the plus ends of microtubules. For example, end-binding (EB) proteins track plus ends autonomously and serve to recruit other important proteins to the plus ends where they serve to regulate microtubule tip dynamics [126]. Another important group of proteins that interact with the microtubules are the motor proteins, which function in movement and transport of organelles along microtubules. Dynein allows retrograde movement toward minus ends, whereas kinesins, of which there are several families, allow anterograde movement toward the tips [127, 128]. Motor proteins may be of particular interest in cancer due to their diverse roles in mitosis, vesicle trafficking, and cellular motility [129]. Dysregulation of mitosis may result in tumorigenesis, while vesicle trafficking may be involved in the altered metabolism underlying cancer cell

survival. Motility facilitated in part by kinesins is required for tumor progression and metastasis.

Rationale for Thesis Work

The IRS proteins mediate signals downstream of the IGF-1R to support breast tumorigenesis and disease progression. Despite the considerable sequence homology shared between the two family members most frequently implicated in breast cancer, IRS-1 and IRS-2, the specific roles of these two proteins in breast carcinoma cell function differ greatly. Differential subcellular localization may affect signaling outcomes through differing access to downstream effectors. Though IRS-1 has been investigated in this context, little is known about the subcellular localization of IRS-2 in breast cancer. Such information has important clinical implications, as the IGF-1 signaling pathway is a common target of treatment, as well as a common suspect in the development of drug resistance. Information about the mechanisms by which downstream signaling events are regulated could lead to the discovery of new drug targets. For my thesis research, I sought to characterize the expression patterns of IRS-1 and IRS-2 in breast tumors and breast carcinoma cell lines and to examine the impact of their localization on downstream signaling, cell function, and patient outcomes in order to determine if the differing roles of IRS-1 and IRS-2 in breast cancer can be explained by differential subcellular localization.

CHAPTER II

Membrane localization of Insulin Receptor Substrate-2 (IRS-2) is associated with decreased overall survival in breast cancer

Jennifer L. Clark¹, Karen Dresser², Chung-Cheng Hsieh¹, Michael Sabel³, Celina G. Klee⁴, Ashraf Khan² and Leslie M. Shaw¹

¹Departments of Cancer Biology and ²Pathology, University of Massachusetts Medical School, Worcester, MA 01605, ³Departments of Surgery and ⁴Pathology, University of Michigan Health System, Ann Arbor, MI 48109

ABSTRACT

Recent studies have identified a role for insulin receptor substrate-2 (IRS-2) in promoting motility and metastasis in breast cancer. However, no published studies to date have examined IRS-2 expression in human breast tumors. We examined IRS-2 expression by immunohistochemistry (IHC) in normal breast tissue, benign breast lesions, and malignant breast tumors from the institutional pathology archives and a tumor microarray from a separate institution. Three distinct IRS-2 staining patterns were noted: diffusely cytoplasmic, punctate cytoplasmic, and localized to the cell membrane. The individual and pooled datasets were analyzed for associations of IRS-2 staining pattern with core clinical parameters and clinical outcomes. Univariate analysis revealed a trend toward decreased overall survival (OS) with IRS-2 membrane staining, and this association became significant upon multivariate analysis ($p = 0.01$). In progesterone receptor negative (PR-) tumors in particular, IRS-2 staining at the membrane correlated with significantly worse OS than other IRS-2 staining patterns ($p < 0.001$). When PR status and IRS-2 staining pattern were evaluated in combination, PR- tumors with IRS-2 at the membrane were associated with a significantly decreased OS when compared with all other combinations ($p = 0.002$). Evaluation of IRS-2 staining patterns could potentially be used to identify patients with PR- tumors who would most benefit from aggressive treatment.

INTRODUCTION

Insulin receptor substrate-1 (IRS-1) and IRS-2 adaptor proteins are downstream signaling intermediates of several receptors that transmit signals to breast carcinoma cell function [6, 33, 130-135]. The most widely studied of these receptors is the insulin-like growth factor-1 receptor (IGF-1R), which has been implicated in breast cancer progression and response to therapy [6, 130-132]. Despite a high level of sequence homology, IRS-1 and IRS-2 play divergent roles in breast cancer [43]. Signaling through IRS-1 promotes breast carcinoma cell proliferation, whereas signals transmitted through IRS-2 regulate breast carcinoma cell motility and invasion, as well as glycolysis [53-60]. Studies from our own lab have demonstrated that IRS-2 acts as a positive regulator of metastasis, while IRS-1 cannot compensate for this function and may negatively regulate metastasis [57, 58]. Taken together, the results from these studies support that IRS-1 and IRS-2 can markedly influence the outcome of signaling through their upstream receptors, and the expression of these proteins is likely to impact the biology of breast tumors.

Although IRS-1 and IRS-2 are expressed relatively ubiquitously in human tissues, differences in their expression patterns have been reported [69]. In the developing mouse mammary gland, IRS-1 is expressed in a subset of luminal mammary epithelial cells in mature ducts and also in the body of the terminal end bud (TEB) [70]. In contrast, IRS-2 is expressed homogeneously in the ductal luminal epithelial cells and also throughout the TEB, including the cap cell layer [70]. These differential expression patterns likely reflect differences in the regulatory mechanisms that control expression of their genes.

IRS-1 is an estrogen-regulated gene, and its expression correlates positively with estrogen receptor (ER) expression in human breast tumors [49, 62, 136-138]. *IRS-1* expression is highest in more well-differentiated, ER-positive (ER+) cell lines and tumors, and its expression may decrease with disease progression, as expression or function of the ER is lost [139]. *IRS-2* is a progesterone-responsive gene, and it is expressed at higher levels in more poorly differentiated, ER negative (ER-) breast carcinoma cells [57, 65]. Given that breast carcinoma cells that express *IRS-2* often lack expression of the progesterone receptor (PR), alternative mechanisms are likely to play a more dominant role in regulating *IRS-2* expression in breast tumors. In this regard, epidermal growth factor (EGF) signaling and hypoxia positively regulate the expression of *IRS-2* [67, 68].

In addition to differential regulation of *IRS-1* and *IRS-2* at the level of gene transcription, intracellular localization is also likely to play an important role in the divergent functions of these adaptor proteins. Although many tumors exhibit diffuse, cytoplasmic expression of *IRS-1*, *IRS-1* can also localize to the nucleus where it can interact with ER- α and modulate its transcriptional activity [63, 136, 139, 140]. An association with increased tamoxifen response and survival for patients with tumors expressing *IRS-1* in the nucleus has been reported [140]. The authors of that study suggested that nuclear *IRS-1* reflects an upregulation of ER signaling, which would render a tumor more sensitive to an ER antagonist such as tamoxifen [140]. To date, there are no published studies examining *IRS-2* expression in human breast tumors. In the current study, we evaluated *IRS-2* expression in invasive ductal carcinomas and

identified distinct IRS-2 expression patterns that have significance for overall patient survival outcomes.

MATERIALS AND METHODS

Tumor sections. Formalin-fixed, paraffin-embedded tumor sections were obtained from the Pathology Department archives and tumor bank at the University of Massachusetts Medical School. Institutional Review Board (IRB) approval was obtained for this study, and informed consent was obtained for all participating subjects. The retrospective study population consisted of patients diagnosed between the years of 1997 and 2007 with breast cancer of any stage. Complete data on tumor size, tumor grade, node status, and receptor status were available. For many patients, follow-up data on recurrence-free survival, overall survival, metastases, therapy, and co-morbid conditions were also available. Median follow-up was 69.5 months for recurrence-free survival and 72.5 months for overall survival.

Tissue Microarray. A tissue microarray was constructed from 154 cases from the surgical pathology files at the University of Michigan Health System [141]. Three 0.6 mm diameter cores were taken from each formalin-fixed, paraffin-embedded block. Cases which did not contain cores with tumor cells were excluded from analysis, resulting in 130 final cases. The study was approved by the IRB, and informed consent was obtained for all subjects. The retrospective study population consisted of patients diagnosed between the years of 1987 and 1991 with invasive breast carcinoma. Complete data on tumor size, tumor grade, node status, receptor status, and other clinicopathologic variables, as well as recurrence-free survival, overall survival, and

therapy were available. Median follow-up time was 80.0 months for recurrence-free survival and 104.4 months for overall survival.

Immunohistochemistry. Immunohistochemical studies were performed on 5-um sections. Archived blocks were stored in a climate-controlled environment. All staining was performed immediately after sectioning to maintain maximum antigenicity for detection. Tissue sections were deparaffinized and rehydrated, and antigen retrieval was carried out with 0.01M citrate buffer, pH 6.0, for slides to be stained for IRS-1, or 0.001M EDTA, pH 8.0, for slides to be stained for IRS-2, and heating in a 770-W microwave oven for 14 minutes. The slides were stained on the Dako Autostainer (Dako, Carpinteria, CA) using EnVision+ (Dako) staining reagents. Tissue sections were blocked with Dual Endogenous Block for 10 minutes and then incubated for 30 minutes with either rabbit polyclonal IRS-1 (C20, Santa Cruz, Santa Cruz, CA) at a concentration of 1:400 or rabbit monoclonal IRS-2 (1849, Epitomics, Burlingame, CA) at a concentration of 1:400. Following a buffer wash, sections were incubated with the EnVision+ Dual Link detection reagent for 30 minutes and then treated with a solution of diaminobenzidine and hydrogen peroxide for 10 minutes to produce the visible brown pigment. DAB Enhancer was used to enrich the final color. The tissue sections were counterstained with hematoxylin, dehydrated, and coverslipped using a permanent mounting medium.

Sections were evaluated for staining pattern using the following criteria: 1) Diffuse staining was defined as even staining throughout the cytoplasm with no clear demarcation of cell borders; 2) Punctate staining was defined as clearly demarcated puncta of staining within the cytoplasm of each cell with or without diffuse background staining of the cytoplasm; 3) Membrane staining was defined as clear demarcation of cell borders by staining with or without diffuse background staining of the cytoplasm. The individual assessing staining patterns was blinded to all prognostic and follow-up data. A second blinded individual assessed a subset of 30 cases for IRS-2 staining patterns with 93.3% concordance. In addition, a subset of the tumors was evaluated using a different antibody that recognizes IRS-2 to confirm the observed staining patterns. The tissue microarray was evaluated using the same criteria that were used for the tumor sections. Three cores per patient were evaluated, and the membrane staining pattern was designated if it was contained in any of the three cores per patient sample.

Imaging. Stained tumor sections were viewed on an Olympus BX41 light microscope (Olympus, Center Valley, PA). Photomicrographs were obtained using an Evolution MPColor camera (Media Cybernetics, Bethesda, MD).

Immunoblotting. Cells were solubilized at 4°C in RIPA buffer, and cell extracts containing equivalent amounts of protein were resolved by SDS-PAGE and transferred to nitrocellulose filters. For samples requiring cytoplasmic/nuclear fractionation, the NE-PER kit (Pierce, Rockford, IL) was used according to the manufacturer's instructions.

The filters were blocked for 1 h with a 50 mM Tris buffer, pH 7.5, containing 0.15 M NaCl, 0.05% Tween 20, and 5% (wt/vol) dry milk, incubated overnight at 4°C in the same buffer containing primary antibodies and then incubated for 1 h in blocking buffer containing peroxidase-conjugated secondary antibodies. Proteins were detected by enhanced chemiluminescence (Pierce). The following antibodies were used for immunoblotting: IRS-1 (#C20, Santa Cruz), IRS-2 (#420293, Calbiochem, Gibbstown, NJ; #1849, Epitomics), GAPDH (#A300-642A, Bethyl, Montgomery, TX), hnRNP A1 (#4B10, Santa Cruz), peroxidase-conjugated goat anti-rabbit IgG (Jackson, West Grove, PA), peroxidase-conjugated goat anti-mouse IgG (Jackson).

Cell lines, shRNA, and transfection. The MDA-MB-231 cell line was obtained from the ATCC Cell Biology Collection. A lentiviral vector containing a small hairpin RNA (shRNA) targeting IRS-2 was obtained from Open Biosystems (Huntsville, AL). MDA-MB-231 cells were infected with virus and stably expressing cells were selected by the addition of 2 ug/mL puromycin. For IHC analysis, cells were pelleted and fixed in 10% zinc formalin before embedding in paraffin blocks.

Statistical analysis. Overall survival was measured from the date of first cancer diagnosis to the date of death from any cause and was censored from the date of last follow-up for survivors. Data for age, tumor size, node status, grade, ER status, PR status, HER2 status, and therapy were obtained as baseline variables. Therapy was defined as any combination of chemotherapy, radiation, or tamoxifen. As most samples

were surgical specimens, surgery was not included. Overall survival was estimated by the Kaplan-Meier method and assessed by the use of log-rank test for univariate analysis. We used the Cox proportional-hazard model to assess and control the simultaneous contribution of baseline covariates in multivariable analyses. First, we estimated the effect of IRS-2 within each individual dataset in the multivariable analysis. We then combined the two datasets in a proportional hazards model that tested for heterogeneity in the effect estimates from the two datasets by the inclusion of multiplicative terms involving the study indicator. The pooled results from the two datasets were presented if there was no significant heterogeneity of the effects for IRS-2 variables. A two-sided p-value of <0.05 was considered to indicate statistical significance. The REMARK criteria were used for this study [142].

RESULTS

IRS staining in normal breast tissue and benign breast disease

Twenty cases from the pathology archives were reviewed to identify all normal and pathological findings. Five cases were found to contain normal ducts. In total, 22 benign lesions were identified in the tissue set. The tissue set was evaluated by IHC for IRS-1 and IRS-2 expression. The IRS-1 antibody used in this study has been characterized in previous studies and stained pancreatic islet cells as expected [139, 143, 144] (Figure 2.1c). We evaluated the specificity of the IRS-2 antibody by staining MDA-MB-231 cells that expressed an IRS-2-specific shRNA to suppress IRS-2 expression. Trypsinized cells were spun down and the cell pellets fixed in zinc formalin, embedded in paraffin, and stained using the same IHC protocol that was used for staining the tissue sections. Parental MDA-MB-231 cells stained positive for IRS-2, and this staining was diminished significantly when IRS-2 expression was suppressed (Figure 2.1a). The antibody also exhibited specificity for IRS-2 by immunoblot (Figure 2.1b). As a positive control, pancreatic islets stained positive for IRS-2 using this antibody (Figure. 2.1c).

All five cases containing normal ducts exhibited nuclear IRS-1 staining in the luminal epithelium (Figure 2.2). 4 of 5 cases also exhibited fine, punctate IRS-1 staining in the cytoplasm in the myoepithelial (basal) cells. IRS-2 was expressed strongly in the myoepithelial cells of the normal ducts, and in 4 of 5 cases it was also expressed diffusely in the cytoplasm of the luminal epithelium (Figure 2.2). However, one case exhibited punctate cytoplasmic staining for IRS-2 in the luminal epithelium, and one case exhibited

Figure 2.1. Analysis of IRS-2 antibody specificity

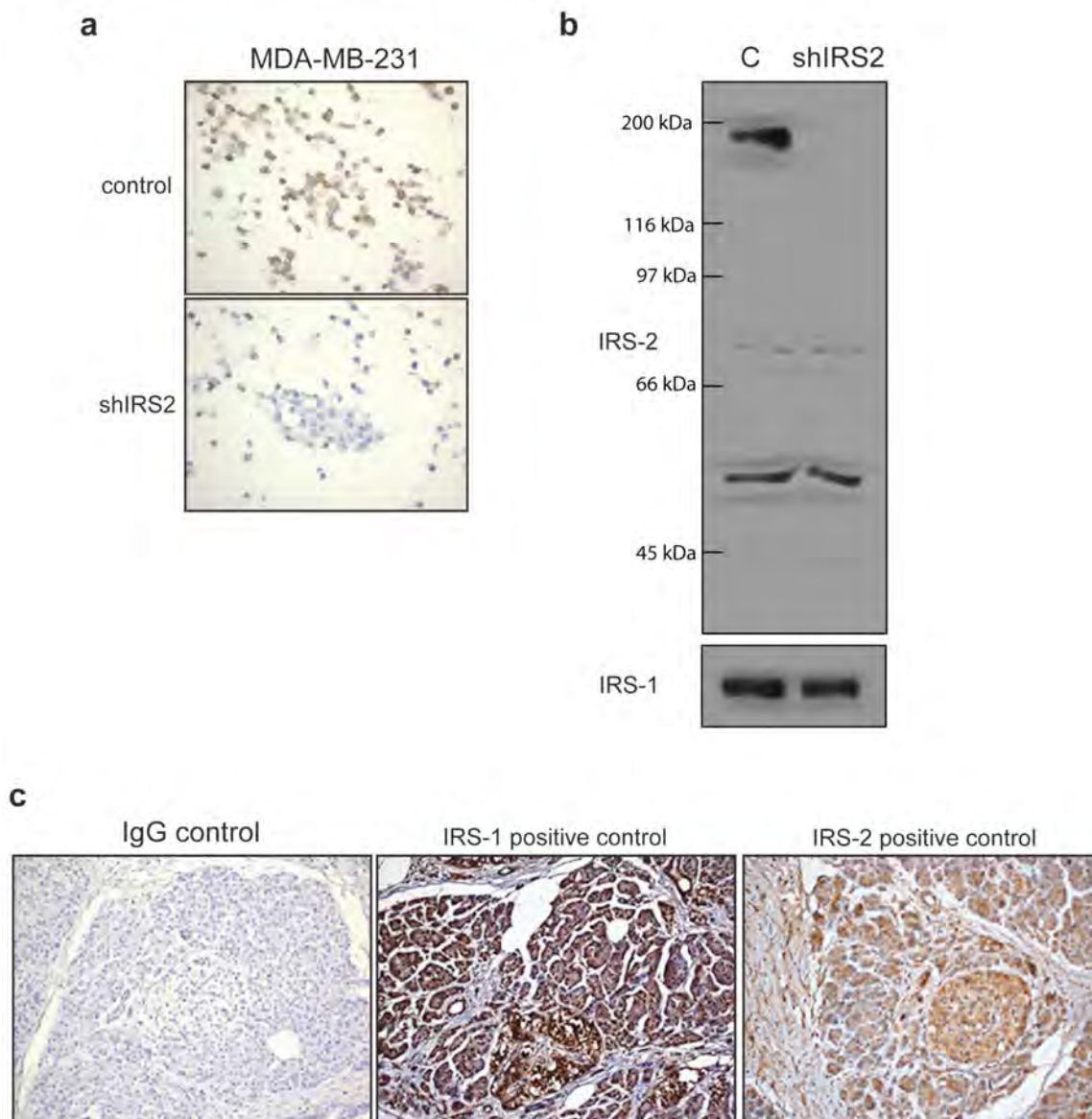


Figure 2.1. Analysis of IRS-2 antibody specificity. **(a)** MDA-MB-231 cells (control) and MDA-MB-231 cells expressing an IRS-2-specific shRNA (shIRS2) were fixed in formalin and embedded in paraffin. Sections were stained by IHC using an IRS-2-specific antibody (#1849, Epitomics). Magnification 20x. **(b)** Aliquots of cell lysates from MDA-MB-231 cells (C) and MDA-MB-231 cells expressing an IRS-2-specific shRNA (shIRS2) were immunoblotted for IRS-2 (#1849, Epitomics) and IRS-1 (#C20, Santa Cruz). **(c)** Immunohistochemical staining of human pancreas with rabbit IgG, IRS-1 (#C20, Santa Cruz), and IRS-2 (#1849, Epitomics). Magnification 40x.

Figure 2.2. IRS expression in normal human breast tissue and benign breast lesions

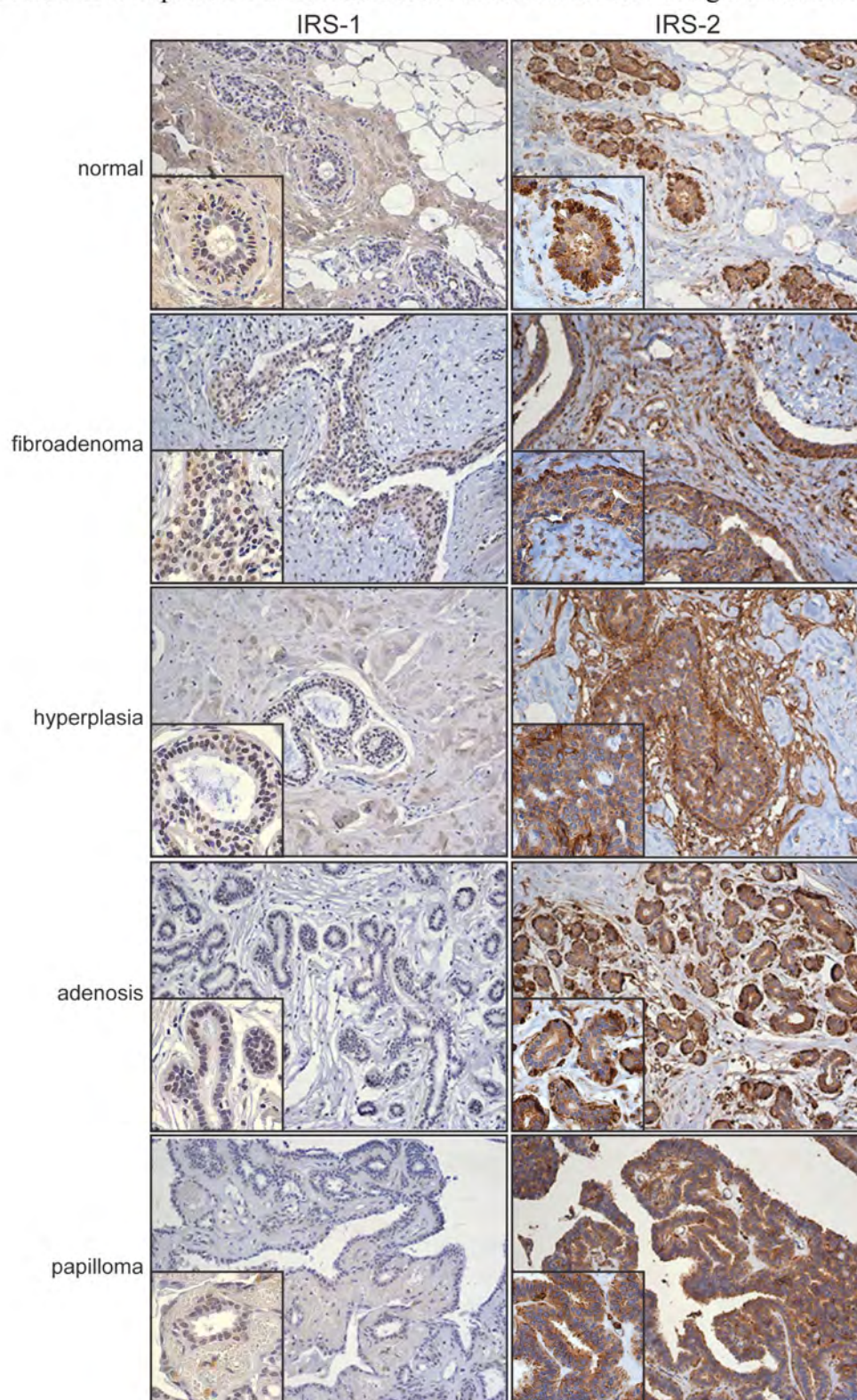


Figure 2.2. IRS expression in normal human breast tissue and benign breast lesions. Representative images of IRS-1 and -2 staining in normal ducts, fibroadenoma, usual ductal hyperplasia, sclerosing adenosis, and intraductal papilloma. Magnification 20x for large images, 40x for insets.

staining at the membrane in addition to diffuse cytoplasmic staining. IRS-2 was not expressed in the nuclei of either the myoepithelial or luminal epithelial cells of normal ducts.

Twenty-two benign lesions were examined consisting of the following: 6 fibroadenomas, 7 cases of ductal hyperplasia (6 of the usual type, 1 of the atypical type), 7 cases of sclerosing adenosis, and 2 intraductal papillomas. Representative images of each type are shown in Figure 2.2. Two cases were negative altogether for IRS-1 staining, including one case of sclerosing adenosis and the atypical ductal hyperplasia. The majority of the benign lesions (77.3%) demonstrated positive nuclear staining for IRS-1 (Figure 2.2), and 20 of 22 cases also exhibited punctate IRS-1 staining of the myoepithelial cells. All of the benign lesions exhibited diffuse cytoplasmic IRS-2 expression in the luminal epithelium, with two cases each demonstrating additional membrane or punctate staining of luminal cells. Strong cytoplasmic IRS-2 staining was also observed in the myoepithelial cells of the benign lesions.

IRS expression patterns in invasive ductal carcinoma

IRS expression was evaluated in 157 invasive ductal carcinoma tumor sections from the pathology archives. This tumor set consisted of the following: grade 1 (21 tumors), grade 2 (39 tumors), and grade 3 (97 tumors). Detailed clinical information was available for a subset of these tumors (128 tumors), and the clinical characteristics of this tumor subset are shown in Table 2.1 (Set 1). Consistent with our findings in normal and

Table 2.1. Clinical characteristics of tumor datasets

	Set 1 <i>n</i> = 128	Set 2 <i>n</i> = 130	p-value
Age (years), No. (%)			
≤50	42 (34.1)	35 (26.9)	0.21
>50	81 (65.9)	95 (73.1)	
unknown	5	-	
Median age (years)	57	60	0.75
Tumor size (stage), No. (%)			
1	72 (57.6)	69 (53.9)	0.57
2	46 (36.8)	46 (35.9)	
3	6 (4.8)	10 (7.8)	
4	1 (0.8)	3 (2.3)	
unknown	3	2	
Node status (stage), No. (%)			
0	50 (48.1)	58 (51.8)	0.64
1	36 (34.6)	32 (28.6)	
2	9 (8.65)	14 (12.5)	
3	9 (8.65)	8 (7.1)	
unknown	24	18	
Grade, No. (%)			
1	17 (13.7)	12 (9.8)	<0.0001
2	21 (16.9)	54 (44.3)	
3	86 (69.4)	56 (45.9)	
unknown	4	8	
Estrogen receptor, No. (%)			
negative	52 (41.6)	42 (34.4)	0.25
positive	73 (58.4)	80 (65.6)	
unknown	3	8	
Progesterone receptor, No. (%)			
negative	40 (32.5)	56 (45.5)	0.04
positive	83 (67.5)	67 (54.5)	
unknown	5	7	
HER2, No. (%)			
negative	79 (62.7)	90 (73.2)	0.08
positive	47 (37.3)	33 (26.8)	
unknown	2	7	
IRS-2 staining pattern			
membrane	42 (33.9)	19 (14.7)	0.001
diffuse	49 (39.5)	72 (55.8)	
punctate	33 (26.6)	38 (29.5)	
unknown	4	1	
Adjuvant therapy			
any	90	108	0.23
none	9	18	
unknown	29	4	
Median follow-up for recurrence free survival (months)	69.5	80.0	<0.001
Median follow-up for overall survival (months)	72.5	104.4	<0.001

benign breast tissue and previously published results, IRS-1 was expressed in the nuclei and cytoplasm of invasive tumors (Figure 2.3a) [136, 139, 140]. IRS-2 was not expressed in the nucleus in any of the invasive tumors (Figure 2.3a). Analysis of SUM-159PT and MDA-MB-231 breast carcinoma cells after fractionation into cytoplasmic and nuclear fractions confirmed the nuclear localization patterns of IRS-1 and IRS-2 in the human tumors. IRS-1 was localized in both the nucleus and cytoplasm in both cell lines, while IRS-2 was localized only in the cytoplasm (Figure 2.3b).

Upon further analysis of the IRS-2 staining in the invasive tumors, three distinct staining patterns were observed: diffuse cytoplasmic staining (diffuse; Figure 2.4a), punctate cytoplasmic staining (punctate; Figure 2.4b), and membrane staining (membrane; Figure 2.4c). While diffuse cytoplasmic staining was the dominant IRS-2 staining pattern in normal ducts and benign lesions, punctate and membrane staining patterns increased in tumors. This alteration in IRS-2 staining patterns during malignant progression was demonstrated in one case in which normal ducts, ductal carcinoma *in situ* (DCIS), and invasive tumor were all present. IRS-2 staining of the normal ductal epithelium was diffusely cytoplasmic, whereas membrane staining was observed in the adjacent DCIS and invasive tumor (Figure 2.4j).

To confirm the IRS-2 staining patterns in a second tumor set, we evaluated a tissue microarray from a separate institution containing 130 new patient cases. The clinical characteristics of this tumor subset are summarized in Table 2.1 (Set 2). The

Figure 2.3. IRS expression in human breast tumors and cell lines

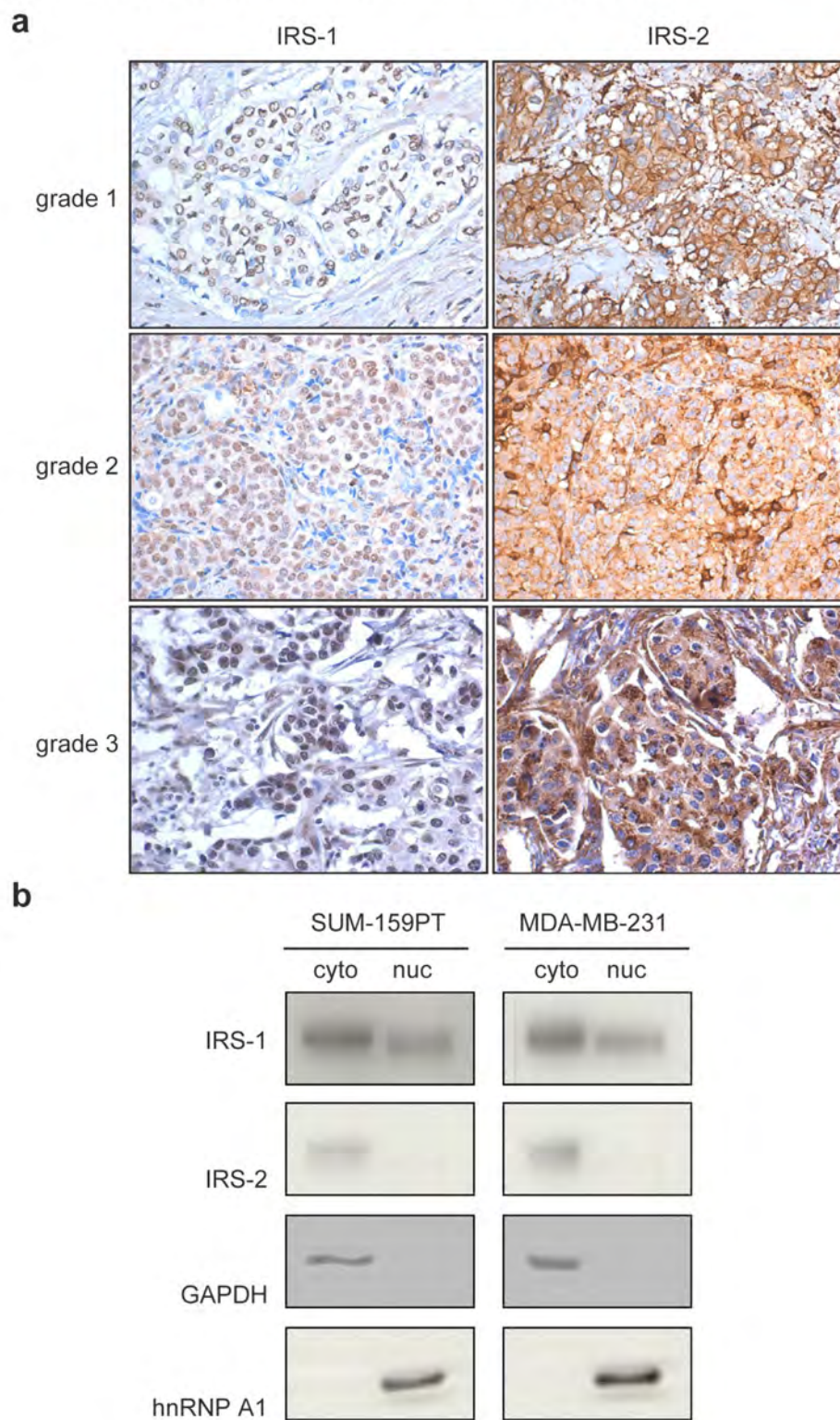


Figure 2.3. IRS expression in human breast tumors and cell lines. **(a)** Representative images of IRS-1 and -2 staining in grade 1, grade 2, and grade 3 breast tumors. Magnification 40x for all images. **(b)** Cytoplasmic (cyto) and nuclear (nuc) fractions from SUM-159PT and MDA-MB-231 breast carcinoma cells were immunoblotted with antibodies specific for IRS-1, IRS-2, GAPDH (cytoplasmic control) and hnRNP A1 (nuclear control).

Figure 2.4. IRS-2 localization in human breast tumors

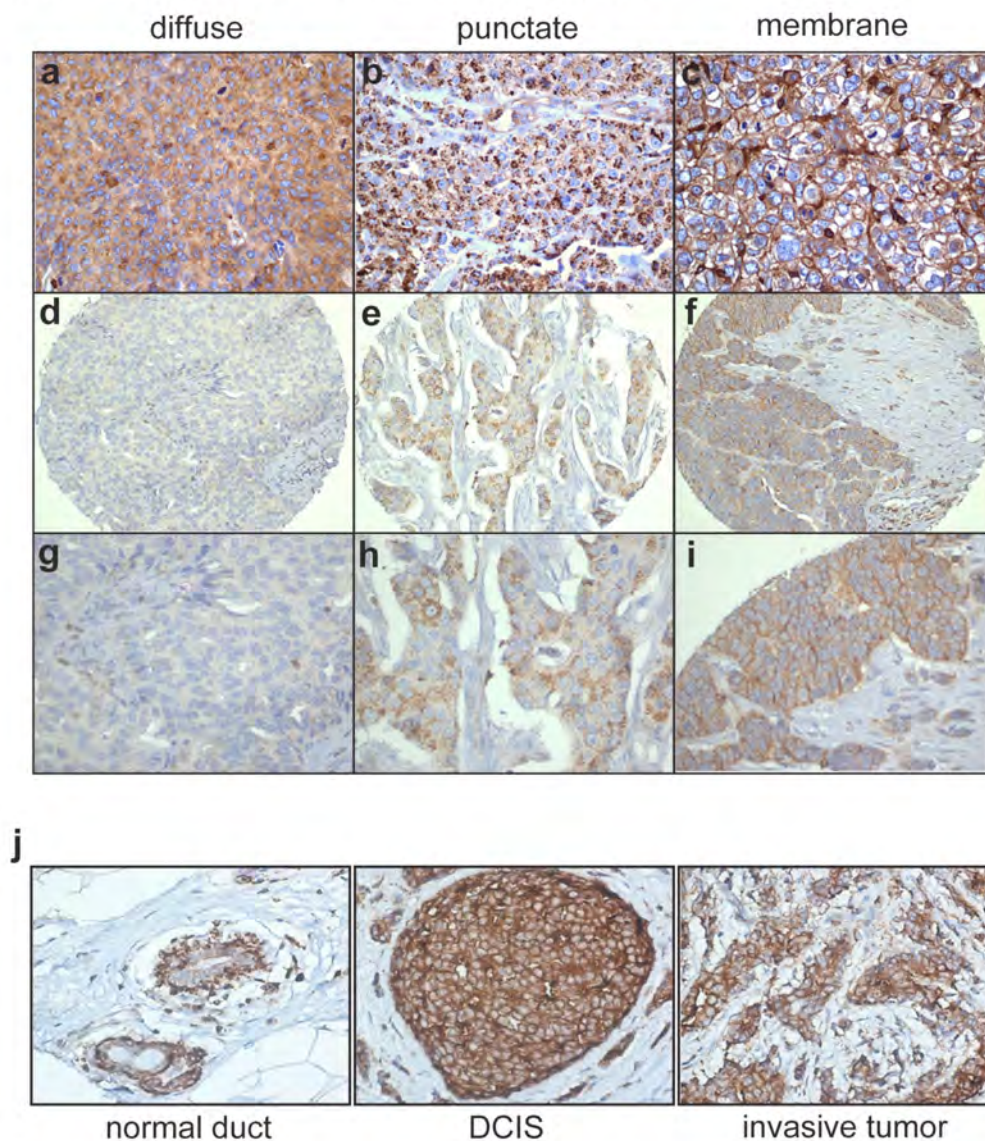


Figure 2.4. IRS-2 localization in human breast tumors. (a-c) Representative images showing diffuse, punctate, and membrane IRS-2 staining patterns in breast tumors. Magnification 40x for all images. (d-i) Representative images from the tissue microarray showing diffuse, punctate, and membrane IRS-2 staining patterns in breast tumor cores. Magnification 20x (d-f), 40x (g-i). (j) IRS-2 staining in a normal duct, adjacent DCIS, and invasive tumor within the same tissue section.

microarray was stained for IRS-2 by IHC and evaluated by the same individual who evaluated Set 1. All three IRS-2 staining patterns were observed (Figure 2.4), although in different percentages than were observed for Set 1. This may reflect the differences in the distribution of tumors by grade in the two individual datasets (Table 2.1).

Correlations with clinical and pathological characteristics

The two datasets were analyzed individually and then pooled for the association of IRS-2 staining patterns with survival outcomes. Clinical parameters and overall survival trends for the pooled dataset are presented in Table 2.2. Initially, survival data were analyzed for the tumor subset defined as Set 1 in Table 2.1, and correlations were drawn to IRS-2 staining pattern. Although not statistically significant, a trend toward decreased overall survival with IRS-2 membrane staining was noted on the initial univariate analysis. This trend became statistically significant in the follow-up multivariate analysis when the dataset was adjusted for confounders such as grade, tumor size, node status, receptor status, and therapy (HR = 4.61, 95%CI 1.35-15.71, $p = 0.02$) (Table 2.3 and Figure 2.5a). No statistically significant associations with overall survival were observed for the diffuse or punctate staining patterns in either the univariate or multivariate analysis (Table 2.4, Figures 2.6a and 2.7a). In the analysis of recurrence-free survival, the effect estimates for IRS-2 staining patterns were similar in direction and magnitude as those found in the analysis of overall survival.

Table 2.2. Survival analysis of clinical parameters in the two datasets

	Univariate ^a	Multivariate ^c		
	p-value	HR ^b	95% CI	p-value
Tumor size (stage)				
1	<0.0001	1.00	---	<0.001
2		2.12	1.28-3.51	
3		5.78	2.66-12.56	
4		4.39	1.18-16.39	
Node status (stage)				
0	<0.0001	1.00	---	0.03
1		1.95	1.13-3.38	
2		2.67	1.30-5.49	
3		1.73	0.76-3.95	
Grade				
1	0.11	1.00	---	0.07
2		0.82	0.35-1.92	
3		1.72	0.70-4.24	
Adjuvant therapy				
any	0.02	1.00	---	
none		2.64	1.25-5.59	0.01
unknown		1.77	0.74-4.25	0.20
Estrogen receptor (ER)				
negative	0.11	1.00	---	0.14
positive		1.62	0.86-3.06	
Progesterone receptor (PR)				
negative	0.002	1.00	---	
positive		0.41	0.23-0.74	0.003
HER2 receptor				
negative	0.21	1.00	---	
positive		0.85	0.51-1.40	0.51

Table 2.2. ^aUnivariate p-values were obtained from the log rank test. ^bHazard ratios shown were adjusted for age (as a continuous variable) and study, as well as other core clinical variables (as categorical variables) shown in the table, including tumor size, node status, grade, adjuvant therapy, ER, PR, and HER2. ^cP-values for tumor size, stage, and grade in multivariate analysis were obtained by treating each, in turn, as an ordered variable while adjusting for other covariates as categorical variables.

Table 2.3. Survival analysis for IRS-2 staining patterns

Set 1 only (n = 128)	Univariate	Multivariate		
	p-value	HR	95% CI	p-value
IRS-2 staining pattern ^a				
membrane	0.69	1.00	---	---
diffuse		0.25	0.07-0.87	0.03
punctate		0.14	0.03-0.72	0.02
IRS-2 membrane staining ^a				
negative	0.43	1.00	---	---
positive		4.61	1.35-15.71	.02
Membrane staining (PR ⁻ only) ^{a,b}				
negative	0.04	1.00	---	---
positive		18.69	1.26-276.47	0.03
PR/membrane ^a				
PR ⁻ /membrane ⁻	0.03	1.00	---	---
PR ⁺ /membrane ⁻		0.97	0.20-4.70	0.97
PR ⁻ /membrane ⁺		4.59	0.98-21.62	0.054
PR ⁺ /membrane ⁺		4.52	0.44-46.90	0.21
Set 2 only (n = 130)				
IRS-2 staining pattern ^a				
membrane	0.58	1.00	---	---
diffuse		0.48	0.19-1.21	0.12
punctate		0.70	0.26-1.90	0.48
IRS-2 membrane staining ^a				
negative	0.29	1.00	---	---
positive		1.94	0.80-4.71	0.14
Membrane staining (PR ⁻ only) ^{a,c}				
negative	0.85	1.00	---	---
positive		5.72	1.44-22.65	0.01
PR/membrane ^a				
PR ⁻ /membrane ⁻	0.021	1.00	---	---
PR ⁺ /membrane ⁻		0.37	0.18-0.79	0.01
PR ⁻ /membrane ⁺		3.06	0.96-9.78	0.06
PR ⁺ /membrane ⁺		0.42	0.09-1.88	0.26
Pooled (n = 258)				
IRS-2 staining pattern ^a				
membrane	0.57	1.00	---	---
diffuse		0.43	0.22-0.82	0.01
punctate		0.52	0.26-1.05	0.07
IRS-2 membrane staining ^a				
negative	0.31	1.00	---	---
positive		2.20	1.20-4.06	0.01
Membrane staining (PR ⁻ only) ^{a,d}				
negative	0.30	1.00	---	---
positive		6.15	2.25-16.80	<0.001
PR/membrane ^a				
PR ⁻ /membrane ⁻	0.010	1.00	---	---
PR ⁺ /membrane ⁻		0.53	0.28-0.99	0.05
PR ⁻ /membrane ⁺		3.36	1.58-7.16	0.002
PR ⁺ /membrane ⁺		0.60	0.20-1.84	0.37

Table 2.3. ^aMultivariate results were obtained from a model that adjusted for the core covariates including age, study (for the combined analysis), tumor size, node status, grade, adjuvant therapy, ER, PR, and HER2. The results for IRS-2 staining pattern and IRS-2 membrane staining were obtained from separate models adjusting for the same set of the core covariates. ^bn = 40, Set 1 contained only 29 PR⁻ cases which had all covariates. ^cn = 56 ^dn = 96

Figure 2.5. Analysis of IRS-2 staining patterns, progesterone receptor status, and overall survival

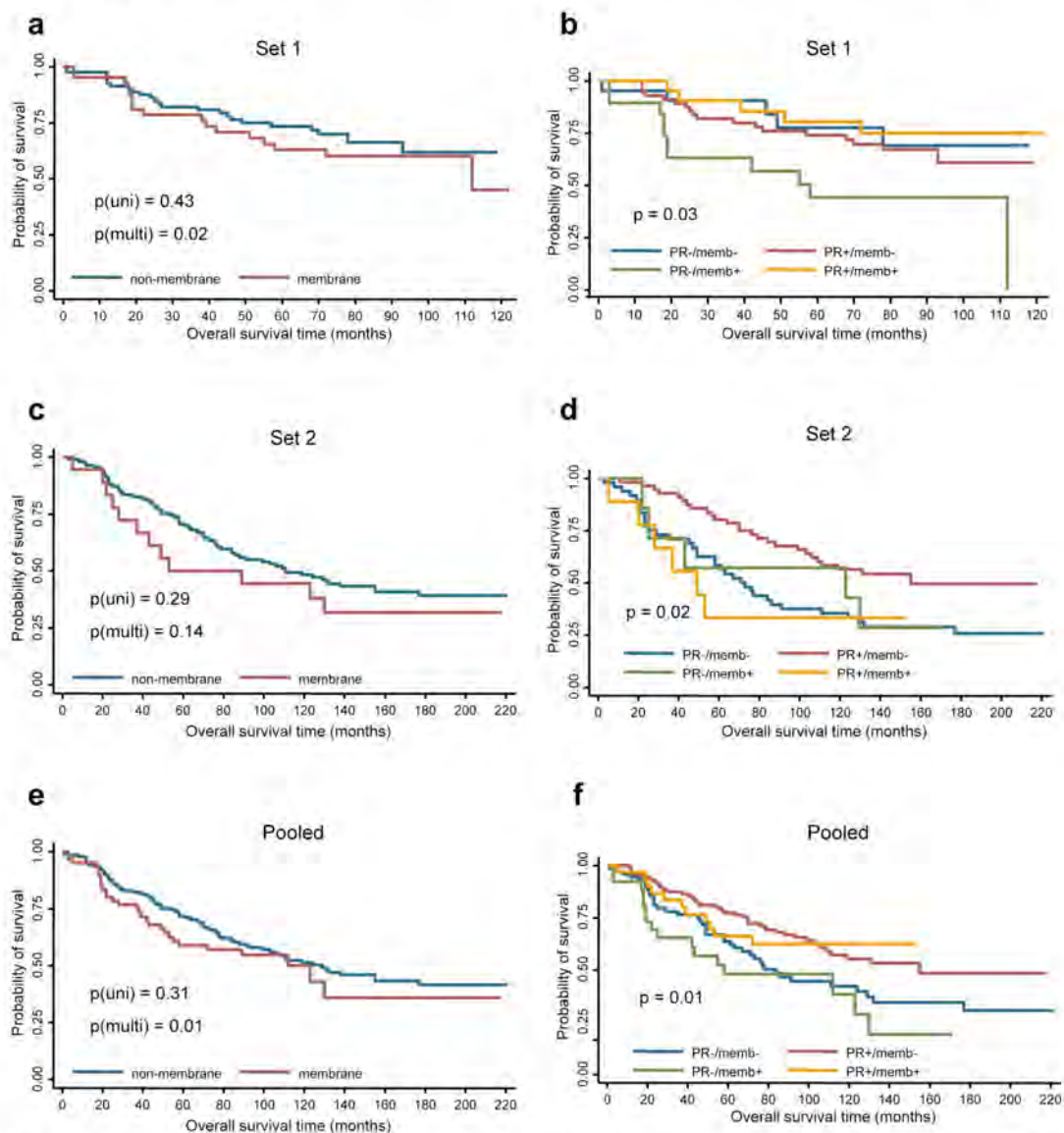


Figure 2.5. Analysis of IRS-2 staining patterns, progesterone receptor status, and overall survival. **(a, c, e)** Kaplan-Meier survival curves showing overall survival (OS) in Set 1 **(a)**, Set 2 **(c)**, and the Pooled Set **(e)** for patients with tumors exhibiting IRS-2 staining at the membrane compared with non-membrane IRS-2 staining. P-values for both univariate and multivariate analyses are shown. **(b, c, f)** Kaplan-Meier survival curves showing OS in tumors from Set 1 **(b)**, Set 2 **(d)**, and the Pooled Set **(f)** as a function of both progesterone receptor (PR) and IRS-2 membrane staining status. P-values based on univariate analysis.

Table 2.4. Survival analysis for diffuse and punctate IRS-2 staining patterns

Set 1 only (n = 128)	Univariate	Multivariate		
	p-value	HR	95% CI	p-value
IRS-2 diffuse staining				
negative	0.85	1.00		
positive		0.68	0.27-1.75	0.43
Diffuse staining (PR ⁻ only) ^{a,b}				
negative	0.63	1.00		
positive		1.14	0.08-15.58	0.92
IRS-2 diffuse staining				
PR ⁻ /diffuse ⁻	0.40	1.00		
PR ⁻ /diffuse ⁻		0.47	0.11-2.05	0.31
PR ⁻ /diffuse ⁺		0.63	0.14-2.84	0.54
PR ⁺ /diffuse ⁺		0.34	0.10-1.21	0.10
IRS-2 punctate staining				
negative	0.47	1.00		
positive		0.49	0.16-1.48	0.20
Punctate staining (PR ⁻ only) ^{a,b}				
negative	0.06	1.00		
positive		0.00	0.00-∞	1.00 ^c
PR/punctate				
PR ⁻ /punctate ⁻	0.09	1.00	---	---
PR ⁻ /punctate ⁻		0.33	0.11-1.03	0.06
PR ⁻ /punctate ⁺		0.00	0.00-∞	1.00 ^c
PR ⁺ /punctate ⁺		0.32	0.08-1.37	0.13
Set 2 only (n = 130)				
IRS-2 diffuse staining				
negative	0.92	1.00		
positive		0.64	0.35-1.18	0.15
Diffuse staining (PR ⁻ only) ^{a,d}				
negative	0.94	1.00		
positive		0.31	0.12-0.78	0.01
IRS-2 diffuse staining				
PR ⁻ /diffuse ⁻	0.08	1.00		
PR ⁺ /diffuse ⁻		0.17	0.06-0.51	0.002
PR ⁻ /diffuse ⁺		0.41	0.19-0.92	0.03
PR ⁺ /diffuse ⁺		0.19	0.07-0.50	0.001
IRS-2 punctate staining				
negative	0.68	1.00		
positive		1.38	0.71-2.67	0.34
Punctate staining (PR ⁻ only) ^{a,d}				
negative	0.95	1.00		
positive		1.86	0.72-4.81	0.20
PR/punctate				
PR ⁻ /punctate ⁻	0.07	1.00	---	---
PR ⁻ /punctate ⁻		0.39	0.18-0.85	0.02
PR ⁻ /punctate ⁺		1.69	0.73-3.91	0.22
PR ⁺ /punctate ⁺		0.42	0.15-1.17	0.10
Pooled (n = 258)				
IRS-2 diffuse staining				
negative	0.96	1.00		
positive		0.67	0.42-1.09	0.11
Diffuse staining (PR ⁻ only) ^{a,e}				
negative	0.93	1.00		
positive		0.38	0.18-0.81	0.01

PR/diffuse				
PR ⁻ /diffuse ⁻	0.02	1.00	---	---
PR ⁺ /diffuse ⁻		0.24	0.11-0.54	0.001
PR ⁻ /diffuse ⁺		0.45	0.24-0.85	0.02
PR ⁺ /diffuse ⁺		0.25	0.12-0.53	<0.001
IRS-2 punctate staining				
negative	0.47	1.00		
positive		0.99	0.59-1.67	0.98
Punctate staining (PR ⁻ only) ^{a,c}				
negative	0.38	1.00		
positive		1.03	0.45-2.34	0.95
PR/punctate				
PR ⁻ /punctate ⁻	0.02	1.00	---	---
PR ⁺ /punctate ⁻		0.43	0.23-0.79	0.007
PR ⁻ /punctate ⁺		1.09	0.51-2.36	0.82
PR ⁺ /punctate ⁺		0.39	0.18-0.87	0.02

Table 2.4. ^aMultivariate results were obtained from a model that adjusted for the core covariates including age, study (for the combined analysis), tumor size, node status, grade, adjuvant therapy, ER, PR, and Her-2. The results for IRS-2 staining pattern and IRS-2 diffuse or punctate staining were obtained from separate models adjusting for the same set of the core covariates. ^bn = 40, Set 1 contained only 29 PR⁻ cases which had all covariates. ^cModel fitting did not converge due to sparse data. ^dn = 56 ^en = 96

Figure 2.6. Analysis of IRS-2 diffuse staining pattern, progesterone receptor status, and overall survival

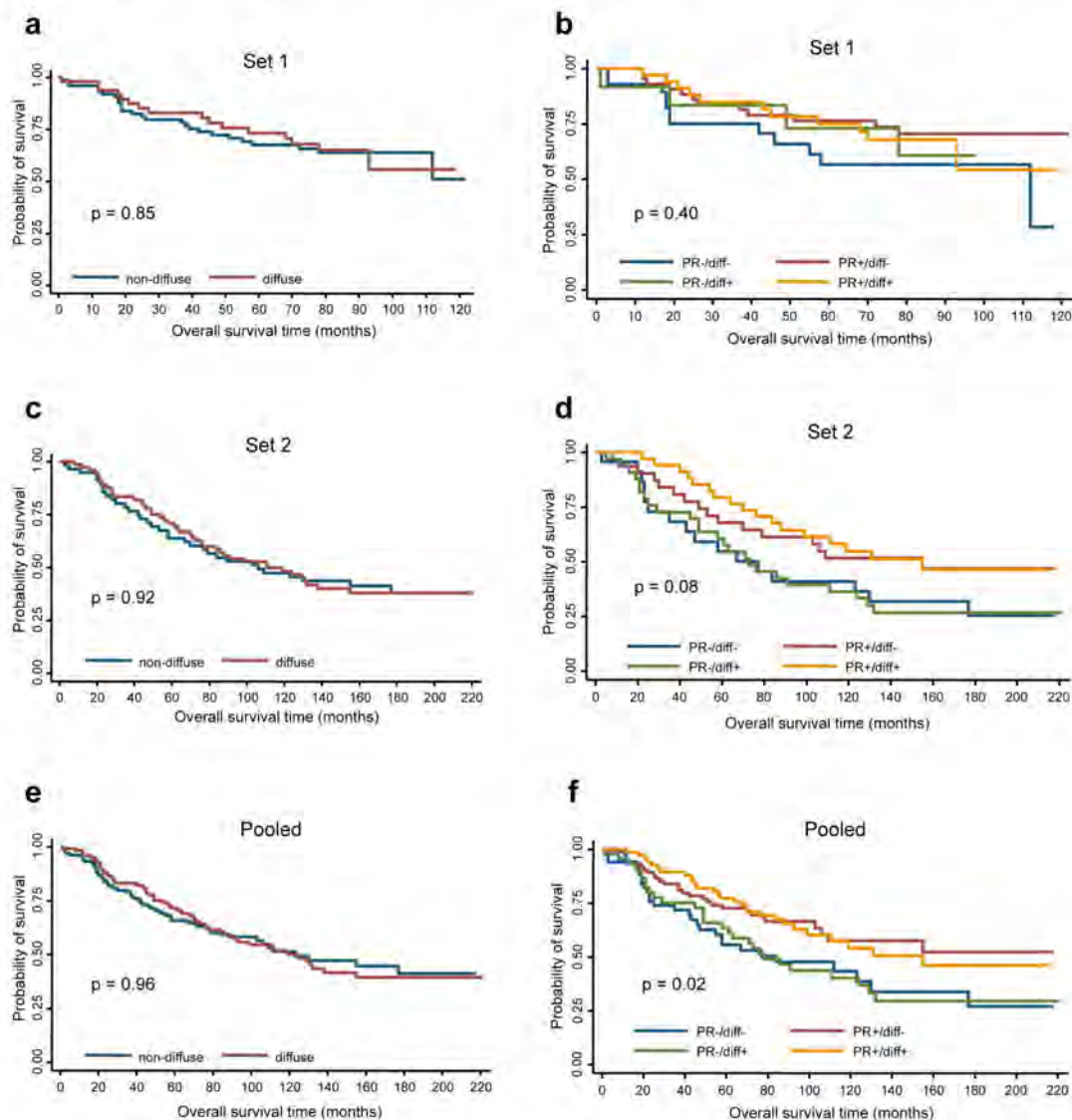


Figure 2.6. Analysis of IRS-2 diffuse staining pattern, progesterone receptor status, and overall survival. **(a, c, e)** Kaplan-Meier survival curves showing overall survival (OS) in Set 1 **(a)**, Set 2 **(c)**, and the Pooled Set **(e)** for patients with tumors exhibiting IRS-2 diffuse staining compared with non-diffuse IRS-2 staining. P-values for both univariate and multivariate analyses are shown. **(b, c, f)** Kaplan-Meier survival curves showing OS in tumors from Set 1 **(b)**, Set 2 **(d)**, and the Pooled Set **(f)** as a function of both progesterone receptor (PR) and IRS-2 diffuse staining status. P-values based on univariate analysis.

Figure 2.7. Analysis of IRS-2 punctate staining pattern, progesterone receptor status, and overall survival

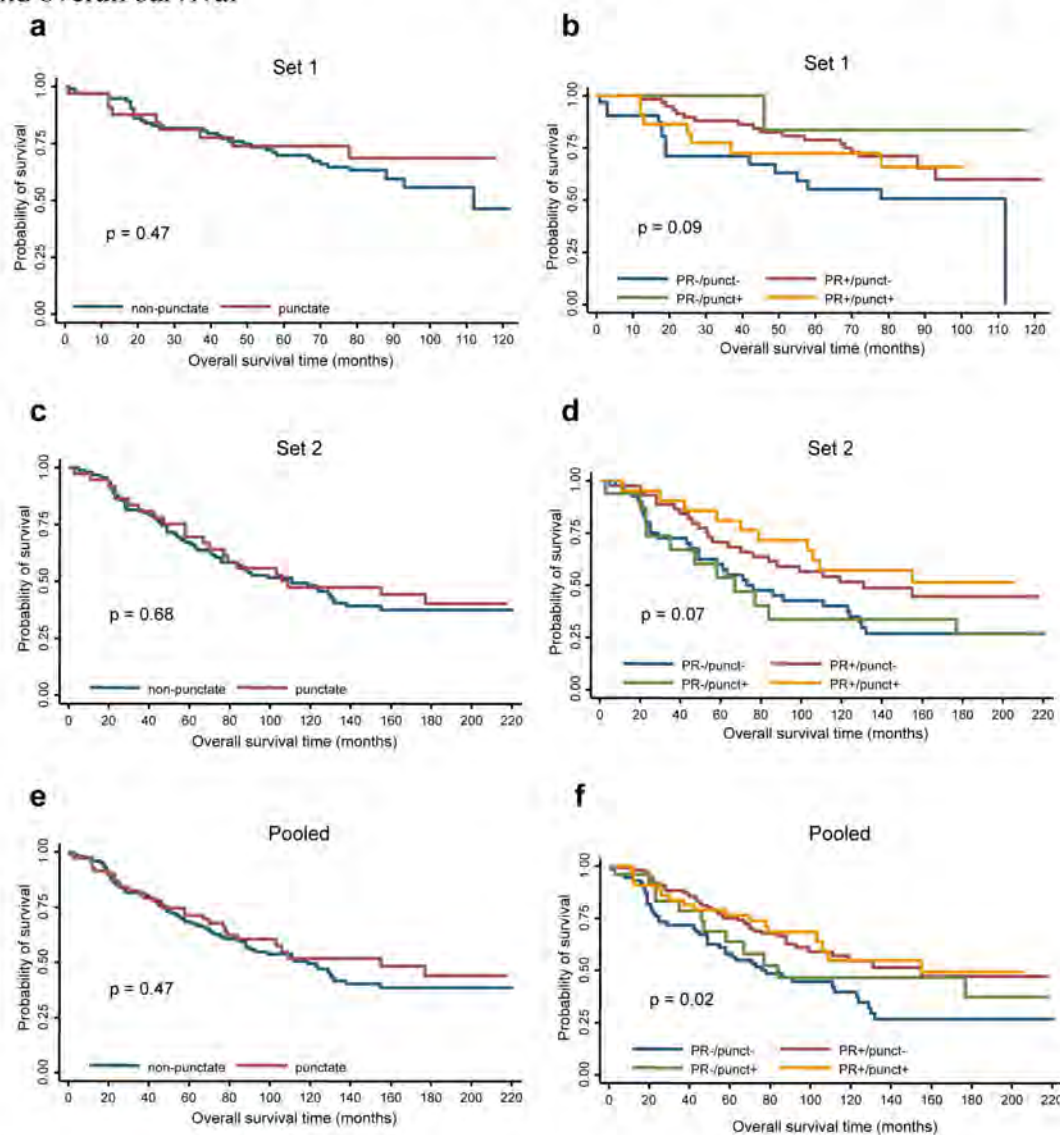


Figure 2.7. Analysis of IRS-2 punctate staining pattern, progesterone receptor status, and overall survival. (a, c, e) Kaplan-Meier survival curves showing overall survival (OS) in Set 1 (a), Set 2 (c), and the Pooled Set (e) for patients with tumors exhibiting IRS-2 punctate staining compared with non-punctate IRS-2 staining. P-values for both univariate and multivariate analyses are shown. (b, c, f) Kaplan-Meier survival curves showing OS in tumors from Set 1 (b), Set 2 (d), and the Pooled Set (f) as a function of both progesterone receptor (PR) and IRS-2 punctate staining status. P-values based on univariate analysis.

The effect of IRS-2 membrane pattern on overall survival was analyzed within each clinical parameter individually. From this analysis, the only clinical parameter to show a significant association with IRS-2 localization at the membrane was PR negative (PR-) status. Univariate analysis revealed that patients with tumors that were PR- and stained positive for IRS-2 at the membrane had significantly worse survival outcomes when compared with patients with tumors that were PR- but did not have IRS-2 membrane staining ($p = 0.04$). To examine further the association of IRS-2 membrane staining and PR expression with regard to patient survival, the data were analyzed by PR status together with IRS-2 membrane staining status. As shown in Figure 2.5b, decreased survival was observed only in the PR- tumors that exhibited IRS-2 membrane staining ($p = 0.03$). Expression of IRS-2 at the membrane did not confer decreased survival in patients with tumors that expressed PR ($p = 0.40$).

Statistical analysis of the tissue microarray dataset (Set 2) produced results consistent with the findings from Set 1 (Table 2.3, Figure 2.5c,d). Though not statistically significant, IRS-2 at the membrane nearly doubled risk of death. Among PR- tumors, membrane staining conferred a statistically significant, nearly six-fold decrease in overall survival on multivariate analysis ($p = 0.01$). When PR status and membrane staining were evaluated in combination, PR- tumors with membrane IRS-2 exhibited a decrease in overall survival compared to all other subtypes ($p = 0.021$), as we had observed for the original tumor dataset (Set 1).

The effect estimates for IRS-2 membrane staining were not statistically different between the two datasets: p-value from the heterogeneity test was 0.47 among all cases and 0.74 among PR- cases. When Sets 1 and 2 were analyzed as a pooled dataset with a total tumor number of 258, the observed trends from the individual datasets became even stronger (Table 2.3, Figure 2.5e,f). On multivariate analysis of the pooled dataset, tumors with IRS-2 at the membrane exhibited a significant decrease in overall survival ($p = 0.01$), and this trend was even more highly significant among PR- tumors ($p < 0.001$). As with each independent set, PR negative status in combination with the IRS-2 membrane staining pattern was associated with a significant decrease in overall survival compared to all other subtypes in the pooled dataset (HR = 3.36, 95%CI 1.58-7.16, $p = 0.002$, as compared to PR-/memb-).

The individual and pooled datasets were also analyzed for the effect of diffuse and punctate IRS-2 staining on overall survival of patients with PR- tumors (Table 2.4, Figures 2.6 and 2.7). On multivariate analysis, the diffuse staining pattern improved survival in patients with PR- tumors in the individual and pooled datasets, although not to the extent that PR+ status improved survival. These results were statistically significant only in Set 2 and the pooled dataset ($p = 0.03$ and 0.02 , respectively). In PR+ tumors, there was no further benefit of the diffuse staining pattern on overall survival rates. A significant effect on survival of combined punctate staining and PR status was observed upon univariate analysis in the pooled dataset only ($p = 0.02$). However, on multivariate analysis, this effect appears to be due to PR status alone.

DISCUSSION

In this study, we present the first report of IRS-2 expression in normal human breast and breast tumors. In the normal breast, IRS-2 is expressed strongly in the myoepithelial cell layer, with a lower level of diffuse cytoplasmic staining in the luminal epithelial cells. This expression pattern persists in benign breast disease. In invasive breast tumors, IRS-2 is localized in one of three staining patterns: diffusely cytoplasmic, punctate in the cytoplasm, and at the plasma membrane. IRS-2 is absent from the nucleus in both normal and tumor tissue. With regard to clinical relevance, IRS-2 membrane staining is associated with decreased overall survival of breast cancer patients. In addition, IRS-2 membrane staining identifies a sub-population of patients with PR-tumors that have significantly worse overall survival outcomes. Taken together, our results demonstrate that IRS-1 and IRS-2 have distinct intracellular localization patterns in human breast tumors, and they reveal a potential role for IRS-2 in the aggressive biology of PR- breast tumors.

Our observation that IRS-1 and IRS-2 are expressed in distinct intracellular compartments reveals a potential mechanism for their divergent roles in breast cancer [54]. The targeting of IRS-1 and IRS-2 to unique intracellular compartments would localize the signals that are generated and determine access of these adaptor proteins to distinct subsets of downstream effectors. As a result, different functional outcomes would occur. In the nucleus, IRS-1 interacts with ER- α and regulates its transcriptional activity [63]. IRS-1 can also interact with β -catenin, the androgen receptor, and upstream

binding factor-1 to positively regulate target gene expression [145, 146]. Regulation of genes such as Cyclin D and c-Myc is likely to contribute to the IRS-1-dependent stimulation of proliferation [145, 147]. In contrast, IRS-2 is excluded from the nucleus and instead can be found in the cytoplasm or at the cell membrane in many invasive breast carcinomas. The localization of IRS-2 at or near the cell membrane would provide access to downstream effectors that are involved in regulating dynamic adhesive and cytoskeletal rearrangements that are required for cell movement [148]. Membrane recruitment of IRS-2 would also localize its signaling to regulate the surface expression of glucose transporter 1 (GLUT1) to promote aerobic glycolysis [59].

Our finding that membrane localization of IRS-2 is associated with poor prognosis supports the hypothesis that IRS-2-mediated signaling promotes tumor progression and metastasis [53, 56-58]. Upon ligand stimulation, the IRS proteins are recruited to upstream receptors where they are phosphorylated on tyrosine residues and initiate signaling [33]. We hypothesize that IRS-2 at the cell membrane is more likely to be tyrosine phosphorylated and actively signaling than the population of IRS-2 that is diffusely expressed in the cytoplasm because the upstream activating receptors are present at the cell membrane. In support of this hypothesis, diffuse localization of IRS-2 was associated with improved survival outcomes in patients with PR- tumors in our study. The population of punctate IRS-2 may result from internalization of the adaptor proteins with surface receptors [149, 150]. However, the question of whether receptor internalization would enhance or attenuate signaling remains to be determined.

Generation of phospho-specific antibodies that can distinguish “active” from “in-active” IRS-2 will be necessary for future studies to confirm the functional status of the membrane, diffuse cytoplasmic, and punctate populations of IRS-2. It will also be important to investigate the expression and activity of upstream regulatory receptors, such as the IGF-1R or insulin receptor, to establish their connection with IRS-2 localization.

For tumors exhibiting membrane staining, those that are PR- demonstrate the worst overall survival outcomes. Loss of PR expression during disease progression, especially following endocrine therapy, is associated with decreased survival [151-154]. In general, loss of PR expression is indicative of a more aggressive tumor behavior. To date, a biological explanation for the increased aggressiveness associated with PR- tumors has not been fully elucidated. The loss of PR expression is thought to represent a down-regulation of ER signaling, a pathway that positively regulates IRS-1 [155]. Previous work in our lab has shown that loss of IRS-1 results in upregulation of IRS-2 expression and function and promotes tumor progression [54]. In PR- tumors, downregulation of IRS-1 function due to absent ER activity would enhance IRS-2 signaling, leading to increased metastatic potential and risk of death. The fact that we did not observe significant correlations between ER expression, IRS-2 membrane staining, and survival may be due to the fact that many of the ER+ tumors in our dataset were PR-, indicating that the ER pathway was not active [156]. Alternatively, loss of PR expression may be the result of enhanced IGF-1R/IRS-2 signaling through PI3K/Akt/mTOR, which

can downregulate PR expression independent of ER activity [157]. Further studies are warranted to determine if specific signaling pathways, particularly PI3K/Akt/mTOR, are preferentially activated in PR- tumors with IRS-2 membrane localization. Interestingly, patients with PR+ tumors that express IRS-2 at the membrane did not exhibit significantly diminished survival outcomes in our combined dataset. This finding supports the hypothesis that ER signaling, and potentially IRS-1, may be dominant with regard to suppressing the impact of IRS-2-mediated signaling. Additional studies to address this question will be important to understand fully the cross-talk between these hormone and growth factor signaling pathways.

Our study is the first report on the expression of IRS-2 in human breast cancer. The fact that the correlations of IRS-2 membrane localization and poor outcomes in PR- patients were observed in tumors from two separate institutions and in both whole tumor sections and a tissue array support the validity of these observations. However, to confirm IRS-2 localization as a predictive biomarker in breast cancer, these results need to be carefully validated through evaluation of a much larger cohort of patients with longer follow-up times to increase the statistical power of these findings. Ideally, a prospective study in which tumor biopsies could be taken before and after adjuvant treatment would better control for effects of therapy on IRS-2 localization. We established rules to classify the IRS-2 staining pattern in our study to address the subjectivity of determining IRS-2 localization, and two independent investigators were in greater than 90% concordance with identifying the localization pattern. Analysis of

additional cohorts of patients by independent investigators will be important to confirm that the identification of IRS-2 staining patterns is not investigator-dependent. The molecular mechanisms underlying the present findings also require further investigation. The membrane IRS-2 staining pattern could represent activation of specific pathways, which promote aggressive tumor behavior. Receptor activation upstream, as well as activation of downstream signaling pathways need to be evaluated and correlated to IRS-2 expression patterns. *In vitro* studies in cell lines are also needed to further explore the role of the localization of IRS-2 in breast carcinoma cell motility, invasion, and metabolism.

In summary, we have identified an IRS-2 staining pattern that has prognostic significance for the overall survival of breast cancer patients. This association was found to be even stronger for patients with PR- tumors. Evaluation of IRS-2 staining patterns could potentially be used to identify patients with PR- tumors who would most benefit from aggressive treatment.

ACKNOWLEDGEMENTS

This work was supported by National Institute of Health (NIH) grants CA090583 and CA142782 (LMS); Department of Defense Synergistic Idea Award W81XWH-07-1-0599 (LMS and AK); National Institute of Health grants CA125577, CA107469, and CA154224 (CGK); and Department of Defense Breast Cancer Predoctoral Fellowship W81XWH-10-1-0038 (JLC). LMS is a member of the University of Massachusetts Diabetes and Endocrinology Research Center (DERC) (DK32520) and the University of Massachusetts Memorial Cancer Center of Excellence. We thank Dr. Qin Liu at the University of Massachusetts Medical School for her advice on statistical analysis.

CHAPTER III

Interaction of Insulin Receptor Substrate-2 (IRS-2) with microtubules and KIF2A: Impact on AKT signaling

**Jennifer L. Clark¹, Jose Mercado-Matos¹, Jenny Janusis¹, Jean M. Underwood²,
Jeffrey Nickerson² and Leslie M. Shaw¹**

¹Departments of Cancer Biology and ²Cell Biology, University of Massachusetts Medical
School, Worcester, MA 01605

INTRODUCTION

The insulin receptor substrate (IRS) proteins are cytoplasmic adaptors for the insulin-like growth factor receptor (IGF-1R), and they play a major role in determining the cellular response to stimulation by IGF-1 [135, 158-160]. IGF-1 signaling has been implicated in many aspects of breast cancer including breast tumor initiation and progression, as well as resistance to therapy [6, 130-132]. High serum IGF-1 levels are associated with an increased risk of developing breast cancer, and breast cancer patients have higher levels than healthy controls [3, 4]. The receptor tends to be overexpressed and hyperactivated in breast carcinoma cells [5, 6]; and inhibition of the receptor suppresses cell adhesion, invasion, and metastasis and increases sensitivity to taxol treatment [7]. Notably, the IRS proteins facilitate the activation of PI3K downstream of IGF-1R, which signals through AKT and mTOR to promote survival, motility, protein synthesis, and glucose metabolism [31, 33].

IRS-1 and -2 are expressed ubiquitously in humans, including in the normal and malignant mammary gland epithelium [69]. However, despite considerable sequence homology and the ability to activate many of the same downstream signaling effectors, IRS-1 and IRS-2 have been shown to play divergent roles in breast cancer [43]. *In vitro*, studies to assess the function of the IRS proteins in breast carcinoma cells have revealed that signaling through IRS-1 primarily regulates proliferation and survival, whereas signaling through IRS-2 regulates motility, invasion, and glycolysis [53-61]. For example, in a model system lacking endogenous IRS protein expression, cells proliferate

in response to IGF-1 stimulation when IRS-1 expression is restored ectopically, whereas IGF-1 stimulates motility upon restoration of ectopic IRS-2 expression [53]. Treatment of non-invasive MCF-7 cells expressing progesterone receptor isoform B (PR-B) with progestin increases IRS-2 protein levels and activation, which enhances IGF-1-dependent migration [55, 65]. Furthermore, mouse mammary tumor cells derived from *Irs-2*^{-/-} mice exhibit decreased invasiveness, as well as diminished lactic acid production and glucose uptake, two measures of glycolysis [58, 59]. In contrast, mouse mammary tumor cells lacking *Irs-1*, and signaling only through *Irs-2*, are highly invasive [58]. *In vivo*, overexpression of either IRS-1 or IRS-2 in the mouse mammary gland promotes mammary tumorigenesis [52]. However, metastasis is diminished in the absence of *Irs-2* expression and increased in the absence of *Irs-1* expression [57, 58]. The inactivation of *Irs-1* by serine phosphorylation in metastatic tumor cells suggests a potential role for *Irs-1* in suppressing metastasis [57].

Differential localization patterns of IRS-1 and -2 in human tumors suggest a possible explanation for their divergent functions in breast cancer [161]. In normal breast tissue, ductal carcinoma *in situ* (DCIS), and invasive breast tumors, IRS-1 is primarily found in the nucleus, as well as expressed diffusely in the cytoplasm, frequently correlating with nuclear expression of estrogen receptor (ER), as estrogen is a known regulator of IRS-1 expression [49, 62, 63, 136-140, 161]. IRS-1 levels are modulated in MCF-7 xenografts in an estrogen-dependent manner [137]. In the nucleus, IRS-1 has been implicated in the regulation of estrogen response genes, through its interaction with

the ER at estrogen response elements (ERE) in gene promoters [63]. The interaction of IRS-1 with β -catenin and its regulation of genes such as c-Myc and Cyclin D1 likely contribute to its role in stimulating proliferation [145, 147]. In contrast to IRS-1, IRS-2 is not localized to the nucleus, but rather it is expressed either diffusely or in a punctate pattern in the cytoplasm or at the cell membrane [161]. The diffuse IRS-2 staining pattern is associated with better overall survival, whereas membrane localization of IRS-2 in breast tumors is associated with decreased overall survival, particularly in PR negative (PR-) tumors [161]. Taken together, the human tumor staining data suggest that the subcellular localization of IRS-1 and IRS-2 may impact the tumor cell response to signaling through these adaptor proteins [161].

Few studies have investigated the specific subcellular localization of the IRS proteins in breast carcinoma cell lines or the impact of localization on their regulation and function. Such studies are vital to uncover the molecular mechanisms underlying the divergent functions of these proteins. In the present study, we assessed the subcellular localization of IRS-1 and IRS-2 using immunofluorescence microscopy. We report that IRS-2, but not IRS-1, co-localizes with the microtubule cytoskeleton and demonstrate that this localization is required for activation of AKT downstream of IRS-2.

MATERIALS AND METHODS

Cell lines, shRNA, siRNA, and transfection. The MDA-MB-231, MDA-MB-435, and SUM159 cell lines were obtained from the ATCC Cell Biology Collection. Wildtype (WT), *Irs-1^{-/-}*, and *Irs-2^{-/-}* mammary tumor cell lines were established from MMTV-PyV-MT-derived tumors as previously described [58]. A lentiviral vector containing a small hairpin RNA (shRNA) targeting IRS-2 was obtained from Open Biosystems (Huntsville, AL). MDA-MB-231 cells were infected with virus, and stably expressing cells were selected by the addition of 2 $\mu\text{g/ml}$ puromycin. Pools of 4 specific short interfering RNAs (siRNAs) targeting KIF2A, CLIP170, or luciferase were obtained from Dharmacon (Lafayette, CO). MDA-MB-231 cells were transfected with siRNA diluted in Opti-MEM (Invitrogen, Grand Island, NY) using lipofectamine (Invitrogen) for 48 hours.

Immunofluorescence microscopy. Subconfluent, adherent cells plated on glass coverslips were washed three times with Dulbecco's PBS and fixed in 3.8% formaldehyde in Dulbecco's PBS with 0.5% Tween (PBST) for 1 hr. Fixed cells were permeabilized in 0.1% Triton X-100 in PBST for 15 minutes. Permeabilized cells were blocked for 1 hr using 3% BSA in PBST. Primary antibodies diluted in blocking buffer were added to cells and incubated at room temperature for 1 hr. Secondary antibodies were diluted in the same buffer and cells were incubated at room temperature for an additional 30 minutes. Cells were washed three times with PBST after each antibody incubation. After the final wash, nuclei were stained by incubating cells for 30 minutes with Draq5

(Biostatus, Leicestershire, UK) diluted in PBST. Coverslips were then mounted on glass slides using Prolong Gold (Invitrogen) and allowed to dry overnight. Edges of the coverslips were sealed with nailpolish and slides were viewed on a confocal microscope (Leica, Buffalo Grove, IL). Antibodies used for immunofluorescence include IRS-1 (#C20, Santa Cruz, Santa Cruz, CA), IRS-2 (#1849, Epitomics, Burlingame, CA), α -tubulin (#T5168, Sigma-Aldrich, St. Louis, MO), and rictor (#A300-459A, Bethyl, Montgomery, TX).

Microtubule co-sedimentation. Confluent cells on 10 cm plates were washed twice with PBS and extracted for 20 minutes in 500 μ L PEM (100 mM PIPES, pH 6.9, 2 mM EGTA, 1 mM magnesium chloride) containing 0.1% Triton X-100. Debris was removed by centrifugation at 14,000 rpm for 10 minutes at 4°C. Microtubules were polymerized by incubating 400 μ l of lysate at 37°C for 1 hr with 10 μ M taxol (Sigma-Aldrich), 1 mM GTP, and 1 mM DTT. Lysates were also incubated on ice for 1 hr with 10 μ M nocodazole (Sigma-Aldrich) and 1 mM DTT as a negative control for microtubule precipitation. Following the incubations, polymerization reactions were layered over a 20% sucrose/PEM cushion prewarmed to 37°C. Microtubules were then pelleted at 100,000 x g for 1 hr at 35°C by ultracentrifugation using a TLA-110 rotor (Beckman Coulter, Brea, CA). Pellets were resuspended in 1X Laemmli sample buffer and boiled for 5 minutes. The samples were resolved by SDS-PAGE and transferred to nitrocellulose membranes for immunoblot analysis.

Immunoblotting. Cells were solubilized at 4°C in RIPA lysis buffer (25 mM Tris, pH 8.0, 0.1% sodium dodecyl sulfate, 1% sodium deoxycholate, 1% Nonidet P-40, 150 mM sodium chloride, 10 mM sodium fluoride, 1 mM sodium orthovanadate) containing protease inhibitors (Roche, Basel, Switzerland). Cell extracts containing equivalent amounts of protein were resolved by SDS-PAGE and transferred to nitrocellulose membranes. The membranes were blocked for 1 h with a 50 mM Tris buffer, pH 7.5, containing 0.15 M NaCl, 0.05% Tween 20, and 5% (wt/vol) dry milk or 5% bovine serum albumin (BSA), incubated overnight at 4°C in the same buffer containing primary antibodies and then incubated for 1 h in 5% blocking buffer with milk containing peroxidase-conjugated secondary antibodies. Proteins were detected by enhanced chemiluminescence (Biorad, Hercules, CA). The following antibodies were used for immunoblotting: IRS-1 (#C20, Santa Cruz), IRS-2 (#420293, Calbiochem, Gibbstown, NJ; #3089, Cell Signaling, Danvers, MA), p85 (#05-212, Millipore, Billerica, MA), IGF-1R β (#3025, Cell Signaling), phospho-mTOR S2481 (#2974, Cell Signaling), phospho-mTOR S2448 (#2971, Cell Signaling), mTOR (#2972, Cell Signaling), rictor (#A300-459A, Bethyl), raptor (#2280, Cell Signaling), phospho-S6K (#9205, Cell Signaling), S6K (#9209, Cell Signaling), phospho-AKT S473 (#9271 and #4060, Cell Signaling), phospho-AKT T308 (#2965, Cell Signaling), AKT (#sc-8312, Santa Cruz), α -tubulin (#T5168, Sigma-Aldrich), phospho-MAPK (#9106, Cell Signaling), MAPK (#9102, Cell Signaling), CLIP170 (#sc-28325, Santa Cruz), KIF2A (#ab37005, abcam, Cambridge, MA), KIF3A (#ab11259, abcam), KIF11 (#NB500-181, Novus Biologicals, Littleton, CO), dynein (#sc-13524, Santa Cruz), GAPDH (#A300-642A, Bethyl), peroxidase-

conjugated goat anti-rabbit IgG (Jackson, West Grove, PA), and peroxidase-conjugated goat anti-mouse IgG (Jackson).

Immunoprecipitation. Cells were extracted using either a 20 mM Tris, pH 7.4 buffer containing 1% Nonidet P-40, 136.9 mM sodium chloride, 10% glycerol, and 10 mM sodium fluoride (NP-40 buffer) or a 40 mM HEPES, pH 7.5 buffer containing 120 mM sodium chloride, 1 mM EDTA, 0.3% CHAPS, and 50 mM sodium fluoride (CHAPS buffer). Both buffers also contained 1 mM sodium orthovanadate and protease inhibitors (Roche). Aliquots of cell extracts containing equivalent amounts of protein were incubated overnight at 4°C with antibodies and protein A sepharose beads (Amersham Biosciences, Piscataway, NJ) with constant agitation. The beads were washed three times in extraction buffer. Laemmli sample buffer was added to the samples, which were then incubated at 95°C for 15 minutes. Immune complexes were resolved by SDS-PAGE, transferred to nitrocellulose membranes, and immunoblotted as described. The following antibodies were used for immunoprecipitation: IRS-2 (Bethyl Custom Immunochemistry Services), IRS-1 (#C20, Santa Cruz), IGF-1R (#3025, Cell Signaling), CLIP170 (#sc-28325, Santa Cruz), rabbit IgG (#sc-2027, Santa Cruz), and mouse IgG_{2b} (#ab18421, abcam).

Permeabilization assay. Cells grown to subconfluency on coverslips were washed once with 1x PBS and then extracted for 5 seconds in a membrane/soluble extraction buffer (0.2% Triton X-100, 100 mM KCl, 200 mM sucrose, 10 mM EGTA, 2 mM magnesium

chloride, 200 μ M sodium vanadate, 1 mM PMSF, and 10 mM Pipes, pH 6.8) [162]. Following extraction, cells were immediately fixed in 3.8% formaldehyde in 1X Dulbecco's PBS containing 0.1% Tween. Immunofluorescent staining was performed as described.

Drug treatment and stimulation. Cells were either serum starved overnight or for 4 hours in plain medium. Drugs were added to the medium for the specified time periods prior to stimulation with IGF-1. Nocodazole was used at a concentration of 1 μ M for 30 minutes, vinblastine (Sigma-Aldrich) at a concentration of 18 nM for 30 minutes, and taxol at a concentration of 20 μ M for 2 hours. The mouse tumor cell lines were treated with nocodazole at a concentration of 10 μ M for 1 hour. All drugs were obtained from Sigma-Aldrich (St. Louis, MO). At the end of the treatment period, cells were stimulated for 5 minutes with 20 ng/ml human recombinant IGF-1 (R&D Systems, Minneapolis, MN) prior to lysis.

Cell cycle analysis. For analysis of DNA content, adherent cells were collected by trypsinization and combined with non-adherent cells from the culture medium. After centrifugation, the cell pellet was washed once in cold PBS, and the cells were then fixed in 70% ethanol and stored overnight at -20°C. The fixed cells were washed once in PBS and then resuspended in PBS containing 0.1% Triton-X-100, 0.1 mM EDTA, 0.05 mg/ml RNase A (50 U/mg) and 50 μ g/ml propidium iodide. The cells were analyzed by flow

cytometry using a Becton Dickinson (Franklin Lakes, NJ) FACSCalibur after a 1 hour incubation at room temperature.

RESULTS

IRS-1 and IRS-2 have distinct intracellular localizations

To investigate the localization of IRS-1 and IRS-2 in human breast carcinoma cells, SUM159 and MDA-MB-231 cells treated with or without IGF-1 stimulation were evaluated by immunofluorescence microscopy. IRS-1 exhibited both cytoplasmic and nuclear localization, whereas IRS-2 was exclusively localized within the cytoplasmic compartment, similar to the distribution we had observed previously in human tumors. Although IRS-1 was diffusely distributed in a punctate manner throughout the cytoplasm, IRS-2 staining exhibited a more organized pattern, reminiscent of microtubules. The subcellular localization of IRS-1 and IRS-2 were investigated further by costaining the cells with antibodies that recognize tubulin (Figure 3.1a-h). IRS-2 showed a considerable overlap with tubulin staining and was closely associated with microtubules when viewed under higher magnification (Figure 3.1a-h). In contrast, IRS-1 did not show any colocalization with tubulin (Figure 3.1i).

MDA-MB-231 cells were treated with drugs that alter microtubule stability to determine if the localization of IRS-2 is dependent upon the microtubule cytoskeleton. Taxol (paclitaxel), a taxane drug commonly used in cancer treatment, stabilizes microtubules, whereas nocodazole causes depolymerization of the tubulin cytoskeleton. Cells were evaluated for IRS-2 localization following short-term treatment with each drug. Taxol treatment increased the fluorescence detection of IRS-2, although total IRS-2 levels were unchanged, as evidenced by immunoblot (Figure 3.2a,b). IRS-2 co-

Figure 3.1. Localization of the IRS proteins in breast carcinoma cells

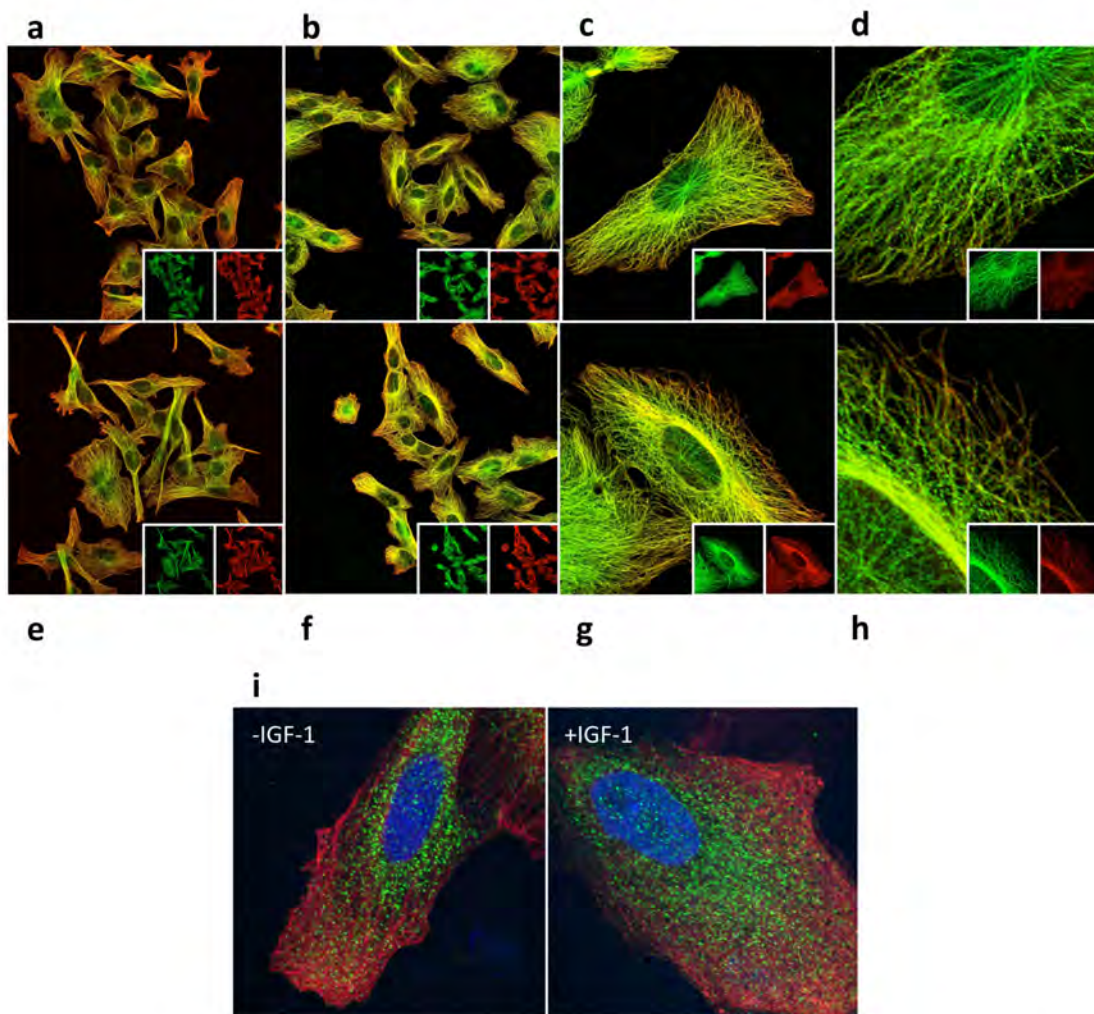


Figure 3.1. Localization of the IRS proteins in breast carcinoma cells. Co-immunofluorescence staining of IRS-2 (green) and tubulin (red) in unstimulated (**a-d**) and IGF-1-stimulated (**e-h**), formalin-fixed (**a,e**) MDA-MB-231 cells (magnification 63x) and (**b,f**) SUM159 cells (magnification 63x). (**c,g**) Co-immunofluorescence staining of IRS-2 (green) and tubulin (red) in an unstimulated (**c**) and IGF-1-stimulated (**g**) formalin-fixed SUM159 cell (magnification 132.3x and 151.2x, respectively) and (**d,h**) the same cell focused on the cell periphery (magnification 346.5x and 441x, respectively). Merged images are shown in each panel, with single channels shown in insets. (**i**) Co-immunofluorescence staining of IRS-1 (green) and tubulin (red) in formalin-fixed SUM159 cells plus or minus IGF-1 stimulation (magnification 161x).

Figure 3.2. Association of IRS-2 with the microtubule cytoskeleton. (a) Co-immunofluorescence staining of IRS-2 (green) and tubulin (red) in MDA-MB-231 cells after treatment with DMSO (control), 20 μ M taxol for 2 hours, or 1 μ M nocodazole for 30 minutes (magnification 40x). (b) MDA-MB-231 cells were treated with DMSO (control), 20 μ M taxol for 2 hours, or 1 μ M nocodazole for 30 minutes. Aliquots of cell extracts containing equivalent amounts of total protein were immunoblotted with IRS-2, actin, and tubulin-specific antibodies. (c) Co-immunofluorescence staining of IRS-2 (green) and tubulin (red) in SUM159 cells after treatment with DMSO (control) or 20 μ M taxol for 2 hours with (Triton) or without (PBS) permeabilization with a Triton X-100-containing buffer prior to formalin fixation (magnification 40x). (d) Cell extracts from MDA-MB-231 cells treated with or without IGF-1 or expressing an shRNA targeting IRS-2 (shIRS2) were incubated with 10 μ M taxol to polymerize tubulin, and microtubules were pelleted by high speed centrifugation. The pellets were immunoblotted with IRS-2 and tubulin-specific antibodies. Neg ctrl, MDA-MB-231 cell lysates treated with nocodazole and kept on ice.

localization with tubulin remained after treatment with taxol. In contrast, treatment with nocodazole resulted in a redistribution of IRS-2 in the cytoplasm and a decrease in fluorescence detection, despite unchanged total protein levels (Figure 3.2a,b). These changes in the detection of IRS-2 after treatment with taxol and nocodazole suggest that the interaction of IRS-2 with microtubules may alter antibody recognition. Treatment of cells with taxol rendered IRS-2 resistant to solubilization by detergent (Triton X-100), supporting a direct association of IRS-2 with microtubules, rather than an indirect association through vesicle binding (Figure 3.2c). The ability of IRS-2 to interact with the microtubule cytoskeleton was demonstrated further by microtubule co-sedimentation. Upon taxol-mediated polymerization of tubulin in MDA-MB-231 cell lysates, IRS-2 was detected in the microtubule pellet after high speed centrifugation (Figure 3.2d).

IGF-1R signaling is dependent upon the microtubule cytoskeleton.

To investigate the role of the microtubule cytoskeleton in IGF-1 signaling, MDA-MB-231 cells were stimulated with IGF-1 after treatment with taxol or nocodazole to stabilize or disrupt microtubules, respectively. IGF-1 signaling was measured by assessing the phosphorylation status of downstream signaling effectors by immunoblot analysis of total cell lysates. Although taxol treatment had no effect on AKT activation (Figure 3.3a), treatment with nocodazole significantly reduced phosphorylation of AKT at both threonine 308 (T308) and serine 473 (S473) (Figure 3.3b). In contrast, MAPK and S6K activation were not affected by nocodazole treatment (Figure 3.3c). A similar inhibition of AKT activation was observed when cells were treated with vinblastine, a

Figure 3.3. Impact of taxol and nocodazole treatment on IGF-1 stimulated AKT activation

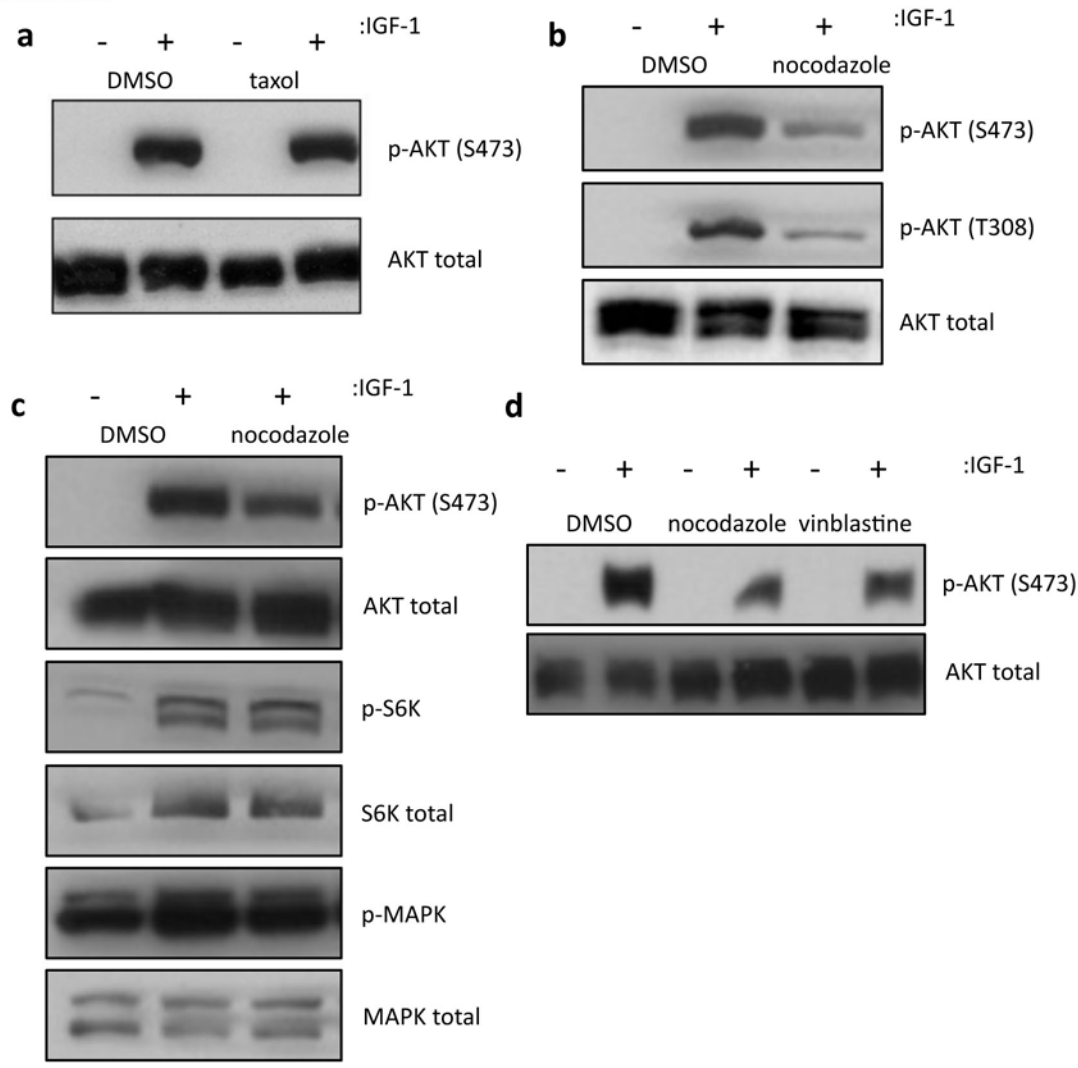


Figure 3.3. Impact of taxol and nocodazole treatment on IGF-1 stimulated AKT activation. (a and b) MDA-MB-231 cells were treated with DMSO (control) and either 20 μ M taxol for 2 hours (a) or 1 μ M nocodazole (b) for 30 minutes and then stimulated with IGF-1 (20 ng/ml) for 5 minutes. Aliquots of cell extracts containing equivalent amounts of total protein were immunoblotted with antibodies specific for phospho-S473AKT or phospho-T308AKT. The immunoblots were subsequently stripped and reprobbed with AKT-specific antibodies. (c) MDA-MB-231 cells were treated with DMSO (control) or 1 μ M nocodazole for 30 minutes and then stimulated with IGF-1 (20 ng/ml) for 5 minutes. Aliquots of cell extracts containing equivalent amounts of total protein were immunoblotted with antibodies specific for phospho-S473AKT, phospho-T389S6K and phospho-MAPK. The phosphoimmunoblots were subsequently stripped and reprobbed with antibodies recognizing total AKT, S6K, and MAPK. (d) MDA-MB-231 cells were treated with DMSO (control) and either 1 μ M nocodazole or 18nM vinblastine for 30 minutes and then stimulated with IGF-1 (20 ng/ml) for 5 minutes. Aliquots of cell extracts containing equivalent amounts of total protein were immunoblotted with antibodies specific for phospho-S473AKT. The immunoblots were subsequently stripped and reprobbed with AKT-specific antibodies.

second drug that also disrupts microtubules and is frequently used in chemotherapy regimens (Figure 3.3d) [114]. Taken together, these results suggest that an intact microtubule cytoskeleton is required for activation of AKT by IGF-1 signaling. The absence of an effect of nocodazole on MAPK and S6K supports that the inhibition of AKT activation is not due to a global downregulation of kinase activation in these cells, but rather a specific effect on the AKT axis.

To investigate the mechanism by which nocodazole disrupts AKT activation, phosphorylation of the IGF-1R and IRS proteins and IRS/PI3K association were examined. Treatment with nocodazole had no effect on IRS-1 or -2 tyrosine phosphorylation or association with the p85 regulatory subunit of PI3K (Figure 3.4). However, phosphorylation of the IGF-1R β -subunit was increased by IGF-1 following nocodazole treatment (Figure 3.4). The IGF-1R is internalized upon activation and either recycled to the cell surface or targeted for lysosomal degradation [150, 163, 164]. This process likely requires trafficking along microtubules. Upon dissolution of the cytoskeleton by nocodazole treatment and subsequent loss of this receptor trafficking pathway, the activated receptor may accumulate at the cell surface or in early endosomes, resulting in sustained activation. Taken together, these results suggest that nocodazole does not disrupt activation of AKT upstream at the level of receptor activation or PI3K recruitment to the IRS proteins.

Figure 3.4. Evaluation of the role of the microtubule cytoskeleton in IGF-1R signaling pathway activation

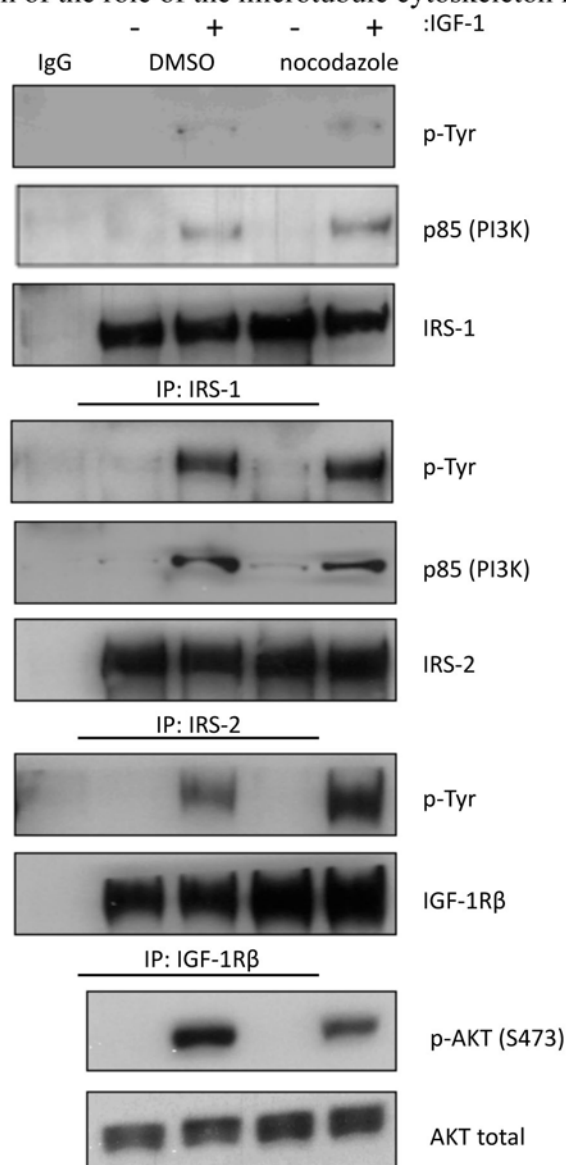


Figure 3.4. Evaluation of the role of the microtubule cytoskeleton in IGF-1R signaling pathway activation. MDA-MB-231 cells were treated with DMSO (control) or 1 μ M nocodazole for 30 minutes and then stimulated with IGF-1 (20 ng/ml) for 5 minutes. Aliquots of the cell extracts containing equivalent amounts of total protein were immunoprecipitated with antisera specific for either IRS-1, IRS-2, or IGF-1R β subunit and immunoblotted with antibodies specific for phosphotyrosine (p-Tyr) and the p85 subunit of PI3K. The p-Tyr immunoblots were subsequently stripped and reprobbed with IRS-1, IRS-2, or IGF-1R β -specific antibodies. Total cell extracts were also immunoblotted with antibodies specific for phospho-S473AKT and total AKT (bottom panels).

mTOR complex 2 (mTORC2), comprised of several proteins including mTOR and rictor, phosphorylates AKT on S473. Phosphorylation of the mTORC2-associated site serine 2481 (S2481) on mTOR was used as a readout for activation of this complex [165]. Nocodazole treatment abolished the IGF-1-dependent increase in phosphorylation at this site (Figure 3.5a), suggesting that an intact microtubule cytoskeleton is required for IGF-1-stimulated mTORC2 activation and subsequent phosphorylation of AKT. Of note, the mTORC1-dependent site serine 2448 (S2448) on mTOR was unaffected by nocodazole treatment (Figure 3.5a), consistent with maintenance of S6K activity (Figure 3.3c) following microtubule disruption and suggesting an mTORC2-specific effect of nocodazole in these cells [165]. We hypothesized that mTORC2 activity might be disrupted by nocodazole due to an association of the complex with microtubules, which is required for proper activation and function. Indeed, both mTOR and rictor co-sedimented with taxol-stabilized microtubules in MDA-MB-231 cell lysates (Figure 3.5b). Consistent with this result, immunofluorescence studies revealed a partial localization of rictor along microtubules in MDA-MB-231 (not shown) and SUM159 cells (Figure 3.5c-f).

IRS-2, but not IRS-1, requires the microtubule cytoskeleton to activate AKT

MDA-MB-231 cells express both IRS-1 and IRS-2 but signal preferentially through IRS-2 in response to IGF-1R activation. To determine if there is a selective role for the microtubule cytoskeleton in IRS-1 or IRS-2 mediated signaling, mammary tumor cells derived from PyMT:WT, PyMT:IRS-1^{-/-} or PyMT:IRS-2^{-/-} mice were treated with

Figure 3.5. Evaluation of the role of the microtubule cytoskeleton in IGF-1 stimulation of mTORC1 and mTORC2 activation

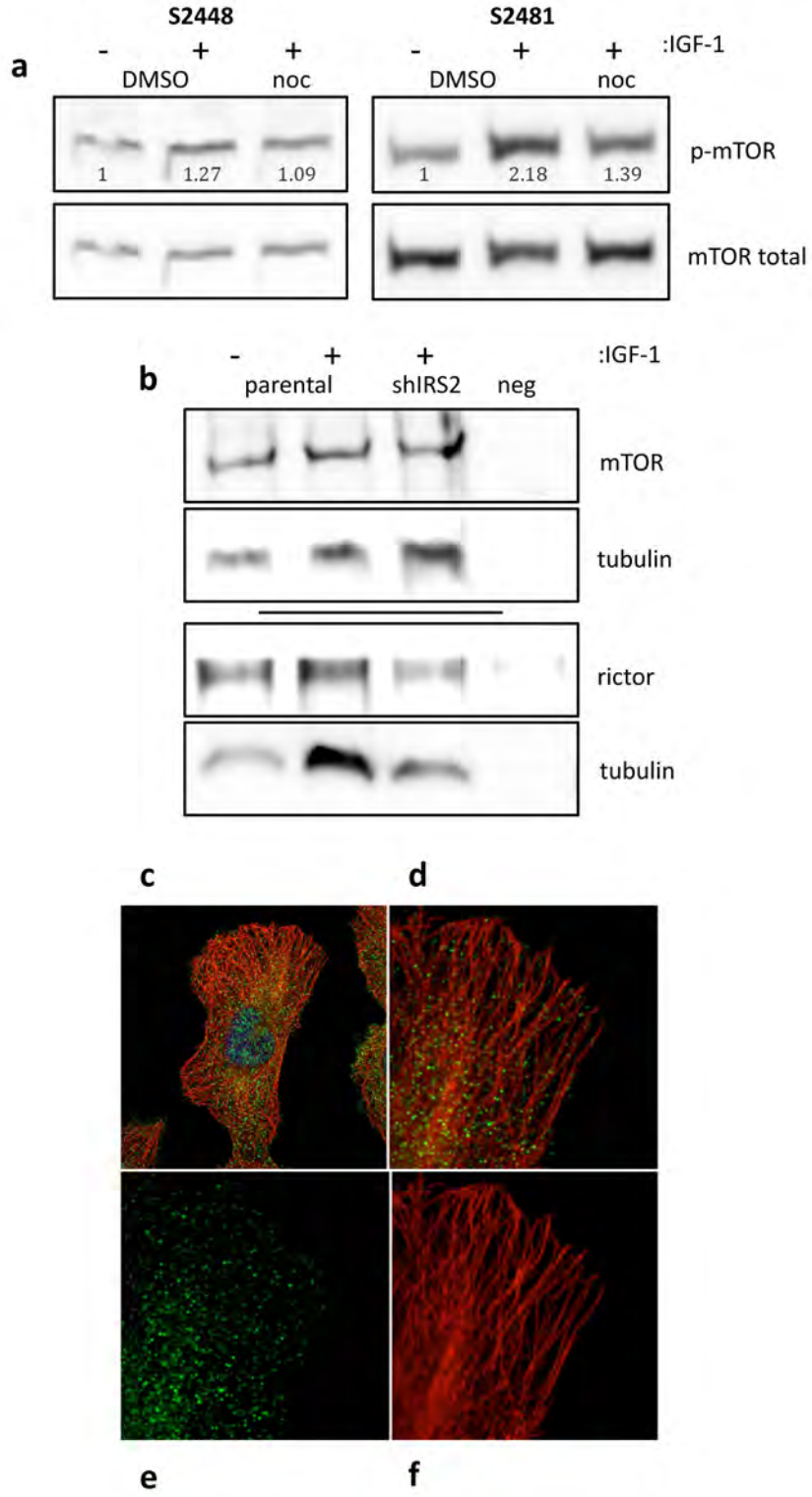


Figure 3.5. Evaluation of the role of the microtubule cytoskeleton in IGF-1 stimulation of mTORC1 and mTORC2 activation. (a) MDA-MB-231 cells were treated with DMSO (control) or 1 μ M nocodazole for 30 minutes and then stimulated with IGF-1 (20 ng/ml) for 5 minutes. Aliquots of cell extracts containing equivalent amounts of total protein were immunoblotted with antibodies specific for phospho-S2448mTOR or phospho-S2481mTOR. The phosphoimmunoblots were subsequently stripped and reprobed with antibodies recognizing total mTOR. The numbers represent phospho-mTOR relative to total mTOR. (b) Cell extracts from MDA-MB-231 cells treated with or without IGF-1 or expressing an shRNA targeting IRS-2 (shIRS2) were incubated with 10 μ M taxol to polymerize tubulin, and microtubules were pelleted by high speed centrifugation. The pellets were immunoblotted with mTOR, rictor, or tubulin-specific antibodies. Neg, MDA-MB-231 cell lysates treated with nocodazole and kept on ice. (c) Co-immunofluorescence staining of rictor (green) and tubulin (red) in an IGF-1-stimulated, formalin-fixed SUM159 cell (magnification 157.5x) (d-f) The same cell shown in (c) with a higher magnification (516.6x). Merged image (d), green channel alone (e) and red channel alone (f).

nocodazole and stimulated with IGF-1. WT cells demonstrated a modest reduction in AKT activation after treatment with nocodazole (Figure 3.6a). PyMT:Irs-1^{-/-} cells, which signal exclusively through Irs-2, exhibited a significant decrease in IGF-1-dependent AKT activation following treatment with nocodazole, similar to the reduction observed in MDA-MB-231 cells (Figure 3.6a). In contrast, AKT activation increased significantly in PyMT:Irs-2^{-/-} cells in response to IGF-1 stimulation following nocodazole treatment (Figure 3.6a). These results suggest that only IGF-1 signaling through IRS-2 is dependent on an intact microtubule cytoskeleton. Signaling to AKT through IRS-1 is not microtubule-dependent.

The selective role of IRS-2 in the sensitivity of cells to microtubule disruption was explored further by knocking down IRS-2 in MDA-MB-231 cells through stable transfection with a specific shRNA. The knockdown efficiency achieved in these cells was ~80%. Total AKT activation in response to IGF-1 stimulation was reduced markedly in the shIRS-2 cells compared to parental cells, consistent with an IRS-2 dependence for IGF-1 signaling in this cell line (Figure 3.6b). Treatment of the shIRS-2 cells with nocodazole caused an additional small reduction in AKT activation, suggesting that the remaining IRS-2 present in the cell (~20%) is still signaling to AKT through a microtubule-dependent mechanism (Figure 3.6b). mTORC2 activation was also evaluated by measuring S2481 phosphorylation. Stimulation with IGF-1 increased phosphorylation at this site two-fold over basal levels in MDA-MB-231 cells (Figure 3.6b). Treatment of these cells with nocodazole abolished this IGF-1-induced

Figure 3.6. Selective impact of nocodazole on IRS-2 mediated signaling

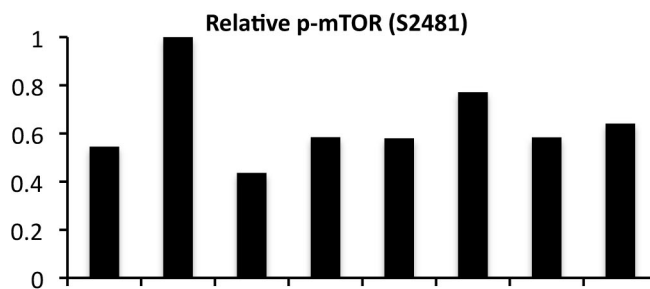
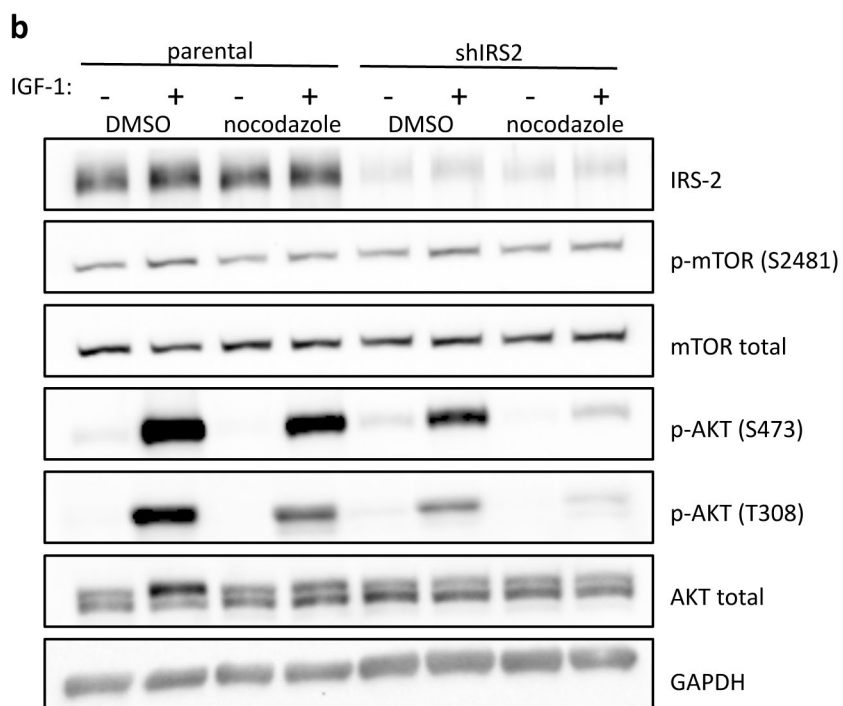
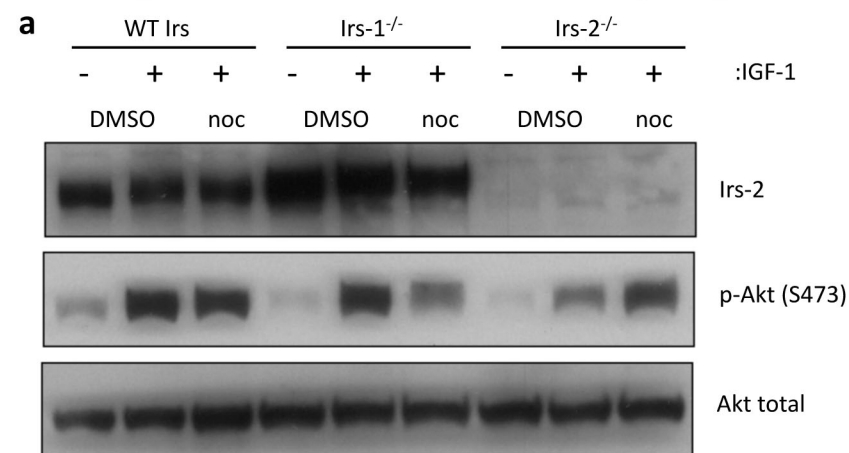


Figure 3.6. Selective impact of nocodazole on IRS-2 mediated signaling. (a) PyVMT:WT Irs, Irs-1^{-/-}, and Irs-2^{-/-} cells were treated with DMSO (control) or 10 uM nocodazole for 1 hour and then stimulated with IGF-1 (20 ng/ml) for 5 minutes. Aliquots of cell extracts containing equivalent amounts of total protein were immunoblotted with antibodies specific for Irs-2 or phospho-S473Akt. The phosphoAkt immunoblot was subsequently stripped and reprobbed with antibodies recognizing total Akt. (b) MDA-MB-231 cells or cells expressing an shRNA targeting IRS-2 were treated with DMSO (control) or 1 uM nocodazole for 30 minutes and then stimulated with IGF-1 (20 ng/ml) for 5 minutes. Aliquots of cell extracts containing equivalent amounts of total protein were immunoblotted with antibodies specific for Irs-2, phospho-S2481mTOR, phospho-S473AKT, phospho-T308AKT and GAPDH. The phosphoblots were subsequently stripped and reprobbed with antibodies recognizing total proteins. The graph represents p-mTOR relative to total mTOR.

upregulation of S2481 (Figure 3.6b). When IRS-2 expression was suppressed, S2481 was not increased by IGF-1 stimulation, even in the presence of an intact microtubule cytoskeleton, suggesting that both IRS-2 and intact microtubules are required for mTORC2 activation downstream of IGF-1 in these cells (Figure 3.6b).

To investigate further the connection between IRS-2 and microtubule dependent AKT activation, a panel of cell lines differing in IRS status was tested for their response to nocodazole. The results are summarized in Table 3.1. Cell lines that signal predominantly through IRS-2, due either to lack of IRS-1 expression or diminished IRS-1 activation in response to IGF-1, responded to treatment with nocodazole by downregulating AKT and mTORC2 activity (Table 3.1). These cell lines, MDA-MB-231, MDA-MB-435, and PyMT:Irs-1^{-/-}, also exhibited greater morphological changes in response to nocodazole treatment (Table 3.1, Figure 3.7). In contrast, AKT and mTORC2 activity remained at or above basal levels following nocodazole treatment in cell lines that signal predominantly through other means, including SUM159, PyMT:Irs-2^{-/-}, and PyMT:WT (Table 3.1). These same cell lines also maintained a more normal overall cell morphology, despite solubilization of the microtubule cytoskeleton (Table 3.1, Figure 3.7).

Mechanism of IRS-2 interaction with microtubules

One mechanism by which IRS-2 could associate with the microtubules is through an interaction with molecular motor proteins that transport organelles, protein complexes

Table 3.1. Nocodazole response summary

Cell line	Species	IRS-2 dependent	AKT/mTORC2	Morphology
MDA-MB-231	human	yes	↓↓	shrinkage
MDA-MB-435	human	yes	↓↓	slight shrinkage, membrane protrusions
Irs-1 ^{-/-} mammary tumor	mouse	yes	↓	membrane protrusions
SUM159	human	no	no change	no change in cell shape despite tubulin depolymerization
wt Irs mammary tumor	mouse	intermediate	no change	no change in cell shape despite tubulin depolymerization
Irs-2 ^{-/-} mammary tumor	mouse	no	↑	slight shrinkage, slightly resistant to depolymerization

Figure 3.7. Differential sensitivity of breast carcinoma cells to nocodazole

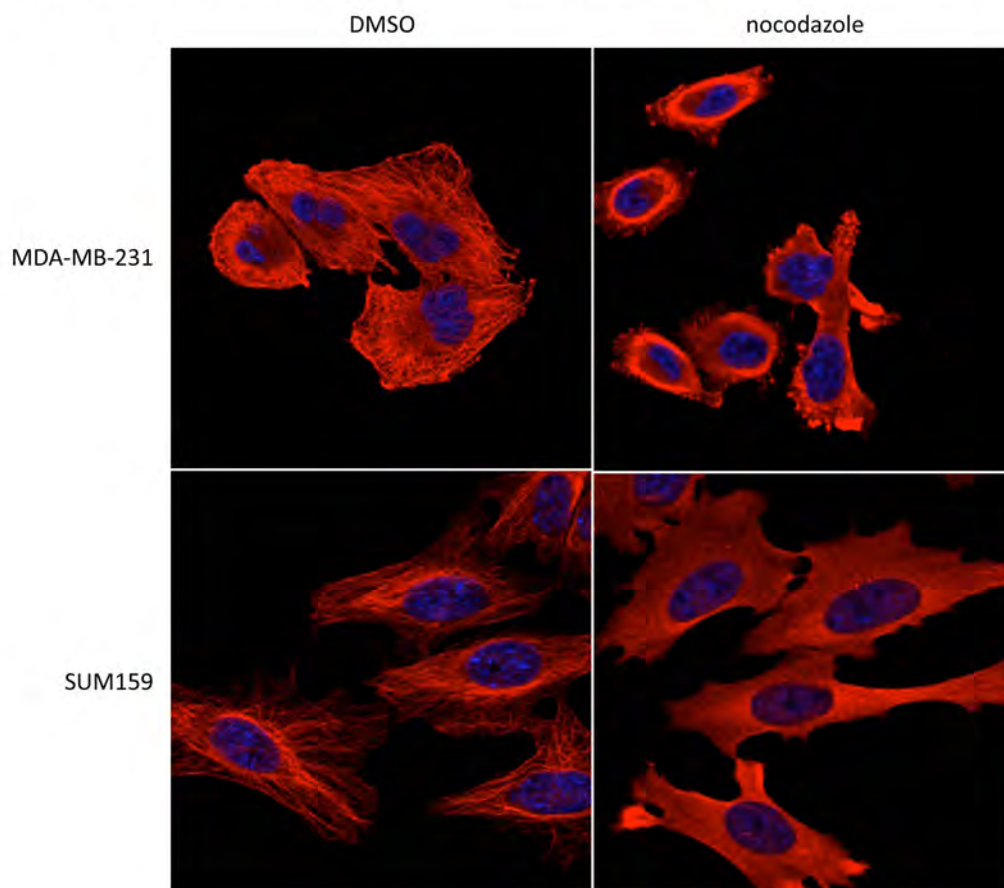


Figure 3.7. Differential sensitivity of breast carcinoma cells to nocodazole. Co-immunofluorescence staining of tubulin (red) in formalin-fixed MDA-MB-231 and SUM159 cells treated with DMSO (control) or 10 μ M nocodazole for 30 min (magnification 126x). Nuclei stained with draq5 (blue).

and mRNAs to specific destinations within the cell. The kinesin family of motor proteins mediates transport primarily in an anterograde direction from the minus to the fast growing plus end of the microtubule, whereas dynein mediates transport in the retrograde direction. There are 45 kinesin superfamily members (KIFs) in mice and humans, all of which share a highly conserved motor domain but have unique “cargo-binding” domains that determine their specific interactions and transport of cargo [129]. To investigate the possibility that IRS-2 interacts with microtubules indirectly through a molecular motor protein, we assessed its ability to interact with either dynein or specific KIFs that had been previously implicated in either insulin/IGF-1 signaling (KIF3A) or in cancer (KIF2A and KIF11) [166-170]. KIF2A co-immunoprecipitated with IRS-2 from MDA-MB-231 cell extracts, and this interaction was confirmed in PyMT mouse mammary tumor cells (Figure 3.8a,b). No interaction of IRS-2 with KIF3A, KIF11, or dynein was detected (Figure 3.8a). The association of IRS-1 with the same motor proteins was also examined to determine if a unique potential for IRS-2 to traffic along microtubules might be responsible for the divergent roles of these two adaptor proteins in breast cancer. Indeed, KIF2A and the other motor proteins tested did not co-immunoprecipitate with IRS-1 (Figure 3.8c). To determine if the association of IRS-2 with KIF2A is required for the stimulation of AKT activation by IGF-1, KIF2A expression was suppressed using siRNA, which resulted in a knockdown efficiency of ~80%. When KIF2A expression was suppressed, AKT phosphorylation at the S473 site was decreased by 20-30% (Figure 3.8d). In contrast, suppression of the plus end binding protein CLIP-170, which also interacts with IRS-2, was shown not to affect AKT activation (Figure 3.8e,f).

Figure 3.8. Interaction of IRS-2 with microtubule associated proteins (MAPs)

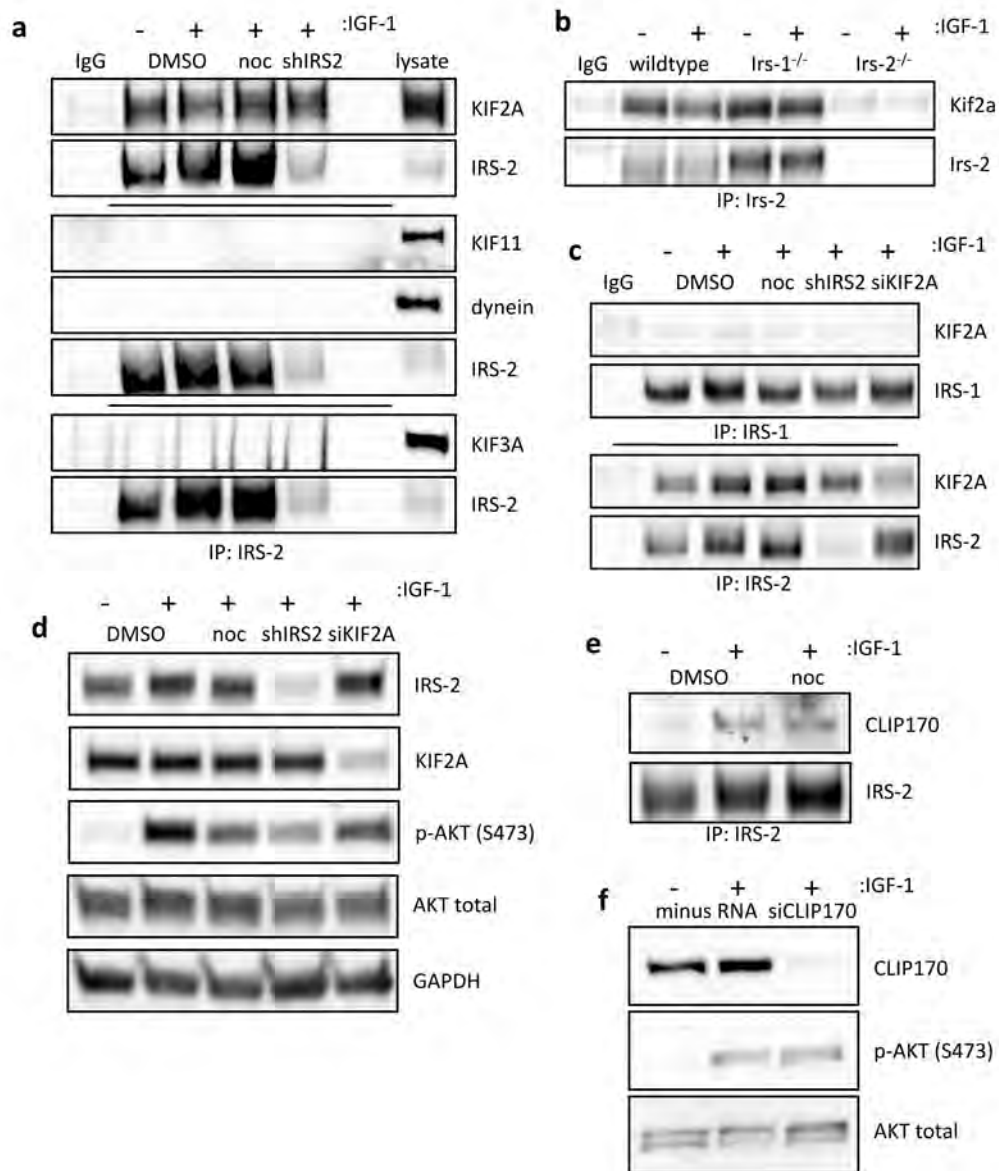


Figure 3.8. Interaction of IRS-2 with microtubule associated proteins (MAPs). (a) MDA-MB-231 cells or MDA-MB-231 cells expressing an IRS-2 specific shRNA (shIRS2) were treated with DMSO (control) or 1 μ M nocodazole for 30 minutes and then stimulated with IGF-1 (20 ng/ml) for 5 minutes. Aliquots of cell extracts containing equivalent amounts of total protein were immunoprecipitated with antisera specific for IRS-2 and immunoblotted with antibodies specific for the kinesins KIF2A, KIF11, and KIF3A, dynein, and IRS-2. IgG, negative control immunoprecipitation. (b) PyVMT:WT Irs, Irs-1^{-/-}, and Irs-2^{-/-} cells were stimulated with IGF-1 (20 ng/ml) for 5 minutes. Aliquots of cell extracts containing equivalent amounts of total protein were immunoprecipitated with antisera specific for IRS-2 and immunoblotted with antibodies specific for Kif2a and Irs-2. IgG, negative control immunoprecipitation. (c and d) MDA-MB-231 cells, MDA-MB-231 cells expressing an IRS-2 specific shRNA (shIRS2) or MDA-MB-231 cells transfected with KIF2A-specific siRNA were treated with DMSO (control) or 1 μ M nocodazole for 30 minutes and then stimulated with IGF-1 (20 ng/ml) for 5 minutes. (c) Aliquots of cell extracts containing equivalent amounts of total protein were immunoprecipitated with antisera specific for IRS-1 or IRS-2 and immunoblotted with antibodies specific for KIF2A, IRS-1, and IRS-2. IgG, negative control immunoprecipitation. (d) Aliquots of cell extracts containing equivalent amounts of total protein were immunoblotted with antibodies specific for the IRS-2, KIF2A, phospho-S473AKT, and GAPDH. The phosphoAKT blot was subsequently stripped and reprobed with antibodies recognizing total AKT. (e) MDA-MB-231 cells were treated with DMSO (control) or 1 μ M nocodazole for 30 minutes and then stimulated with IGF-1 (20 ng/ml) for 5 minutes. Aliquots of cell extracts containing equivalent amounts of total protein were immunoprecipitated with antisera specific for IRS-2 and immunoblotted with antibodies specific for CLIP-170 and IRS-2. (f) MDA-MB-231 cells or MDA-MB-231 cells transfected with CLIP-170-specific siRNA were stimulated with IGF-1 (20 ng/ml) for 5 minutes. Aliquots of cell extracts containing equivalent amounts of total protein were immunoblotted with antibodies specific for the CLIP-170 and phospho-S473AKT. The phosphoAKT blot was subsequently stripped and reprobed with antibodies recognizing total AKT.

IRS-2 determines cellular responses to microtubule disruption

The role of IRS-2 in mediating functional outcomes associated with microtubule disruption was assessed by cell cycle analysis of parental and shIRS-2 MDA-MB-231 cells after treatment with nocodazole or vinblastine for 48 hours. A significant increase in the sub-G1 population occurred in response to both nocodazole and vinblastine treatment, consistent with an induction of apoptosis (Figure 3.9a,b). In contrast, after 48 hrs of treatment, shIRS-2 cells did not die, but rather underwent a G2/M arrest (Figure 3.9a-d). These results suggest that cells that signal through IRS-2 may be more susceptible to drugs which depolymerize microtubules and respond by undergoing apoptosis, consistent with downregulation of the pro-survival protein AKT. Cells that must signal to AKT through other means, as in the IRS-2 knockdown cells, are less susceptible to death from these drugs because they are capable of maintaining AKT activity in the absence of intact microtubules.

Figure 3.9. Role of IRS-2 in the cellular response to microtubule disruption

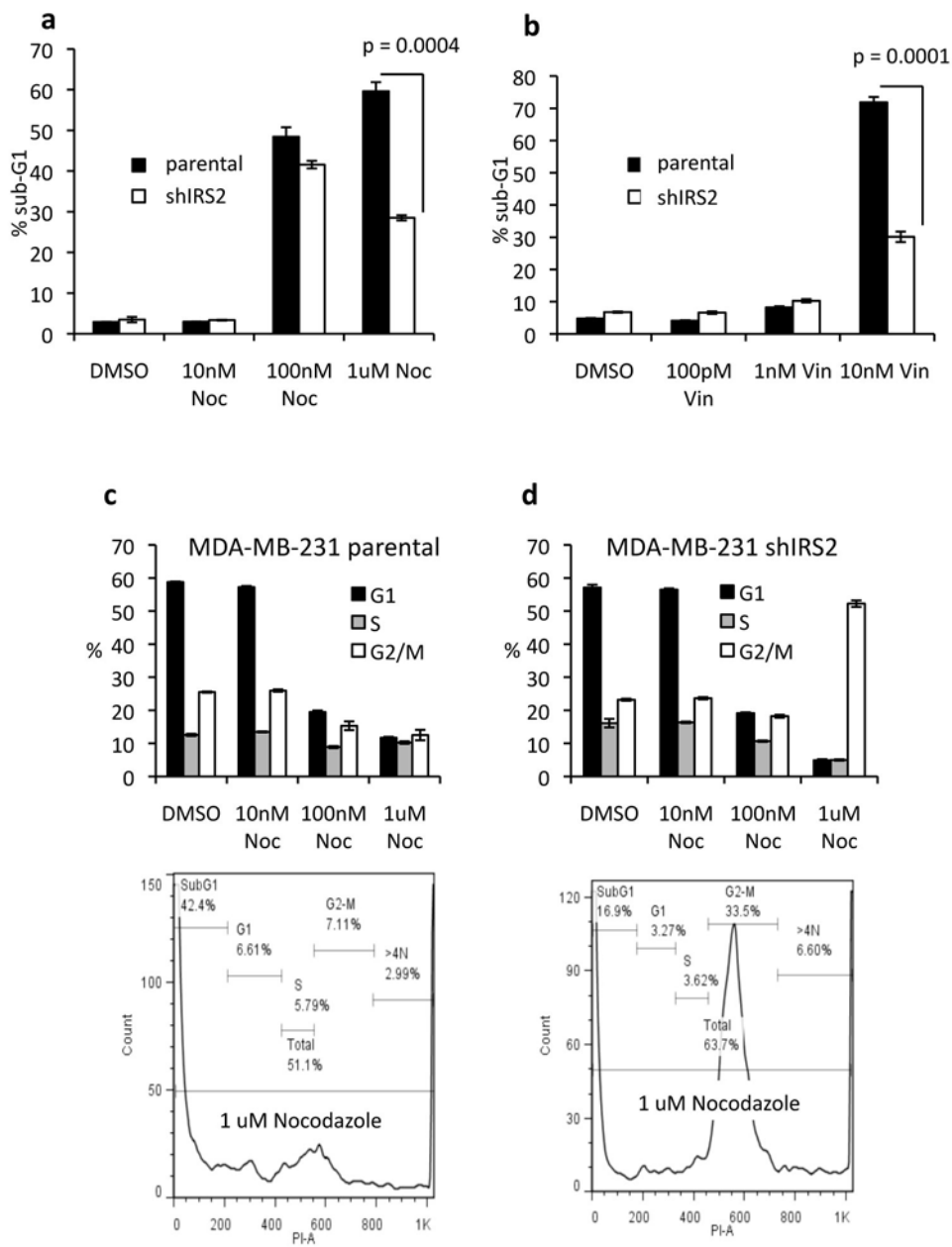


Figure 3.9. Role of IRS-2 in the cellular response to microtubule disruption. MDA-MB-231 cells were treated with DMSO or the specified concentrations of nocodazole **(a)** or vinblastine **(b)** for 48 hours and then stained with propidium iodide and analyzed by flow cytometry. Shown are the % of cells in the sub-G1 peak. **(c and d)** MDA-MB-231 cells **(c)** or MDA-MB-231 cells expressing an IRS-2 specific shRNA **(d)** were treated with the specified concentrations of nocodazole for 48 hours and then stained with propidium iodide and analyzed by flow cytometry. Lower panels show the FACS plots for the 1 μ M nocodazole treatment condition. Data represent the mean (\pm SEM) of a representative experiment performed in triplicate.

DISCUSSION

We report in the current study that IRS-2, but not IRS-1, co-localizes with the microtubule cytoskeleton in breast carcinoma cell lines. Depolymerization of microtubules by nocodazole or vinblastine disrupts the localization pattern of IRS-2, whereas stabilization with taxol preserves its localization, and enhances the resistance of IRS-2 to solubilization by detergent. Disruption of the microtubule cytoskeleton inhibits AKT activation in cells that signal preferentially through IRS-2, without affecting activation of IGF-1R, PI3K, or IRS-2 upstream, nor signaling through S6K and MAPK, suggesting that an intact microtubule cytoskeleton is required specifically for IRS-2-dependent AKT activation. Intact microtubules are also required for mTORC2 activation in response to IGF-1. IRS-2, but not IRS-1, associates with the kinesin family member KIF2A, and this interaction is important for the activation of AKT through IRS-2, as suppression of KIF2A expression decreased IGF-1-dependent AKT activation. Treatment of parental MDA-MB-231 cells that express IRS-2 with either nocodazole or vinblastine resulted in significant levels of cell death. However, cells with reduced IRS-2 expression underwent G2/M arrest instead of cell death, suggesting that the expression of IRS-2 determines the cellular response to microtubule-disrupting drugs. The interaction of IRS-2, but not IRS-1, with KIF2A and the association of IRS-2 with the microtubule cytoskeleton provides a mechanism by which signaling downstream of these adaptor proteins can be targeted to distinct intracellular compartments to promote divergent cell functions in breast cancer.

We have demonstrated that an intact microtubule cytoskeleton is required for activation of AKT downstream of IRS-2. The interaction of IRS-2 with microtubules suggests two possible mechanisms for its action. Microtubules may act as a scaffold for an IGF-1R/IRS-2 signaling complex, bringing together kinases and their substrates in close proximity. Such a mechanism has been suggested previously for IRS-1 and insulin receptor signaling [124]. Alternatively, but possibly not mutually exclusive, the ability of IRS-2 to traffic along the microtubules may be required for proper activation of AKT. Our data suggest that an intact microtubule cytoskeleton is required for the trafficking of the internalized IGF-1R as microtubule disruption results in an accumulation of the activated receptor, likely because it is no longer being targeted for a degradation pathway. Internalization may allow trafficking of the activated receptor along the microtubules to a subcellular location where signaling to activate AKT can occur, and this is regulated by its interaction with IRS-2. Our finding that IRS-2 associates with the kinesin KIF2A suggests a potential mechanism for the role of the microtubules in supporting signaling through IRS-2. Kinesins generally function in anterograde transport of protein complexes and vesicles, suggesting an involvement in trafficking IRS-2 toward the plasma membrane where it can interact with IGF-1R and become phosphorylated. However, the kinesin-13 family to which KIF2A belongs is also characterized by tubulin depolymerizing activity [129, 171]. Depolymerization of tubulin at microtubule plus ends might allow for limited retrograde movement to bring two vesicles together or to “pull” a vesicle containing the internalized receptor into the cell. Another kinesin, KIF3, has been shown to facilitate the translocation of endosomal vesicles containing GLUT4 to

the cell surface for exocytosis in response to insulin; and in preadipocytes, KIF3A facilitates recruitment and activation of IRS-1 to the microtubules at the basal body of the primary cilium to promote activation of AKT [166, 167]. If KIF2A has a similar role in IGF-1R/IRS-2 signaling, the microtubules are likely serving both purposes, as a scaffold to organize signaling complexes and as a pathway for trafficking of signaling components to specific subcellular locations.

The association of IRS-2 with microtubules and the kinesin KIF2A suggests a mechanism underlying the differing functions of IRS-1 and IRS-2 in breast carcinoma cells. Whereas IRS-2 is closely associated with the cytoskeleton and appears to require intact microtubules for proper signaling, IRS-1 does not co-localize with tubulin or interact with KIF2A, consistent with a previous report that IRS-1 function and localization is not microtubule-dependent [172]. Localization of these two proteins to distinct subcellular compartments in breast carcinoma cells could impact access to substrates and signaling outcomes, explaining their divergent roles in breast cancer. Specifically, the unique association of IRS-2 with microtubules could explain this protein's ability to support signaling for motility, metabolism, and tumor progression. For example, motility and invasion require a dynamic cytoskeleton, which is mediated in part by microtubules and microtubule-associated proteins. In addition to interacting with KIF2A, we discovered that IRS-2 also associates with CLIP-170, a plus-end binding protein involved in tip dynamics. CLIP170 has been shown to regulate invasion in MDA-MB-231 cells through interactions with Rac1 [173]. With regard to metabolism,

we have previously reported that trafficking of glucose transporter 1 (GLUT1) to the cell surface is dependent on IRS-2 and is regulated by PI3K/mTor signaling [59]. GLUT4 translocation to the membrane in adipocytes has been shown to be dependent on intact microtubules, suggesting that IRS-2 may regulate GLUT1 translocation by directing movement of vesicles along microtubules to the plasma membrane [59, 174]. Future studies will be needed to explore the role of microtubule integrity and association with IRS-2 on invasion and motility, glycolysis, and GLUT1 trafficking.

In our model system, IGF-1-induced phosphorylation of mTOR at the mTORC2-associated site S2481 was regulated by both IRS-2 and microtubule integrity. Consistent with this finding, the mTORC2 component rictor partially localizes along microtubules. To our knowledge, regulation of mTORC2 activity by either IRS-2 or the microtubules is a novel finding. Our study of a panel of breast carcinoma and mammary tumor cell lines suggests that this regulation is likely cell type dependent, as this phenomenon was only detected in the cell lines that respond to nocodazole by downregulating AKT and that have demonstrated a preference for IRS-2 in mediating signaling downstream of IGF-1R (Table 3.1). Further studies will be needed to confirm that S2481 phosphorylation on mTOR does in fact define activation of mTORC2 in this system. In addition, the effect of microtubule disruption on the activation of other downstream effectors of mTORC2, such as the AGC kinases Serum- and Glucocorticoid-induced Protein Kinase 1 (SGK1) and Protein Kinase C (PKC) should be assessed to understand the full impact of IRS-2/microtubule-dependent signaling in breast carcinoma cells [83, 86].

The results of our study have implications for the use of microtubule-disrupting drugs, such as vinblastine, for the treatment of breast cancer. Our data indicate that signaling through IRS-2 is associated with tumor cell response to these drugs, whereas signaling through alternate pathways, such as through IRS-1, is independent of microtubules and unaffected by these chemotherapeutic drugs. These differential responses raise the possibility that IRS-2 expression or activation could be used as a biomarker to identify patients for treatment with these drugs. We reported previously that expression of IRS-2 at the cell membrane is associated with a statistically significant decrease in overall survival in breast cancer patients [161]. We hypothesize that IRS-2 at the cell membrane is indicative of active signaling, and patients with this staining pattern may be more sensitive to microtubule-disrupting drugs than patients without active IRS-2 signaling. In order to test this hypothesis, a large cohort of patients, as well as accurate treatment and recurrence information, would be required in order to draw the appropriate correlations with statistical significance. The results of our study are consistent with the work of other groups that suggest that AKT plays a central role in the tumor cell response to microtubule-disrupting drugs [175-178]. Our data reveal that the mechanism by which a tumor cell upregulates AKT activity will also influence response to these drugs. Finally, there is evidence to support that the expression of KIF2A, which has microtubule depolymerizing activity, may influence tumor cell response to microtubule disrupting drugs [179]. Therefore, the interaction of IRS-2 with KIF2A may also contribute to its impact on sensitivity to these drugs, and assessing KIF2A expression may also aid in the selection of patients for treatment.

ACKNOWLEDGEMENTS

This work was supported by National Institute of Health (NIH) grants CA090583 and CA142782 (LMS) and Department of Defense Breast Cancer Predoctoral Fellowship W81XWH-10-1-0038 (JLC). LMS is a member of the University of Massachusetts Diabetes and Endocrinology Research Center (DERC) (DK32520) and the University of Massachusetts Memorial Cancer Center of Excellence. I also acknowledge the assistance of Stephen Doxsey and his laboratory at UMass Medical School for sharing both helpful advice and reagents.

CHAPTER IV

Discussion

Summary of Findings

I have examined the localization of insulin receptor substrate-2 (IRS-2) in breast cancer and its relevance to downstream signaling, response to therapy, and patient outcomes. In human breast tumors, IRS-2 exhibited three distinct staining patterns: diffuse cytoplasmic, punctate cytoplasmic, and at the plasma membrane [161]. The plasma membrane staining pattern was associated significantly with poor overall survival, particularly when examined in combination with progesterone receptor (PR) negativity [161]. In contrast, patients whose tumors exhibited diffuse cytoplasmic staining trended toward improved survival outcomes [161]. In human breast carcinoma cell lines, IRS-2 was found specifically to associate with the microtubules. Upon disruption of the microtubule cytoskeleton, insulin-like growth factor-1- (IGF-1)-induced activation of AKT and mTORC2 was suppressed, suggesting that the microtubules are required for signaling downstream of IRS-2. In support of a trafficking mechanism, IRS-2 was found to interact with the microtubule motor protein KIF2A, whose suppression results in a partial inhibition of AKT phosphorylation. Cell cycle analysis also revealed that suppression of IRS-2 in the nocodazole-sensitive MDA-MB-231 cell line resulted in a relative resistance to drug-induced cell death. Taken together, my data suggest that signaling through IRS-2 to AKT is microtubule-dependent and denotes sensitivity to microtubule disruption.

Explanation for Divergent Roles of IRS-1 and IRS-2

The results of my studies have uncovered an explanation for the divergent roles of IRS-1 and IRS-2 in breast cancer despite sequence homology and similar activities. Differential localization of IRS-1 and IRS-2 appears to direct differential signaling. Specifically, signaling to AKT and mTOR through IRS-2 is microtubule-dependent, whereas signaling through IRS-1 is not. Disruption of the association of IRS-2 with microtubules and microtubule associated proteins (MAPs) results in a partial inhibition of downstream signaling, while signaling through IRS-1 is unaffected. My results suggest that the unique localization of IRS-2 to the microtubules directs its signaling and functions.

I hypothesize that the unique ability of IRS-2 to promote movement, whether in the form of cell motility, local invasion, or distant metastasis, is due to its association with the microtubule cytoskeleton. IRS-2 may play a special role in the dynamic changes which take place during cell movement, especially considering its association with the tubulin depolymerase KIF2A. In addition, the ability of IRS-2 to regulate GLUT1 trafficking, likely along microtubules, may be due to its localization there. The signals which IRS-2 promotes from the cytoskeleton for glucose transport and glycolysis might be involved in producing the local chemical changes that allow destruction of the basement membrane and subsequent invasion. The same signals may be transmitted through IRS-1, but in contrast, localization of these signals to an alternative cytosolic compartment or to the nucleus would result in a very different cellular outcome. In order

to fully evaluate this hypothesis, a similar study to my own would have to be performed for IRS-1. The specific compartment to which IRS-1 is localized in the cytoplasm should be identified and this localization similarly disrupted in order to evaluate the role of that localization in directing downstream signaling. If possible, pending identification of the domains which specify localization, IRS-1 could be forced to the cytoskeleton and IRS-2 to the as of yet unidentified compartment to which IRS-1 normally localizes to determine if localization does in fact define the signaling capabilities of these two proteins.

Clinical Relevance of IRS-2 Expression Patterns in Tumors

Localization of IRS-2 to the plasma membrane in a set of invasive tumors was associated with poor survival, both in the entire tumor set and in the PR negative (PR-) subset [161]. We and others have previously reported that IRS-2 is associated with motility, invasion, and aerobic glycolysis, all mediators of tumor progression [56, 59, 60, 67], and we have shown in a mouse model that *Irs-2* is a promoter of tumor metastasis [54]. Taken together, we hypothesize that the plasma membrane staining pattern, which is associated with poor prognosis, likely represents enhanced IRS-2 activity, perhaps due to interaction with membrane-bound receptors [161]. In contrast, the diffuse cytoplasmic pattern was associated with improved survival, indicating that IRS-2 may be inactive in this context [161]. Further studies are warranted to determine if these expression patterns represent IRS-2 activation status, ideally through direct evaluation of IRS-2 phosphorylation either through phosphotyrosine immunoblot of IRS-2 immunoprecipitates from tumor lysates or through production of a specific phospho-IRS-

2 antibody for direct evaluation of tumor lysates or paraffin sections. Alternatively, pathway activation could be studied through evaluation of IGF-1R β activation in the same manner.

It is plausible that IRS-2 expression patterns in breast tumors might be useful as biomarkers following a larger, long-term study. Although the membrane staining pattern was associated with poor survival in the entire dataset, the potential use of IRS-2 as a biomarker may be most useful for PR- disease, as the membrane staining pattern was only found to be statistically significant within this subgroup upon multivariate analysis compared to other prognostic indicators (ie. node status, estrogen receptor (ER) expression, HER2 expression, etc.) [161]. The ability to predict better or worse survival is particularly useful in the PR- setting, as these aggressive tumors are associated with poor survival rates and more recurrent disease [151-153]. A patient lacking the membrane staining pattern that is statistically more likely to survive PR- disease might warrant more aggressive (and subsequently more toxic) treatment, as the survival benefit might outweigh the morbidity associated with drug toxicity. Alternatively, the membrane staining pattern may denote a particularly aggressive PR- tumor, warranting more aggressive treatment, while a patient with PR- disease lacking the IRS-2 membrane staining pattern might forgo such treatment due to their improved prognosis. Further studies analyzing detailed treatment outcomes are required to determine how IRS-2 staining pattern information might be used to predict patient response to conservative versus aggressive treatment approaches in patients with PR- breast cancer.

IRS-2 expression patterns might also be of clinical utility in guiding more specific treatment decisions. My studies have shown that IRS-2 activity is associated with more cell death in response to treatment with microtubule-disrupting drugs. If the plasma membrane expression pattern is indeed representative of active IRS-2, then by extension, this pattern would represent enhanced sensitivity to microtubule-disrupting drugs like vinorelbine, a vinca alkaloid commonly used in the treatment of breast cancer [114]. Likewise, patients whose tumors exhibit diffuse cytoplasmic IRS-2, which we hypothesize is inactive, might be poor candidates for such treatment because these tumors are less sensitive to cell death and may be more likely to resist treatment. In order to test this hypothesis, further studies would require a large tumor set, ideally with pre- and post-treatment samples. Detailed treatment information, particularly regarding taxane and vinca alkaloid use, would be a necessity. Response versus recurrence could be correlated to IRS-2 expression patterns and activation status to determine if IRS-2 activity dictates response to these drugs. In addition, evaluation of downstream signaling activation, namely AKT phosphorylation, before and after treatment could be correlated to clinical response and development of resistance. Such a study would also serve to elucidate the role of the microtubules and their disruption in the activation of AKT in the context of a tumor *in vivo*, as opposed to cells in culture.

Further Study of the Punctate Cytoplasmic IRS-2 Expression Pattern

The punctate cytoplasmic IRS-2 expression pattern did not correlate significantly with survival in our study, although there was a trend toward improved outcome [161].

We hypothesize that IRS-2 may be associated with an internalized receptor in this context [163]. Electron microscopy of select tumors should be used to determine if this is the case. If so, the question of IRS-2 activity remains. Perhaps the slightly improved survival associated with these tumors is due to a sequestration or degradation of the IRS-2 signal upon internalization with the receptor [164, 180]. It is also possible that IRS-2 is associated with a membrane-bound organelle, independent of receptor internalization, and co-staining with markers of the endosomal compartments and other organelles may be necessary to identify the specific localization of IRS-2 in these tumors. When a specific compartment has been identified, further studies should examine the activity of IRS-2 in that compartment and the impact of this localization on signaling and response to microtubule disruption.

Localization of IRS-2 to an autophagic vesicle is also a possible explanation for the punctate pattern of staining. IRS-2 might be directly involved in the formation or activity of autophagic vesicles. Alternatively, dysregulation of autophagy, as often occurs in tumor cells, might result in an accumulation of autophagic vacuoles which may contain undegraded proteins, including IRS-2 [181]. In either case, correlation of this pattern to tumor aggressiveness and prognosis would be difficult, as autophagy is associated with both oncogenic and tumor suppressive activity [181]. Interestingly, *in vitro* treatment of cancer cells with nocodazole or vinblastine causes an accumulation of ineffective autophagic vacuoles containing undigested protein. Perhaps IRS-2 is an innocent bystander of normal physiology which becomes accumulated in these vesicles in

the tumor cells of patients who have been treated with vinca alkaloids [182, 183]. Regarding this possibility, treatment information should be obtained for the patients in my study whose tumors exhibited the punctate IRS-2 staining pattern. In addition, these tumors could be evaluated for a marker of autophagy like light chain 3 (LC3), including co-immunofluorescence studies with IRS-2 to determine if IRS-2 is co-localized with an autophagic vesicle.

The Role of the Microtubules in AKT Activation

Several groups have demonstrated a role for the microtubules in signaling through the PI3K/AKT axis. Eyster, et al. suggest that the microtubules provide a surface for the insulin signaling complex and insulin-stimulated GLUT4 trafficking [124]. In cells with constitutively active AKT signaling, inhibition of this pathway with the PI3K inhibitor LY294002 destabilizes microtubules, resulting in an enhanced apoptotic response to microtubule-disrupting drugs [184]. Hyperactivation of AKT has been shown to increase resistance to chemotherapeutics which disrupt microtubules [185]. Consistent with my findings, treatment of both normal endothelial cells and tumor cells with drugs that disrupt microtubules have been shown to downregulate AKT [186, 187]. This downregulation similarly enhances apoptosis [186]. Also consistent with my study, no effect of these drugs was found on a panel of other kinases [187].

In this study, I have uncovered a role for the microtubules in the activation of AKT specifically downstream of IRS-2. Interestingly, this phenomenon was only

observed in cell lines that predominantly signal through IRS-2, as opposed to other adaptors, such as IRS-1. The unique localization of IRS-2 to the microtubules suggests that the association of IRS-2 with microtubules, or a MAP, may be required for AKT activation. Indeed, IRS-2 was found to interact with the motor protein KIF2A, and suppression of KIF2A partially decreased activation of AKT upon stimulation with IGF-1. Furthermore, the association of IRS-2 with KIF2A was unique. No such association was detected with IRS-1, further supporting the IRS-2-specific nature of microtubule-dependent AKT activation.

It has been shown that IGF-1R internalization supports sustained phosphorylation of AKT and that blocking internalization prevents AKT activation [150]. It has also been shown that AKT moves toward the plasma membrane upon stimulation [188]. Based on those findings, I propose a model in which trafficking of AKT along microtubules into the vicinity of the internalized receptor is required for phosphorylation and activation of the protein downstream of IRS-2. When trafficking is disrupted, with a microtubule-disrupting drug, for example, the receptor cannot be internalized, nor can AKT be trafficked to the activated receptor.

Internalization and trafficking must not be required for upstream events, as microtubule disruption has no effect on IRS tyrosine phosphorylation or association with PI3K. Once activated upon IGF-1 stimulation, IRS-2 would partially facilitate the trafficking of this IGF-1R-containing vesicle into the cell through its association with the

microtubule depolymerase KIF2A. Alternatively, KIF2A may cooperate with a retrograde motor during internalization, as has been suggested for kinesin-3 in retrograde transport of endosomes [189]. The upstream signaling complex is now sitting on the microtubule, providing a surface for the interaction of downstream signaling proteins, including PDK1, which will associate with phosphatidylinositol (3,4,5)-trisphosphate (PIP₃) on the outer membrane of the internalized vesicle, and its target threonine 308 (T308) on AKT which is itself trafficked toward the membrane and associates with PIP₃ under stimulatory conditions. Phosphorylation of AKT at the mTORC2-dependent serine 473 (S473) site is similarly microtubule-dependent and requires trafficking of AKT along microtubules. My work has shown that mTOR and rictor associate with the microtubules in MDA-MB-231 cells, and this localization likely dictates that intact microtubules and the ability of AKT to traffic are required for S473 phosphorylation by mTORC2. The proposed model of AKT activation is outlined in Figure 4.1.

Potential Relevance of KIF2A in Breast Cancer

KIF2A is a member of the kinesin-13 family, a group of motor proteins with adenosine triphosphatase (ATPase) activity involved in microtubule trafficking and regulation of the mitotic spindle [190]. While all kinesins have tubulin depolymerizing activity at plus ends, kinesin-13 members are uniquely capable of depolymerizing tubulin at both the minus and plus ends of microtubules [191, 192]. The localization and activity of KIF2A is partially modulated by phosphorylation [190]. Phosphorylation at the serine 196 (S196) site by Aurora B results in a downregulation of depolymerizing activity [193].

Figure 4.1. Model of IRS-2-mediated AKT activation

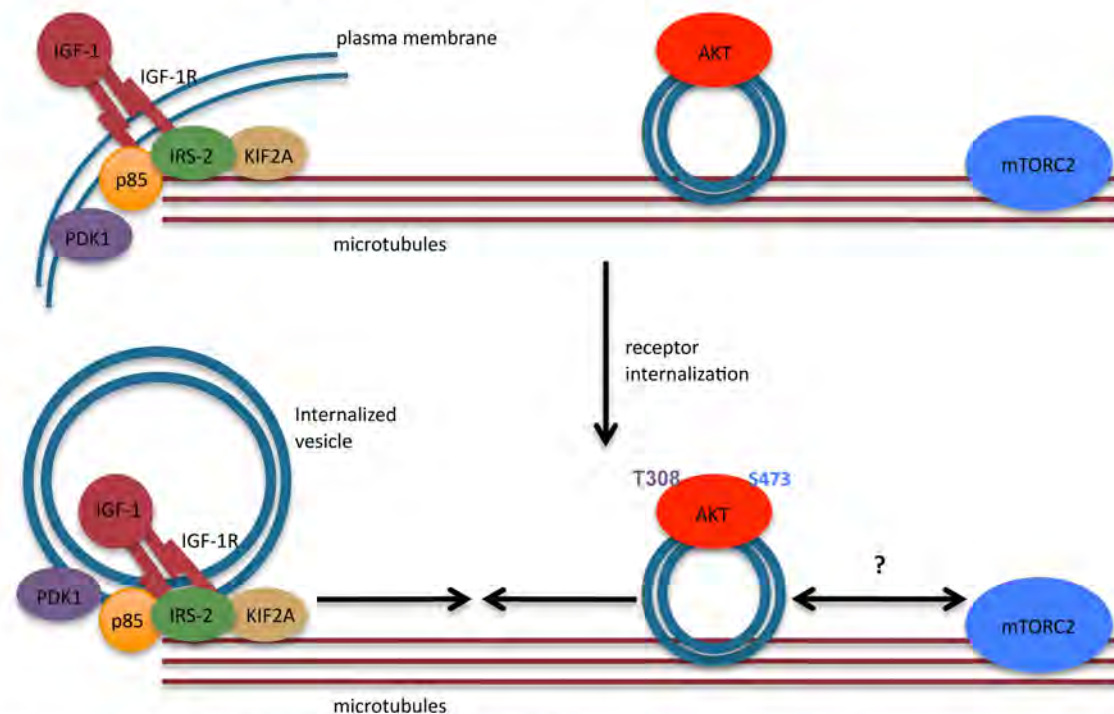


Figure 4.1. Model of IRS-2-mediated AKT activation. IRS-2 associates with the activated IGF-1R at the plasma membrane. IRS-2 is phosphorylated by the receptor tyrosine kinase and becomes active, recruiting the p85 subunit of PI3K. The receptor and signaling complex is internalized, likely due in part to the association of IRS-2 with KIF2A and the microtubules. The signaling complex may then come into contact with AKT, which is also trafficked along microtubules, allowing phosphorylation of T308 by PDK1. mTORC2 is also associated with the microtubules and phosphorylates S473 on AKT through a microtubule-dependent mechanism.

Association with binding partners, particularly plus end binding proteins, further modulates the activities of kinesin-13 family members [190]. In this regard, it is possible that KIF2A interacts with CLIP170, as I have shown both of these proteins to be associated with IRS-2.

The kinesin-13 family member mitotic centromere-associated kinesin (MCAK) has been correlated to tumor progression and poor survival in a variety of studies [194]. *In vitro* studies found that suppression of MCAK inhibited the growth of breast cancer cells [195]. KIF2A has not been well studied in this context, but one group did find that overexpression of KIF2A was associated with lymph node metastasis and advanced stage in oral cancer [168]. In terms of treatment, KLP10A, a kinesin-13 family member in *Drosophila* is associated with sensitivity to colchicine [179]. The authors of that study suggest that overexpression of tubulin depolymerizing kinesins result in a tubulin destabilization that sensitizes cells to pharmacologic microtubule disruption [179].

The unique ability of IRS-2 to promote motility and invasion may be due not only to its association with microtubules, as discussed previously, but also to its interaction with KIF2A. In HeLa cells, suppression of KIF2A expression by microRNA-183 (miR-183) is associated with decreased migration [196]. Other kinesins have also been implicated in migration and invasion. In pancreatic cancer cells, treatment with the compound dimethylenastron inhibits both migration and invasion by targeting KIF11 [170]. Overexpression of KIF18A in colorectal cancer cells enhances migration and

invasion, while suppression of this kinesin results in the opposite effect [197]. The microtubule depolymerase activities of KIF2A, which may be modulated in part by its association with components of the IGF-1 signaling pathway, may play a role in the dynamic changes in cytoskeletal structure which take place at the leading edge of a migrating and/or invading cell.

KIF2A expression in breast tumors may also be useful as a biomarker of drug sensitivity. The depolymerizing activity of KIF2A may be partially responsible for the sensitivity of MDA-MB-231 cells to microtubule-disrupting drugs observed in my studies. As phosphorylation of KIF2A at the S196 site is associated with inhibition of depolymerizing activity, this site could be evaluated in our system and in tumor samples to determine if KIF2A depolymerase is active. If KIF2A is partially responsible for sensitivity to nocodazole treatment, low levels of S196 phosphorylation would be expected in sensitive cell lines like MDA-MB-231 and PyVMT: *Irs-1*^{-/-} and higher phosphorylation levels (or low total KIF2A levels) in resistant cell lines like SUM159 and PyVMT: *Irs-2*^{-/-}. Taking a step further, based on our hypothesis that the membrane expression pattern of IRS-2 in tumors is associated with active signaling and enhanced susceptibility to microtubule disruption, high total KIF2A levels and/or low KIF2A phosphorylation would be expected. A patient study might evaluate both total and phosphorylated KIF2A in a large set of breast tumors and draw correlations to IRS-2 expression patterns and activation, AKT phosphorylation, and sensitivity to treatment with vinca alkaloids.

Potential Role of Microtubules in Differential Signaling to AKT Substrates

The association of IRS-2 with microtubules appears to direct specific signals downstream of this protein, as opposed to the related IGF-1R adaptor IRS-1. I hypothesize that the microtubules further direct differential signaling downstream of AKT. One study of a panel of drugs found that vinblastine, but not taxol, treatment of osteosarcoma cells causes the nuclear accumulation of the forkhead family transcription factor FOXO, which regulates cell cycle progression and survival [198, 199]. Unphosphorylated FOXO is active in the nucleus, and upon phosphorylation by AKT, FOXO activity is inhibited by nuclear export [199]. It has also been reported that AKT phosphorylated on T308 only, lacking phosphorylation of the mTORC2-dependent S473 site, is unable to phosphorylate FOXO, although other AKT targets remain activated [200]. Taken together, this suggests that the microtubules are required specifically for phosphorylation of FOXO by AKT and that this may be due to a requirement of intact microtubules by mTORC2 for the S473 phosphorylation on AKT. Further studies should disrupt mTORC2 in my system without disrupting the cytoskeleton to determine if AKT deficient in S473 phosphorylation only can still target FOXO in the presence of intact microtubules.

Novel Finding that Microtubules May Be Required for mTORC2 Activation

We report in this study the novel finding that an intact microtubule cytoskeleton is required for activation of mTORC2. Relatively little is known about the activation and activities of this complex. One study has implicated the ribosome in activation [89]. The

authors of that study found that the active complex physically interacts with the ribosome and that this interaction was modulated by insulin signaling [89]. My findings do not exclude a role for the ribosome, as ribosomes have been shown to interact with microtubules and MAPs [201, 202]. In my study, I found specifically that microtubules are required for the mTORC2-associated phosphorylation on mTOR at serine 2481 (S2481), as well as the mTORC-2 dependent S473 phosphorylation site on AKT. Further studies are warranted to determine if the S2481 site is truly associated with complex formation and activity in my system, as well as to determine if the effects of microtubule disruption on mTORC2 activity are AKT specific or extend to other mTORC2 targets, such as Protein Kinase C- α (PKC- α). The important question remains whether the microtubules directly activate mTORC2 or if they simply serve as a scaffold for the interaction of mTORC2 with ribosomes or other activating proteins unknown at this time. Disruption of the ribosome-microtubule interaction without disrupting microtubule architecture should elucidate the role of this interaction in mTORC2 activation.

Overall Significance

The results of my study of IRS-2 expression patterns in breast tumors indicate that the plasma membrane localization of this protein is associated with poor survival, particularly in PR- disease. Furthermore, this marker subdivides PR- tumors into better and worse survival groups, separating more aggressive disease from less aggressive, PR+-like disease. Following further studies, IRS-2 localization patterns could be used as a biomarker to predict patient outcomes in breast cancer patients with PR- tumors.

The current use of ER, PR, and HER2 as markers of prognosis and sensitivity to treatment has significant limitations, as patient outcomes frequently fail to match the prognosis predicted by receptor status. This is particularly true of PR- disease, as the mechanisms of PR loss vary widely [155]. Given these limitations, the ability to more accurately predict survival in this aggressive cancer subtype could be of great usefulness in the clinic to guide treatment appropriate to the true prognosis.

The results of my studies have further implications for the understanding of signaling through IRS-2, particularly the involvement of IRS-2 in AKT activation. Although it has been previously reported that the microtubules are required for activation of AKT in certain cell types and contexts [186, 187], I report the novel finding that signaling specifically through IRS-2 is microtubule-dependent. As AKT regulates a wide number of signals for a variety of functions, knowledge of the mechanisms of AKT regulation is important for the development of new cancer therapies and circumventing resistance. In addition, these results suggest another potential use for IRS-2 as a biomarker in breast cancer, as IRS-2 activity may be associated with enhanced response to microtubule-disrupting chemotherapy, such as vinorelbine treatment. This finding could make vinorelbine, commonly used in the advanced stages of the disease, a first-line treatment for certain patients who may subsequently have improved outcomes.

I have also uncovered a role for the kinesin and microtubule depolymerase KIF2A in the IRS-2-mediated activation of AKT. Not only does this finding have potential

implications for therapy with microtubule-affecting drugs, but KIF2A might also be used as a biomarker, differentiating tumors which might be more or less susceptible to treatment with taxanes or vinca alkaloids. Furthermore, these results link signaling to microtubule dynamics, providing a partial explanation for IRS-2-mediated motility and invasion and contributing to the general knowledge of these events in cancer.

Finally, I report the novel finding that both IRS-2 and microtubules regulate mTORC2 activity. Though others have reported a potential role for the ribosome or PIP3 in mTORC2 activation, very little is known about the mechanism by which this complex is activated or its activities [89, 90]. In addition, I report that two complex components, rictor and mTOR, are associated with the microtubule cytoskeleton, also a novel finding to our knowledge. Though mTORC2 has been implicated in the regulation of the actin cytoskeleton and has been associated with an actin cytoskeletal fraction in cell lysates [87, 203, 204], this result suggests that mTORC2 might also regulate the microtubule cytoskeleton, suggesting a broader role for this complex in the regulation of trafficking and cell architecture previously unknown.

APPENDIX***Interaction of Insulin Receptor Substrate-2 (IRS-2) with
mTORC2***

To determine if IRS-2 and rictor interact, IRS-2 was immunoprecipitated from MDA-MB-231 cell lysates, and associated proteins were analyzed by Western blot. Rictor, but not the mTORC1 component raptor, co-immunoprecipitated with IRS-2 (Figure A.1a). Serum starvation and IGF-1 stimulation have no effect on the degree of interaction, and the interaction is maintained upon microtubule disruption with nocodazole. When cell extraction was performed using a buffer containing CHAPS instead of NP-40, which preserves mTOR-rictor interactions, mTOR also co-immunoprecipitated with IRS-2 (Figure A.1b). These results suggest that an IRS-2/mTORC2 complex is localized to the microtubule cytoskeleton.

The interaction of IRS-2 with rictor in this system might be responsible for the microtubule dependence of mTORC2 activation and subsequent AKT phosphorylation on serine 473 (S473). This might also explain why phosphorylation on both threonine 308 (T308) and S473 on AKT require intact microtubules. AKT must traffick along microtubules in order to associate with both the internalized receptor vesicle to which PDK1 is likely localized, as well as mTORC2 which is partially localized to the microtubules. IRS-2 may coordinate both events through its association with the microtubules and the kinesin KIF2A, linking the cytoskeleton to both upstream and downstream IGF-1 signaling events.

An association of IRS-2 with rictor has been previously reported in the nucleus in a mouse model of diabetic nephropathy [205]. In this study, the presence of the nuclear

IRS-2-ricor complex was associated with accumulation of activated Protein Kinase C (PKC) in the nucleus, which the authors suggest might modulate gene transcription [205]. It is possible that localization of an IRS-2-mTORC2 complex to the microtubules is directing a specific downstream signal from that compartment. The results of my studies would suggest that AKT is the preferential mTORC2 target downstream of the microtubules. Other downstream signals should also be examined, to determine if localization of this complex directs differential signaling.

Figure A.1. Association of IRS-2 with mTORC2

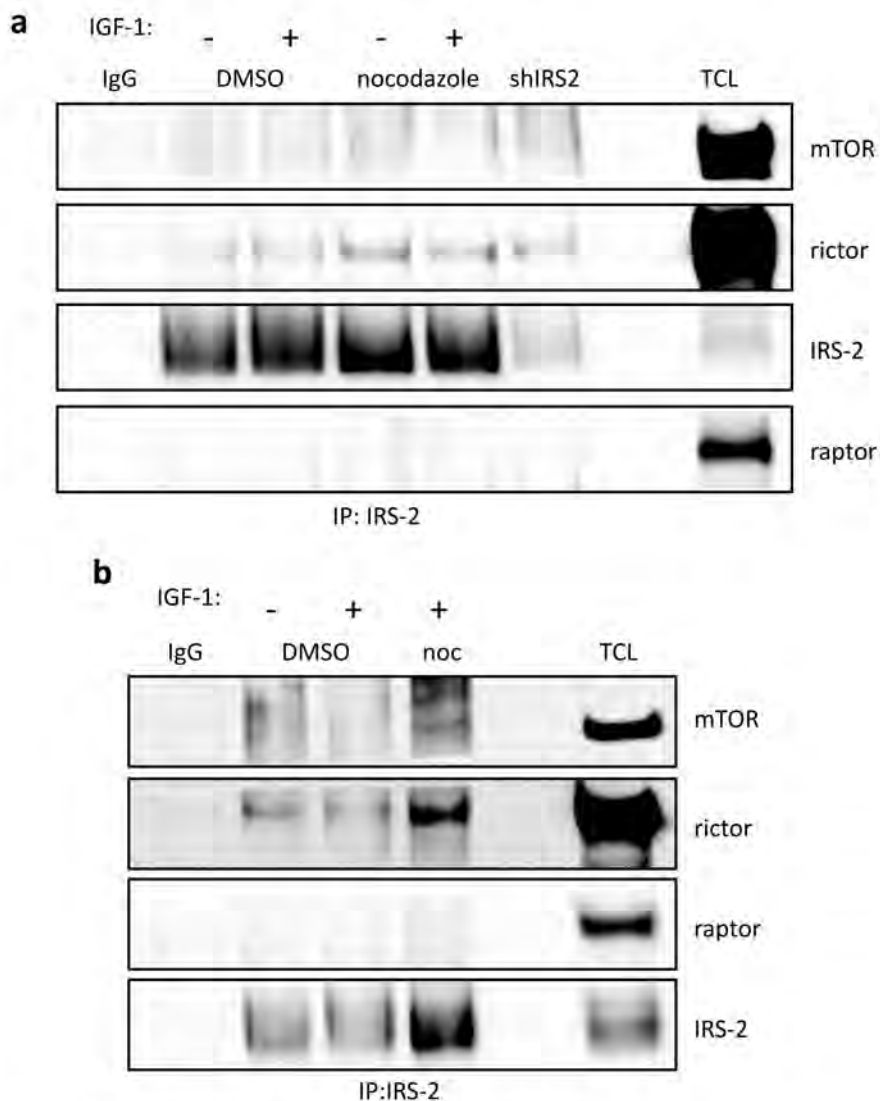


Figure A.1. Association of IRS-2 with mTORC2. MDA-MB-231 cells treated with DMSO (control) or 1 μ M nocodazole for 30 minutes or expressing an shRNA specific for IRS-2 were then stimulated with IGF-1 (20 ng/ml) for 5 minutes. Aliquots of the NP-40 buffer (a) or CHAPS buffer (b) cell extracts containing equivalent amounts of total protein were immunoprecipitated with antisera specific for IRS-2 and immunoblotted with antibodies specific for mTOR, rictor, and raptor. The rictor immunoblots were subsequently stripped and reprobbed with IRS-2-specific antibodies. TCL, total cell lysate. IgG, negative control immunoprecipitation.

BIBLIOGRAPHY

1. ACS, *Breast Cancer Facts & Figures 2011-2012*, 2011, American Cancer Society, Inc.: Atlanta.
2. Chaffer, C.L. and R.A. Weinberg, *A perspective on cancer cell metastasis*. Science, 2011. **331**(6024): p. 1559-64.
3. Hankinson, S.E., et al., *Circulating concentrations of insulin-like growth factor-I and risk of breast cancer*. Lancet, 1998. **351**(9113): p. 1393-6.
4. Peyrat, J.P., et al., *Plasma insulin-like growth factor-I (IGF-I) concentrations in human breast cancer*. Eur J Cancer, 1993. **29A**(4): p. 492-7.
5. Papa, V., et al., *Insulin-like growth factor-I receptors are overexpressed and predict a low risk in human breast cancer*. Cancer Res, 1993. **53**(16): p. 3736-40.
6. Resnik, J.L., et al., *Elevated insulin-like growth factor I receptor autophosphorylation and kinase activity in human breast cancer*. Cancer Res, 1998. **58**(6): p. 1159-64.
7. Dunn, S.E., et al., *A dominant negative mutant of the insulin-like growth factor-I receptor inhibits the adhesion, invasion, and metastasis of breast cancer*. Cancer Res, 1998. **58**(15): p. 3353-61.
8. Stewart, A.J., et al., *Role of insulin-like growth factors and the type I insulin-like growth factor receptor in the estrogen-stimulated proliferation of human breast cancer cells*. J Biol Chem, 1990. **265**(34): p. 21172-8.
9. Lee, A.V., et al., *Activation of estrogen receptor-mediated gene transcription by IGF-I in human breast cancer cells*. J Endocrinol, 1997. **152**(1): p. 39-47.
10. Siddle, K., *The insulin receptor and type I IGF receptor: comparison of structure and function*. Prog Growth Factor Res, 1992. **4**(4): p. 301-20.
11. Jones, J.I. and D.R. Clemmons, *Insulin-like growth factors and their binding proteins: biological actions*. Endocr Rev, 1995. **16**(1): p. 3-34.
12. Gullu, G., S. Karabulut, and M. Akkiprik, *Functional roles and clinical values of insulin-like growth factor binding protein-5 in different types of cancers*. Chin J Cancer, 2012.
13. Rosendahl, A.H., et al., *IGFBP1 and IGFBP3 polymorphisms predict circulating IGFBP-3 levels among women from high-risk breast cancer families*. Breast Cancer Res Treat, 2011. **127**(3): p. 785-94.
14. Akkiprik, M., et al., *Multifunctional roles of insulin-like growth factor binding protein 5 in breast cancer*. Breast Cancer Res, 2008. **10**(4): p. 212.
15. Li, X., et al., *Expression level of insulin-like growth factor binding protein 5 mRNA is a prognostic factor for breast cancer*. Cancer Sci, 2007. **98**(10): p. 1592-6.
16. Dokmanovic, M., et al., *Trastuzumab regulates IGFBP-2 and IGFBP-3 to mediate growth inhibition: implications for the development of predictive biomarkers for trastuzumab resistance*. Mol Cancer Ther, 2011. **10**(6): p. 917-28.

17. Mohanraj, L. and Y. Oh, *Targeting IGF-I, IGF-BPs and IGF-I receptor system in cancer: the current and future in breast cancer therapy*. Recent Pat Anticancer Drug Discov, 2011. **6**(2): p. 166-77.
18. Becker, M.A., et al., *IGFBP ratio confers resistance to IGF targeting and correlates with increased invasion and poor outcome in breast tumors*. Clin Cancer Res, 2012.
19. Ahn, B.Y., et al., *Genetic screen identifies insulin-like growth factor binding protein 5 as a modulator of tamoxifen resistance in breast cancer*. Cancer Res, 2010. **70**(8): p. 3013-9.
20. Oh, Y., et al., *Antiproliferative actions of insulin-like growth factor binding protein (IGFBP)-3 in human breast cancer cells*. Prog Growth Factor Res, 1995. **6**(2-4): p. 503-12.
21. Oh, Y., et al., *Demonstration of receptors for insulin-like growth factor binding protein-3 on Hs578T human breast cancer cells*. J Biol Chem, 1993. **268**(35): p. 26045-8.
22. Pratt, S.E. and M.N. Pollak, *Insulin-like growth factor binding protein 3 (IGFBP3) inhibits estrogen-stimulated breast cancer cell proliferation*. Biochem Biophys Res Commun, 1994. **198**(1): p. 292-7.
23. Huynh, H., X.F. Yang, and M. Pollak, *A role for insulin-like growth factor binding protein 5 in the antiproliferative action of the antiestrogen ICI 182780*. Cell Growth Differ, 1996. **7**(11): p. 1501-6.
24. Schedlich, L.J., et al., *Insulin-like growth factor-binding protein (IGFBP)-3 and IGFBP-5 share a common nuclear transport pathway in T47D human breast carcinoma cells*. J Biol Chem, 1998. **273**(29): p. 18347-52.
25. Butt, A.J., et al., *Enhancement of tumor necrosis factor-alpha-induced growth inhibition by insulin-like growth factor-binding protein-5 (IGFBP-5), but not IGFBP-3 in human breast cancer cells*. Endocrinology, 2005. **146**(7): p. 3113-22.
26. Pessin, J.E. and A.L. Frattali, *Molecular dynamics of insulin/IGF-I receptor transmembrane signaling*. Mol Reprod Dev, 1993. **35**(4): p. 339-44; discussion 344-5.
27. Sawka-Verhelle, D., et al., *Insulin receptor substrate-2 binds to the insulin receptor through its phosphotyrosine-binding domain and through a newly identified domain comprising amino acids 591-786*. J Biol Chem, 1996. **271**(11): p. 5980-3.
28. Backer, J.M., C. Wjasow, and Y. Zhang, *In vitro binding and phosphorylation of insulin receptor substrate 1 by the insulin receptor. Role of interactions mediated by the phosphotyrosine-binding domain and the pleckstrin-homology domain*. Eur J Biochem, 1997. **245**(1): p. 91-6.
29. Dey, B.R., et al., *Evidence for the direct interaction of the insulin-like growth factor I receptor with IRS-1, Shc, and Grb10*. Mol Endocrinol, 1996. **10**(6): p. 631-41.
30. Sun, X.J., et al., *Role of IRS-2 in insulin and cytokine signalling*. Nature, 1995. **377**(6545): p. 173-7.

31. Hadari, Y.R., et al., *Insulin and insulinomimetic agents induce activation of phosphatidylinositol 3'-kinase upon its association with pp185 (IRS-1) in intact rat livers*. J Biol Chem, 1992. **267**(25): p. 17483-6.
32. Auger, K.R., et al., *PDGF-dependent tyrosine phosphorylation stimulates production of novel polyphosphoinositides in intact cells*. Cell, 1989. **57**(1): p. 167-75.
33. Mardilovich, K., S.L. Pankratz, and L.M. Shaw, *Expression and function of the insulin receptor substrate proteins in cancer*. Cell Commun Signal, 2009. **7**: p. 14.
34. White, M.F., *IRS proteins and the common path to diabetes*. Am J Physiol Endocrinol Metab, 2002. **283**(3): p. E413-22.
35. Araki, E., et al., *Alternative pathway of insulin signalling in mice with targeted disruption of the IRS-1 gene*. Nature, 1994. **372**(6502): p. 186-90.
36. Tamemoto, H., et al., *Insulin resistance and growth retardation in mice lacking insulin receptor substrate-1*. Nature, 1994. **372**(6502): p. 182-6.
37. Withers, D.J., et al., *Disruption of IRS-2 causes type 2 diabetes in mice*. Nature, 1998. **391**(6670): p. 900-4.
38. Schubert, M., et al., *Insulin receptor substrate-2 deficiency impairs brain growth and promotes tau phosphorylation*. J Neurosci, 2003. **23**(18): p. 7084-92.
39. Lavan, B.E., W.S. Lane, and G.E. Lienhard, *The 60-kDa phosphotyrosine protein in insulin-treated adipocytes is a new member of the insulin receptor substrate family*. J Biol Chem, 1997. **272**(17): p. 11439-43.
40. Bjornholm, M., et al., *Absence of functional insulin receptor substrate-3 (IRS-3) gene in humans*. Diabetologia, 2002. **45**(12): p. 1697-702.
41. Lavan, B.E., et al., *A novel 160-kDa phosphotyrosine protein in insulin-treated embryonic kidney cells is a new member of the insulin receptor substrate family*. J Biol Chem, 1997. **272**(34): p. 21403-7.
42. Cai, D., et al., *Two new substrates in insulin signaling, IRS5/DOK4 and IRS6/DOK5*. J Biol Chem, 2003. **278**(28): p. 25323-30.
43. White, M.F., *The IRS-signalling system in insulin and cytokine action*. Philos Trans R Soc Lond B Biol Sci, 1996. **351**(1336): p. 181-9.
44. Wu, J., et al., *Structural and biochemical characterization of the KRLB region in insulin receptor substrate-2*. Nat Struct Mol Biol, 2008. **15**(3): p. 251-8.
45. Sun, X.J., et al., *Expression and function of IRS-1 in insulin signal transmission*. J Biol Chem, 1992. **267**(31): p. 22662-72.
46. Tanti, J.F., et al., *Serine/threonine phosphorylation of insulin receptor substrate 1 modulates insulin receptor signaling*. J Biol Chem, 1994. **269**(8): p. 6051-7.
47. Paz, K., et al., *A molecular basis for insulin resistance. Elevated serine/threonine phosphorylation of IRS-1 and IRS-2 inhibits their binding to the juxtamembrane region of the insulin receptor and impairs their ability to undergo insulin-induced tyrosine phosphorylation*. J Biol Chem, 1997. **272**(47): p. 29911-8.
48. Ueno, M., et al., *Regulation of insulin signalling by hyperinsulinaemia: role of IRS-1/2 serine phosphorylation and the mTOR/p70 S6K pathway*. Diabetologia, 2005. **48**(3): p. 506-18.

49. Koda, M., et al., *Expression of insulin receptor substrate 1 in primary breast cancer and lymph node metastases*. J Clin Pathol, 2005. **58**(6): p. 645-9.
50. Rocha, R.L., et al., *Insulin-like growth factor binding protein-3 and insulin receptor substrate-1 in breast cancer: correlation with clinical parameters and disease-free survival*. Clin Cancer Res, 1997. **3**(1): p. 103-9.
51. Slattery, M.L., et al., *Genetic variation in IGF1, IGFBP3, IRS1, IRS2 and risk of breast cancer in women living in Southwestern United States*. Breast Cancer Res Treat, 2007. **104**(2): p. 197-209.
52. Dearth, R.K., et al., *Mammary tumorigenesis and metastasis caused by overexpression of insulin receptor substrate 1 (IRS-1) or IRS-2*. Mol Cell Biol, 2006. **26**(24): p. 9302-14.
53. Byron, S.A., et al., *Insulin receptor substrates mediate distinct biological responses to insulin-like growth factor receptor activation in breast cancer cells*. Br J Cancer, 2006. **95**(9): p. 1220-8.
54. Gibson, S.L., Z. Ma, and L.M. Shaw, *Divergent roles for IRS-1 and IRS-2 in breast cancer metastasis*. Cell Cycle, 2007. **6**(6): p. 631-7.
55. Ibrahim, Y.H., et al., *Progesterone receptor-B regulation of insulin-like growth factor-stimulated cell migration in breast cancer cells via insulin receptor substrate-2*. Mol Cancer Res, 2008. **6**(9): p. 1491-8.
56. Jackson, J.G., et al., *Regulation of breast cancer cell motility by insulin receptor substrate-2 (IRS-2) in metastatic variants of human breast cancer cell lines*. Oncogene, 2001. **20**(50): p. 7318-25.
57. Ma, Z., et al., *Suppression of insulin receptor substrate 1 (IRS-1) promotes mammary tumor metastasis*. Mol Cell Biol, 2006. **26**(24): p. 9338-51.
58. Nagle, J.A., et al., *Involvement of insulin receptor substrate 2 in mammary tumor metastasis*. Mol Cell Biol, 2004. **24**(22): p. 9726-35.
59. Pankratz, S.L., et al., *Insulin receptor substrate-2 regulates aerobic glycolysis in mouse mammary tumor cells via glucose transporter 1*. J Biol Chem, 2009. **284**(4): p. 2031-7.
60. Zhang, X., et al., *Motility response to insulin-like growth factor-I (IGF-I) in MCF-7 cells is associated with IRS-2 activation and integrin expression*. Breast Cancer Res Treat, 2004. **83**(2): p. 161-70.
61. Cesarone, G., et al., *RNAi-mediated silencing of insulin receptor substrate 1 (IRS-1) enhances tamoxifen-induced cell death in MCF-7 breast cancer cells*. J Cell Biochem, 2006. **98**(2): p. 440-50.
62. Mauro, L., et al., *Estradiol increases IRS-1 gene expression and insulin signaling in breast cancer cells*. Biochem Biophys Res Commun, 2001. **288**(3): p. 685-9.
63. Morelli, C., et al., *Nuclear insulin receptor substrate 1 interacts with estrogen receptor alpha at ERE promoters*. Oncogene, 2004. **23**(45): p. 7517-26.
64. Sisci, D., et al., *The estrogen receptor alpha:insulin receptor substrate 1 complex in breast cancer: structure-function relationships*. Ann Oncol, 2007. **18 Suppl 6**: p. vi81-5.

65. Vassen, L., W. Wegrzyn, and L. Klein-Hitpass, *Human insulin receptor substrate-2 (IRS-2) is a primary progesterone response gene*. Mol Endocrinol, 1999. **13**(3): p. 485-94.
66. Cui, X., et al., *Progesterone crosstalks with insulin-like growth factor signaling in breast cancer cells via induction of insulin receptor substrate-2*. Oncogene, 2003. **22**(44): p. 6937-41.
67. Mardilovich, K. and L.M. Shaw, *Hypoxia regulates insulin receptor substrate-2 expression to promote breast carcinoma cell survival and invasion*. Cancer Res, 2009. **69**(23): p. 8894-901.
68. Cui, X., et al., *Epidermal growth factor induces insulin receptor substrate-2 in breast cancer cells via c-Jun NH(2)-terminal kinase/activator protein-1 signaling to regulate cell migration*. Cancer Res, 2006. **66**(10): p. 5304-13.
69. Giovannone, B., et al., *Insulin receptor substrate (IRS) transduction system: distinct and overlapping signaling potential*. Diabetes Metab Res Rev, 2000. **16**(6): p. 434-41.
70. Lee, A.V., et al., *Developmental and hormonal signals dramatically alter the localization and abundance of insulin receptor substrate proteins in the mammary gland*. Endocrinology, 2003. **144**(6): p. 2683-94.
71. Ahmad, S., N. Singh, and R.I. Glazer, *Role of AKT1 in 17beta-estradiol- and insulin-like growth factor I (IGF-I)-dependent proliferation and prevention of apoptosis in MCF-7 breast carcinoma cells*. Biochem Pharmacol, 1999. **58**(3): p. 425-30.
72. Burow, M.E., et al., *PI3-K/AKT regulation of NF-kappaB signaling events in suppression of TNF-induced apoptosis*. Biochem Biophys Res Commun, 2000. **271**(2): p. 342-5.
73. Bacus, S.S., et al., *AKT2 is frequently upregulated in HER-2/neu-positive breast cancers and may contribute to tumor aggressiveness by enhancing cell survival*. Oncogene, 2002. **21**(22): p. 3532-40.
74. Perez-Tenorio, G. and O. Stal, *Activation of AKT/PKB in breast cancer predicts a worse outcome among endocrine treated patients*. Br J Cancer, 2002. **86**(4): p. 540-5.
75. Sokolosky, M.L., et al., *Involvement of Akt-1 and mTOR in sensitivity of breast cancer to targeted therapy*. Oncotarget, 2011. **2**(7): p. 538-50.
76. Zhang, Y., et al., *Elevated insulin-like growth factor I receptor signaling induces antiestrogen resistance through the MAPK/ERK and PI3K/Akt signaling routes*. Breast Cancer Res, 2011. **13**(3): p. R52.
77. Alessi, D.R., et al., *3-Phosphoinositide-dependent protein kinase-1 (PDK1): structural and functional homology with the Drosophila DSTPK61 kinase*. Curr Biol, 1997. **7**(10): p. 776-89.
78. Alessi, D.R., et al., *Characterization of a 3-phosphoinositide-dependent protein kinase which phosphorylates and activates protein kinase Balpha*. Curr Biol, 1997. **7**(4): p. 261-9.

79. Stephens, L., et al., *Protein kinase B kinases that mediate phosphatidylinositol 3,4,5-trisphosphate-dependent activation of protein kinase B*. *Science*, 1998. **279**(5351): p. 710-4.
80. Sarbassov, D.D., et al., *Phosphorylation and regulation of Akt/PKB by the rictor-mTOR complex*. *Science*, 2005. **307**(5712): p. 1098-101.
81. Hauge, C., et al., *Mechanism for activation of the growth factor-activated AGC kinases by turn motif phosphorylation*. *EMBO J*, 2007. **26**(9): p. 2251-61.
82. Ikenoue, T., et al., *Essential function of TORC2 in PKC and Akt turn motif phosphorylation, maturation and signalling*. *EMBO J*, 2008. **27**(14): p. 1919-31.
83. Facchinetti, V., et al., *The mammalian target of rapamycin complex 2 controls folding and stability of Akt and protein kinase C*. *EMBO J*, 2008. **27**(14): p. 1932-43.
84. Currie, R.A., et al., *Role of phosphatidylinositol 3,4,5-trisphosphate in regulating the activity and localization of 3-phosphoinositide-dependent protein kinase-1*. *Biochem J*, 1999. **337** (Pt 3): p. 575-83.
85. Oh, W.J. and E. Jacinto, *mTOR complex 2 signaling and functions*. *Cell Cycle*, 2011. **10**(14): p. 2305-16.
86. Garcia-Martinez, J.M. and D.R. Alessi, *mTOR complex 2 (mTORC2) controls hydrophobic motif phosphorylation and activation of serum- and glucocorticoid-induced protein kinase 1 (SGK1)*. *Biochem J*, 2008. **416**(3): p. 375-85.
87. Sarbassov, D.D., et al., *Rictor, a novel binding partner of mTOR, defines a rapamycin-insensitive and raptor-independent pathway that regulates the cytoskeleton*. *Curr Biol*, 2004. **14**(14): p. 1296-302.
88. Tato, I., et al., *Amino acids activate mammalian target of rapamycin complex 2 (mTORC2) via PI3K/Akt signaling*. *J Biol Chem*, 2011. **286**(8): p. 6128-42.
89. Zinzalla, V., et al., *Activation of mTORC2 by association with the ribosome*. *Cell*, 2011. **144**(5): p. 757-68.
90. Gan, X., et al., *Evidence for direct activation of mTORC2 kinase activity by phosphatidylinositol 3,4,5-trisphosphate*. *J Biol Chem*, 2011. **286**(13): p. 10998-1002.
91. Dibble, C.C., J.M. Asara, and B.D. Manning, *Characterization of Rictor phosphorylation sites reveals direct regulation of mTOR complex 2 by S6K1*. *Mol Cell Biol*, 2009. **29**(21): p. 5657-70.
92. Gonzalez, E. and T.E. McGraw, *The Akt kinases: isoform specificity in metabolism and cancer*. *Cell Cycle*, 2009. **8**(16): p. 2502-8.
93. Bellacosa, A., et al., *Molecular alterations of the AKT2 oncogene in ovarian and breast carcinomas*. *Int J Cancer*, 1995. **64**(4): p. 280-5.
94. Nakatani, K., et al., *Up-regulation of Akt3 in estrogen receptor-deficient breast cancers and androgen-independent prostate cancer lines*. *J Biol Chem*, 1999. **274**(31): p. 21528-32.
95. Mende, I., et al., *Oncogenic transformation induced by membrane-targeted Akt2 and Akt3*. *Oncogene*, 2001. **20**(32): p. 4419-23.

96. Yuan, Z.Q., et al., *AKT2 inhibition of cisplatin-induced JNK/p38 and Bax activation by phosphorylation of ASK1: implication of AKT2 in chemoresistance.* J Biol Chem, 2003. **278**(26): p. 23432-40.
97. Cheng, G.Z., et al., *Twist transcriptionally up-regulates AKT2 in breast cancer cells leading to increased migration, invasion, and resistance to paclitaxel.* Cancer Res, 2007. **67**(5): p. 1979-87.
98. Xing, H., et al., *Activation of fibronectin/PI-3K/Akt2 leads to chemoresistance to docetaxel by regulating survivin protein expression in ovarian and breast cancer cells.* Cancer Lett, 2008. **261**(1): p. 108-19.
99. Downward, J., *Mechanisms and consequences of activation of protein kinase B/Akt.* Curr Opin Cell Biol, 1998. **10**(2): p. 262-7.
100. Diehl, J.A., et al., *Glycogen synthase kinase-3beta regulates cyclin D1 proteolysis and subcellular localization.* Genes Dev, 1998. **12**(22): p. 3499-511.
101. Katayama, K., N. Fujita, and T. Tsuruo, *Akt/protein kinase B-dependent phosphorylation and inactivation of WEE1Hu promote cell cycle progression at G2/M transition.* Mol Cell Biol, 2005. **25**(13): p. 5725-37.
102. Okumura, E., et al., *Akt inhibits Myt1 in the signalling pathway that leads to meiotic G2/M-phase transition.* Nat Cell Biol, 2002. **4**(2): p. 111-6.
103. Gesbert, F., et al., *BCR/ABL regulates expression of the cyclin-dependent kinase inhibitor p27Kip1 through the phosphatidylinositol 3-Kinase/AKT pathway.* J Biol Chem, 2000. **275**(50): p. 39223-30.
104. Rossig, L., et al., *Akt-dependent phosphorylation of p21(Cip1) regulates PCNA binding and proliferation of endothelial cells.* Mol Cell Biol, 2001. **21**(16): p. 5644-57.
105. Hara, K., et al., *Amino acid sufficiency and mTOR regulate p70 S6 kinase and eIF-4E Bp1 through a common effector mechanism.* J Biol Chem, 1998. **273**(23): p. 14484-94.
106. Gingras, A.C., et al., *4E-BP1, a repressor of mRNA translation, is phosphorylated and inactivated by the Akt(PKB) signaling pathway.* Genes Dev, 1998. **12**(4): p. 502-13.
107. Cross, D.A., et al., *Inhibition of glycogen synthase kinase-3 by insulin mediated by protein kinase B.* Nature, 1995. **378**(6559): p. 785-9.
108. Kane, S., et al., *A method to identify serine kinase substrates. Akt phosphorylates a novel adipocyte protein with a Rab GTPase-activating protein (GAP) domain.* J Biol Chem, 2002. **277**(25): p. 22115-8.
109. Zeigerer, A., M.K. McBrayer, and T.E. McGraw, *Insulin stimulation of GLUT4 exocytosis, but not its inhibition of endocytosis, is dependent on RabGAP AS160.* Mol Biol Cell, 2004. **15**(10): p. 4406-15.
110. Tang, E.D., et al., *Negative regulation of the forkhead transcription factor FKHR by Akt.* J Biol Chem, 1999. **274**(24): p. 16741-6.
111. Qi, X.J., G.M. Wildey, and P.H. Howe, *Evidence that Ser87 of BimEL is phosphorylated by Akt and regulates BimEL apoptotic function.* J Biol Chem, 2006. **281**(2): p. 813-23.

112. Yamaguchi, H. and H.G. Wang, *The protein kinase PKB/Akt regulates cell survival and apoptosis by inhibiting Bax conformational change*. *Oncogene*, 2001. **20**(53): p. 7779-86.
113. del Peso, L., et al., *Interleukin-3-induced phosphorylation of BAD through the protein kinase Akt*. *Science*, 1997. **278**(5338): p. 687-9.
114. Sausville, E.A. and D.L. Longo, *Principles of Cancer Treatment: Surgery, Chemotherapy, and Biologic Therapy*, in *Harrison's Principles of Internal Medicine*, D.L. Kasper, et al., Editors. 2005, McGraw-Hill: New York. p. 464-482.
115. Avila, J., *Microtubule dynamics*. *FASEB J*, 1990. **4**(15): p. 3284-90.
116. Mitchison, T. and M. Kirschner, *Dynamic instability of microtubule growth*. *Nature*, 1984. **312**(5991): p. 237-42.
117. Wadsworth, P. and M. McGrail, *Interphase microtubule dynamics are cell type-specific*. *J Cell Sci*, 1990. **95 (Pt 1)**: p. 23-32.
118. Weisenberg, R.C. and W.J. Deery, *Role of nucleotide hydrolysis in microtubule assembly*. *Nature*, 1976. **263**(5580): p. 792-3.
119. Assmann, V., et al., *The pattern of expression of the microtubule-binding protein RHAMM/IHABP in mammary carcinoma suggests a role in the invasive behaviour of tumour cells*. *J Pathol*, 2001. **195**(2): p. 191-6.
120. Yoon, S.O., S. Shin, and A.M. Mercurio, *Hypoxia stimulates carcinoma invasion by stabilizing microtubules and promoting the Rab11 trafficking of the alpha6beta4 integrin*. *Cancer Res*, 2005. **65**(7): p. 2761-9.
121. Whipple, R.A., et al., *Epithelial-to-mesenchymal transition promotes tubulin detyrosination and microtentacles that enhance endothelial engagement*. *Cancer Res*, 2010. **70**(20): p. 8127-37.
122. Cassimeris, L., et al., *Fueled by microtubules: Does tubulin dimer/polymer partitioning regulate intracellular metabolism?* *Cytoskeleton (Hoboken)*, 2012.
123. Eyster, C.A. and A.L. Olson, *Compartmentalization and regulation of insulin signaling to GLUT4 by the cytoskeleton*. *Vitam Horm*, 2009. **80**: p. 193-215.
124. Eyster, C.A., et al., *Microtubule network is required for insulin signaling through activation of Akt/protein kinase B: evidence that insulin stimulates vesicle docking/fusion but not intracellular mobility*. *J Biol Chem*, 2006. **281**(51): p. 39719-27.
125. Dehmelt, L. and S. Halpain, *The MAP2/Tau family of microtubule-associated proteins*. *Genome Biol*, 2005. **6**(1): p. 204.
126. Akhmanova, A. and M.O. Steinmetz, *Microtubule +TIPs at a glance*. *J Cell Sci*, 2010. **123**(Pt 20): p. 3415-9.
127. Schnapp, B.J. and T.S. Reese, *Dynein is the motor for retrograde axonal transport of organelles*. *Proc Natl Acad Sci U S A*, 1989. **86**(5): p. 1548-52.
128. Hirokawa, N., et al., *Kinesin associates with anterogradely transported membranous organelles in vivo*. *J Cell Biol*, 1991. **114**(2): p. 295-302.
129. Hirokawa, N. and R. Takemura, *Kinesin superfamily proteins and their various functions and dynamics*. *Exp Cell Res*, 2004. **301**(1): p. 50-9.

130. Furlanetto, R.W. and J.N. DiCarlo, *Somatomedin-C receptors and growth effects in human breast cells maintained in long-term tissue culture*. *Cancer Res*, 1984. **44**(5): p. 2122-8.
131. Turner, B.C., et al., *Insulin-like growth factor-I receptor overexpression mediates cellular radioresistance and local breast cancer recurrence after lumpectomy and radiation*. *Cancer Res*, 1997. **57**(15): p. 3079-83.
132. Johnston, S.R., M. Dowsett, and I.E. Smith, *Towards a molecular basis for tamoxifen resistance in breast cancer*. *Ann Oncol*, 1992. **3**(7): p. 503-11.
133. White, M.F., R. Maron, and C.R. Kahn, *Insulin rapidly stimulates tyrosine phosphorylation of a Mr-185,000 protein in intact cells*. *Nature*, 1985. **318**(6042): p. 183-6.
134. Patti, M.E., et al., *4PS/insulin receptor substrate (IRS)-2 is the alternative substrate of the insulin receptor in IRS-1-deficient mice*. *J Biol Chem*, 1995. **270**(42): p. 24670-3.
135. Yamauchi, T., et al., *Growth hormone and prolactin stimulate tyrosine phosphorylation of insulin receptor substrate-1, -2, and -3, their association with p85 phosphatidylinositol 3-kinase (PI3-kinase), and concomitantly PI3-kinase activation via JAK2 kinase*. *J Biol Chem*, 1998. **273**(25): p. 15719-26.
136. Sisci, D., et al., *Expression of nuclear insulin receptor substrate 1 in breast cancer*. *J Clin Pathol*, 2007. **60**(6): p. 633-41.
137. Lee, A.V., et al., *Enhancement of insulin-like growth factor signaling in human breast cancer: estrogen regulation of insulin receptor substrate-1 expression in vitro and in vivo*. *Mol Endocrinol*, 1999. **13**(5): p. 787-96.
138. Molloy, C.A., F.E. May, and B.R. Westley, *Insulin receptor substrate-1 expression is regulated by estrogen in the MCF-7 human breast cancer cell line*. *J Biol Chem*, 2000. **275**(17): p. 12565-71.
139. Schnarr, B., et al., *Down-regulation of insulin-like growth factor-I receptor and insulin receptor substrate-1 expression in advanced human breast cancer*. *Int J Cancer*, 2000. **89**(6): p. 506-13.
140. Migliaccio, I., et al., *Nuclear IRS-1 predicts tamoxifen response in patients with early breast cancer*. *Breast Cancer Res Treat*, 2010. **123**(3): p. 651-60.
141. Kleer, C.G., et al., *EZH2 is a marker of aggressive breast cancer and promotes neoplastic transformation of breast epithelial cells*. *Proc Natl Acad Sci U S A*, 2003. **100**(20): p. 11606-11.
142. McShane, L.M., et al., *REporting recommendations for tumor MARKer prognostic studies (REMARK)*. *Breast Cancer Res Treat*, 2006. **100**(2): p. 229-35.
143. Prisco, M., et al., *Nuclear translocation of insulin receptor substrate-1 by the simian virus 40 T antigen and the activated type I insulin-like growth factor receptor*. *J Biol Chem*, 2002. **277**(35): p. 32078-85.
144. Thirone, A.C., et al., *Modulation of growth hormone signal transduction in kidneys of streptozotocin-induced diabetic animals: effect of a growth hormone receptor antagonist*. *Diabetes*, 2002. **51**(7): p. 2270-81.

145. Chen, J., et al., *Functional significance of type I insulin-like growth factor-mediated nuclear translocation of the insulin receptor substrate-1 and beta-catenin*. J Biol Chem, 2005. **280**(33): p. 29912-20.
146. Lanzino, M., et al., *Insulin receptor substrate 1 modulates the transcriptional activity and the stability of androgen receptor in breast cancer cells*. Breast Cancer Res Treat, 2009. **115**(2): p. 297-306.
147. Wu, A., J. Chen, and R. Baserga, *Nuclear insulin receptor substrate-1 activates promoters of cell cycle progression genes*. Oncogene, 2008. **27**(3): p. 397-403.
148. Petrie, R.J., A.D. Doyle, and K.M. Yamada, *Random versus directionally persistent cell migration*. Nat Rev Mol Cell Biol, 2009. **10**(8): p. 538-49.
149. Monami, G., V. Emiliozzi, and A. Morrione, *Grb10/Nedd4-mediated multiubiquitination of the insulin-like growth factor receptor regulates receptor internalization*. J Cell Physiol, 2008. **216**(2): p. 426-37.
150. Romanelli, R.J., et al., *Insulin-like growth factor type-I receptor internalization and recycling mediate the sustained phosphorylation of Akt*. J Biol Chem, 2007. **282**(31): p. 22513-24.
151. Gross, G.E., et al., *Multiple progesterone receptor assays in human breast cancer*. Cancer Res, 1984. **44**(2): p. 836-40.
152. Balleine, R.L., et al., *Absence of progesterone receptor associated with secondary breast cancer in postmenopausal women*. Br J Cancer, 1999. **79**(9-10): p. 1564-71.
153. Anderson, W.F., et al., *Tumor variants by hormone receptor expression in white patients with node-negative breast cancer from the surveillance, epidemiology, and end results database*. J Clin Oncol, 2001. **19**(1): p. 18-27.
154. Arpino, G., et al., *Estrogen receptor-positive, progesterone receptor-negative breast cancer: association with growth factor receptor expression and tamoxifen resistance*. J Natl Cancer Inst, 2005. **97**(17): p. 1254-61.
155. Cui, X., et al., *Biology of progesterone receptor loss in breast cancer and its implications for endocrine therapy*. J Clin Oncol, 2005. **23**(30): p. 7721-35.
156. Singh, A., et al., *Reporter gene assay demonstrates functional differences in estrogen receptor activity in purified breast cancer cells: a pilot study*. Int J Cancer, 2003. **107**(5): p. 700-6.
157. Cui, X., et al., *Insulin-like growth factor-I inhibits progesterone receptor expression in breast cancer cells via the phosphatidylinositol 3-kinase/Akt/mammalian target of rapamycin pathway: progesterone receptor as a potential indicator of growth factor activity in breast cancer*. Mol Endocrinol, 2003. **17**(4): p. 575-88.
158. Myers, M.G., Jr., et al., *IRS-1 is a common element in insulin and insulin-like growth factor-I signaling to the phosphatidylinositol 3'-kinase*. Endocrinology, 1993. **132**(4): p. 1421-30.
159. Fujioka, T., et al., *Further evidence for the involvement of insulin receptor substrates in epidermal growth factor-induced activation of phosphatidylinositol 3-kinase*. Eur J Biochem, 2001. **268**(15): p. 4158-68.

160. Senthil, D., et al., *The type 2 vascular endothelial growth factor receptor recruits insulin receptor substrate-1 in its signalling pathway*. *Biochem J*, 2002. **368**(Pt 1): p. 49-56.
161. Clark, J.L., et al., *Membrane localization of insulin receptor substrate-2 (IRS-2) is associated with decreased overall survival in breast cancer*. *Breast Cancer Res Treat*, 2011. **130**(3): p. 759-72.
162. Rabinovitz, I., A. Toker, and A.M. Mercurio, *Protein kinase C-dependent mobilization of the alpha6beta4 integrin from hemidesmosomes and its association with actin-rich cell protrusions drive the chemotactic migration of carcinoma cells*. *J Cell Biol*, 1999. **146**(5): p. 1147-60.
163. Yamasaki, H., et al., *Human insulin-like growth factor I receptor 950tyrosine is required for somatotroph growth factor signal transduction*. *J Biol Chem*, 1992. **267**(29): p. 20953-8.
164. Carelli, S., et al., *Degradation of insulin-like growth factor-I receptor occurs via ubiquitin-proteasome pathway in human lung cancer cells*. *J Cell Physiol*, 2006. **208**(2): p. 354-62.
165. Copp, J., G. Manning, and T. Hunter, *TORC-specific phosphorylation of mammalian target of rapamycin (mTOR): phospho-Ser2481 is a marker for intact mTOR signaling complex 2*. *Cancer Res*, 2009. **69**(5): p. 1821-7.
166. Zhu, D., et al., *Growth arrest induces primary-cilium formation and sensitizes IGF-1-receptor signaling during differentiation induction of 3T3-L1 preadipocytes*. *J Cell Sci*, 2009. **122**(Pt 15): p. 2760-8.
167. Imamura, T., et al., *Insulin-induced GLUT4 translocation involves protein kinase C-lambda-mediated functional coupling between Rab4 and the motor protein kinesin*. *Mol Cell Biol*, 2003. **23**(14): p. 4892-900.
168. Wang, C.Q., et al., *Overexpression of Kif2a promotes the progression and metastasis of squamous cell carcinoma of the oral tongue*. *Oral Oncol*, 2010. **46**(1): p. 65-9.
169. Ding, S., et al., *Overexpression of Eg5 predicts unfavorable prognosis in non-muscle invasive bladder urothelial carcinoma*. *Int J Urol*, 2011. **18**(6): p. 432-8.
170. Sun, X.D., et al., *Dimethylnastron suppresses human pancreatic cancer cell migration and invasion in vitro via allosteric inhibition of mitotic kinesin Eg5*. *Acta Pharmacol Sin*, 2011. **32**(12): p. 1543-8.
171. Manning, A.L., et al., *The kinesin-13 proteins Kif2a, Kif2b, and Kif2c/MCAK have distinct roles during mitosis in human cells*. *Mol Biol Cell*, 2007. **18**(8): p. 2970-9.
172. Thomas, E.C., et al., *The subcellular fractionation properties and function of insulin receptor substrate-1 (IRS-1) are independent of cytoskeletal integrity*. *Int J Biochem Cell Biol*, 2006. **38**(10): p. 1686-99.
173. Suzuki, K. and K. Takahashi, *Regulation of lamellipodia formation and cell invasion by CLIP-170 in invasive human breast cancer cells*. *Biochem Biophys Res Commun*, 2008. **368**(2): p. 199-204.

174. Olson, A.L., A.R. Trumbly, and G.V. Gibson, *Insulin-mediated GLUT4 translocation is dependent on the microtubule network*. J Biol Chem, 2001. **276**(14): p. 10706-14.
175. Gagnon, V., et al., *Akt and XIAP regulate the sensitivity of human uterine cancer cells to cisplatin, doxorubicin and taxol*. Apoptosis, 2008. **13**(2): p. 259-71.
176. Nguyen, D.M., et al., *Potentiation of paclitaxel cytotoxicity in lung and esophageal cancer cells by pharmacologic inhibition of the phosphoinositide 3-kinase/protein kinase B (Akt)-mediated signaling pathway*. J Thorac Cardiovasc Surg, 2004. **127**(2): p. 365-75.
177. Yang, S.X., et al., *Akt phosphorylation at Ser473 predicts benefit of paclitaxel chemotherapy in node-positive breast cancer*. J Clin Oncol, 2010. **28**(18): p. 2974-81.
178. Page, C., et al., *Overexpression of Akt/AKT can modulate chemotherapy-induced apoptosis*. Anticancer Res, 2000. **20**(1A): p. 407-16.
179. Schimizzi, G.V., J.D. Currie, and S.L. Rogers, *Expression levels of a kinesin-13 microtubule depolymerase modulates the effectiveness of anti-microtubule agents*. PLoS One, 2010. **5**(6): p. e11381.
180. Sehat, B., et al., *Identification of c-Cbl as a new ligase for insulin-like growth factor-I receptor with distinct roles from Mdm2 in receptor ubiquitination and endocytosis*. Cancer Res, 2008. **68**(14): p. 5669-77.
181. Kimmelman, A.C., *The dynamic nature of autophagy in cancer*. Genes Dev, 2011. **25**(19): p. 1999-2010.
182. Aplin, A., et al., *Cytoskeletal elements are required for the formation and maturation of autophagic vacuoles*. J Cell Physiol, 1992. **152**(3): p. 458-66.
183. Reunanen, H., M. Marttinen, and P. Hirsimäki, *Effects of griseofulvin and nocodazole on the accumulation of autophagic vacuoles in Ehrlich ascites tumor cells*. Exp Mol Pathol, 1988. **48**(1): p. 97-102.
184. Fujiwara, Y., et al., *Blockade of the phosphatidylinositol-3-kinase-Akt signaling pathway enhances the induction of apoptosis by microtubule-destabilizing agents in tumor cells in which the pathway is constitutively activated*. Mol Cancer Ther, 2007. **6**(3): p. 1133-42.
185. VanderWeele, D.J., R. Zhou, and C.M. Rudin, *Akt up-regulation increases resistance to microtubule-directed chemotherapeutic agents through mammalian target of rapamycin*. Mol Cancer Ther, 2004. **3**(12): p. 1605-13.
186. Flusberg, D.A., Y. Numaguchi, and D.E. Ingber, *Cooperative control of Akt phosphorylation, bcl-2 expression, and apoptosis by cytoskeletal microfilaments and microtubules in capillary endothelial cells*. Mol Biol Cell, 2001. **12**(10): p. 3087-94.
187. Zhang, C., et al., *S9, a novel anticancer agent, exerts its anti-proliferative activity by interfering with both PI3K-Akt-mTOR signaling and microtubule cytoskeleton*. PLoS One, 2009. **4**(3): p. e4881.
188. Zhang, X. and T.A. Vik, *Growth factor stimulation of hematopoietic cells leads to membrane translocation of AKT1 protein kinase*. Leuk Res, 1997. **21**(9): p. 849-56.

189. Schuster, M., et al., *Kinesin-3 and dynein cooperate in long-range retrograde endosome motility along a nonuniform microtubule array*. Mol Biol Cell, 2011. **22**(19): p. 3645-57.
190. Ems-McClung, S.C. and C.E. Walczak, *Kinesin-13s in mitosis: Key players in the spatial and temporal organization of spindle microtubules*. Semin Cell Dev Biol, 2010. **21**(3): p. 276-82.
191. Mennella, V., et al., *Functionally distinct kinesin-13 family members cooperate to regulate microtubule dynamics during interphase*. Nat Cell Biol, 2005. **7**(3): p. 235-45.
192. Desai, A., et al., *Kin I kinesins are microtubule-destabilizing enzymes*. Cell, 1999. **96**(1): p. 69-78.
193. Knowlton, A.L., et al., *ICIS and Aurora B coregulate the microtubule depolymerase Kif2a*. Curr Biol, 2009. **19**(9): p. 758-63.
194. Yu, Y. and Y.M. Feng, *The role of kinesin family proteins in tumorigenesis and progression: potential biomarkers and molecular targets for cancer therapy*. Cancer, 2010. **116**(22): p. 5150-60.
195. Shimo, A., et al., *Involvement of kinesin family member 2C/mitotic centromere-associated kinesin overexpression in mammary carcinogenesis*. Cancer Sci, 2008. **99**(1): p. 62-70.
196. Li, G., et al., *Targeting of integrin beta1 and kinesin 2alpha by microRNA 183*. J Biol Chem, 2010. **285**(8): p. 5461-71.
197. Nagahara, M., et al., *Kinesin 18A expression: clinical relevance to colorectal cancer progression*. Int J Cancer, 2011. **129**(11): p. 2543-52.
198. Zanella, F., et al., *Chemical genetic analysis of FOXO nuclear-cytoplasmic shuttling by using image-based cell screening*. Chembiochem, 2008. **9**(14): p. 2229-37.
199. Birkenkamp, K.U. and P.J. Coffey, *Regulation of cell survival and proliferation by the FOXO (Forkhead box, class O) subfamily of Forkhead transcription factors*. Biochem Soc Trans, 2003. **31**(Pt 1): p. 292-7.
200. Bhaskar, P.T. and N. Hay, *The two TORCs and Akt*. Dev Cell, 2007. **12**(4): p. 487-502.
201. Suprenant, K.A., et al., *EMAP, an echinoderm microtubule-associated protein found in microtubule-ribosome complexes*. J Cell Sci, 1993. **104**(2): p. 445-50.
202. Jessus, C., et al., *Interaction between rat brain microtubule associated proteins (MAPs) and free ribosomes from Xenopus oocyte: a possible mechanism for the in ovo distribution of MAPs*. Cell Differ, 1984. **14**(4): p. 295-301.
203. Jacinto, E., et al., *Mammalian TOR complex 2 controls the actin cytoskeleton and is rapamycin insensitive*. Nat Cell Biol, 2004. **6**(11): p. 1122-8.
204. Hresko, R.C., H. Murata, and M. Mueckler, *Phosphoinositide-dependent kinase-2 is a distinct protein kinase enriched in a novel cytoskeletal fraction associated with adipocyte plasma membranes*. J Biol Chem, 2003. **278**(24): p. 21615-22.
205. Singh, B.K., A. Singh, and D.D. Mascarenhas, *A nuclear complex of rictor and insulin receptor substrate-2 is associated with albuminuria in diabetic mice*. Metab Syndr Relat Disord, 2010. **8**(4): p. 355-63.